

Normalization and global analysis of perturbations of the hydrogen atom

K. Efstathiou*

Department of Mathematics, University of Groningen, Groningen 9700 AK, The Netherlands

D. A. Sadovskii†

Département de Physique, Université du Littoral–Côte d’Opale, 59140 Dunkerque, France

(Published 3 August 2010)

The hydrogen atom perturbed by sufficiently small homogeneous static electric and magnetic fields of arbitrary mutual alignment is a specific perturbation of the Kepler system with three degrees of freedom and three parameters. Normalization of the Keplerian symmetry reveals that the parameter space is stratified into resonant zones of systems, each zone with an internal dynamical stratification of its own (Efstathiou, Sadovskii, and Zhilinskiĭ, 2007, *Proc. R. Soc. London, Ser. A* **463**, 1771). Based on the fully integrable approximation, the bundle of invariant tori of individual systems within zones is characterized globally and the qualitative dynamical stratification is uncovered. The techniques involved in this analysis are illustrated with the example of the 1:1 resonance zone (near orthogonal fields) whose structure is known at present. Applications in the corresponding quantum system are also described.

DOI: [10.1103/RevModPhys.82.2099](https://doi.org/10.1103/RevModPhys.82.2099)

PACS number(s): 32.60.+i, 03.65.Vf, 45.05.+x, 03.65.Sq

CONTENTS

I. Introduction	2100	4. Generalized or fractional monodromy	2110
A. Global dynamical analysis	2100	5. Monodromy map and its matrix	2111
1. Characteristics of individual perturbations	2100	E. Quantum-classical correspondence	2111
2. Stratification of the parameter space	2101	1. Quantum joint spectrum lattice	2111
B. Hamiltonian and parameter space	2101	2. Quantum monodromy	2112
C. Historical overview and perspective	2102	3. Generalizations	2112
D. Structure of the paper	2102	F. Main conjecture of the global classification	2112
II. Basic Mathematical Concepts	2103	1. Toric fibrations and their \mathcal{BD}	2112
A. Regularization, first integrals, and their flows	2103	2. Recovering topology of singular fibrations from their \mathcal{BD}	2113
B. Geometry of the reduction map	2103	3. Extending to systems with hyperbolic singular fibers	2113
1. First or Keplerian reduction	2103	4. Extending to nearly integrable systems	2113
2. Resonant Pauliean symmetry S^1 and zones	2104	III. Results: Qualitative Types of Perturbations	2113
3. Singular reduction of Pauliean symmetry	2105	A. Symmetry strata and their stabilizers	2113
C. The study of the integrable fibration	2105	B. Classification of systems in the 1:1 zone	2114
1. Energy-momentum map \mathcal{EM}	2106	C. Systems in the 1:2 zone	2115
2. Critical points of \mathcal{EM}	2106	1. Most typical 1:2 structure	2116
a. Critical points of rank 2	2106	2. Fractional monodromy	2116
b. Critical points of rank 1	2106	D. Higher-order resonance zones	2117
c. Restrictions due to symmetry and topology	2107	E. Systems with additional Lie symmetry	2117
3. Fibers of the energy-momentum map \mathcal{EM}	2107	IV. The Integrable Approximation	2117
a. Relative equilibria (RE)	2107	A. Keplerian normalization and reduction	2118
b. Singular fibers	2108	1. KS regularization	2118
4. \mathcal{BD} as stratified unfolded \mathcal{EM} image	2108	2. Normalization of the Keplerian symmetry	2118
D. Global action-angle variables and monodromy	2108	3. Reduction of the Keplerian symmetry	2118
1. Basic case of Hamiltonian monodromy	2109	B. Energy correction	2119
2. Specifics of monodromy	2110	C. Standard form of the linear term and resonances	2120
3. Multivalued action functions	2110	D. Normalization and reduction of the Pauliean symmetry	2120
		1. Resonances, zones, and second normalization	2120
		a. Second normalization in $S^2 \times S^2$	2121
		b. Second normalization in \mathbb{R}^8	2121

*k.efstathiou@rug.nl

†sadovski@univ-littoral.fr

2. Reduction of the Pauliean symmetry	2122	7. Other regularization and normal form techniques	2143
a. Invariants of the $k_-:k_+$ resonant S^1 action	2122	8. Studies of parametric families, classification, and bifurcations	2144
b. Pauliean orbit space \mathcal{O}_n	2122	D. Monodromy	2145
c. Second reduced phase space $P_{n,m}$	2123	E. Similar systems	2146
d. Second reduced phase spaces $P_{n,m}^{1:1}$ and $P_{n,m}^{1:2}$	2123	IX. Conclusion and Perspectives	2146
e. Spherical deformation of $P_{n,m}^{k_-:k_+}$	2123	List of Symbols	2147
f. Second reduced energy correction on $P_{n,m}$	2124	Acknowledgments	2148
g. Reduced dynamics and trajectories on $P_{n,m}$	2124	References	2148
E. Ambiguity of the integrable approximation	2124		
V. Dynamical Strata in the Parameter Space	2125		
A. Energy-momentum map \mathcal{EM} and its image \mathcal{BD}	2125		
1. Constant h level sets of the reduced system	2125		
2. Relative equilibria and other critical fibers	2126		
3. Bifurcation diagrams	2126		
B. Energy-momentum map \mathcal{EM} of 1:1 systems	2126		
1. Constant h level sets of reduced 1:1 systems	2126		
2. Relative equilibria and other critical fibers of 1:1 systems	2127		
a. Case A_0	2127		
b. Case $A_{1,1}$	2127		
c. Case A_2	2127		
d. Case A_1	2128		
e. Case B_0	2128		
f. Case B_1	2128		
3. Constant ns bifurcation diagrams \mathcal{BD}_n of 1:1 systems and their structural stability	2128		
C. Analysis of 1:2 systems and higher resonances	2129		
VI. Monodromy	2129		
A. Computation of monodromy	2129		
1. Rotation angles in systems with two degrees of freedom	2129		
2. Rotation angles in systems with $K > 2$ degrees of freedom and $K-1$ diagonal S^1 actions	2130		
B. General properties of the monodromy map	2131		
1. Monodromy matrix and changes of cycle bases	2131		
2. The sum rules	2131		
3. Deformation principle	2131		
4. The sign of monodromy	2132		
5. Geometric monodromy theorem	2132		
C. Monodromy of systems in the 1:1 zone	2132		
1. Monodromy of the n -shell system on $S^2 \times S^2$	2132		
2. Monodromy on $\mathbb{R}^8 _{\zeta=0}$	2133		
3. Monodromy in \mathbb{R}^6	2134		
VII. Quantum Dynamical Stratification	2135		
A. Quantized second normal form	2135		
B. Quantized first normal form $\widehat{\Delta E}$	2136		
C. Quantum joint spectra	2136		
VIII. Bibliographic Remarks	2137		
A. The general idea of our approach	2138		
B. Topics outside our scope	2138		
C. Review of relevant literature	2138		
1. Second-order perturbation theory of the 1980s	2139		
2. Geometry of the reduction map	2140		
3. Restrictions to specific systems	2140		
4. Dynamical symmetry, equivalent operators	2141		
5. Reduced dynamics, rotator models	2141		
6. KS regularization and applications	2142		

I. INTRODUCTION

Global analysis from the theory of integrable dynamical systems point of view is the key to this review. We study perturbations of the hydrogen atom by sufficiently small homogeneous static electric (\mathbf{F}) and magnetic (\mathbf{G}) fields of any mutual orientation. In spite of this system being one of the most widely studied in quantum and classical mechanics (see Sec. VIII), its consistent global dynamical description began to be finalized recently by Cushman and Sadovskii (1999, 2000) and is presently limited to the subset of systems with nearly orthogonal fields¹ called by Efstathiou, Sadovskii, and Zhilinskiĭ (2007) the 1:1 resonance zone and so remains incomplete. We detail the scheme of the global analysis and explain it with the example of the 1:1 and 1:2 zones.

A. Global dynamical analysis

We assume conditions under which an integrable approximation can be used for a dynamical classification of our systems, and the influence of unbound motion and irregular dynamics can be subdued at our level of detail (cf. Sec. VIII.B). Subsequently, we proceed with the global analysis of the integrable approximation, which has two principal aspects: (i) complete topological characterization of each individual perturbation for given fixed values of parameters and (ii) partition of the whole parameter space into dynamical strata representing systems of the same topological type.

1. Characteristics of individual perturbations

The first aspect is primary and requires considerable effort. Each individual system in the three-parameter family of perturbations under study is, typically, a system with three degrees of freedom (3-DOF) without strict Lie symmetries. After normalizing this system and constructing an integrable approximation, we give a global description of the latter by analyzing the fibration of the phase space defined by the common level sets of its first integrals. In particular we describe the fiber bundle of regular Liouville tori \mathbb{T}^3 by establishing global *connections* between them. In that we follow the standard ap-

¹See Efstathiou, Sadovskii, and Zhilinskiĭ, (2007), Schleif and Delos (2007, 2008), and Efstathiou *et al.* (2008, 2009), and discussion in Sec. VIII.C.8.

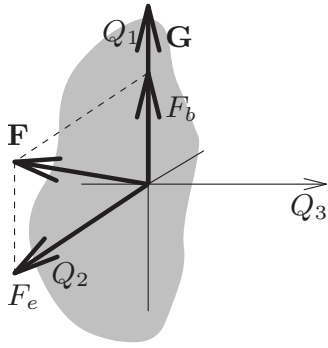


FIG. 1. Orientation of electric and magnetic fields \mathbf{F} and \mathbf{G} .

proach in the contemporary theory of integrable Hamiltonian dynamical systems described by Cushman and Bates (1997) and in a wider sense by Bolsinov and Fomenko (2004) [see also Michel and Zhilinskiĭ (2001a), Efsthathiou (2005), and Efsthathiou and Sadovskii (2005)]. The obtained qualitative dynamical characteristics can be then attributed to the original nonintegrable system if the latter satisfies the conditions of the Kolmogorov-Arnol'd-Moser (KAM) theory and retains sufficiently many invariant tori (Rink, 2004; Broer *et al.*, 2007).

2. Stratification of the parameter space

Once all systems in our three-parameter family are characterized, the second stage of the analysis involves finding how these systems form strata in the parameter space which is a domain in \mathbb{R}^3 . Within this space, we distinguish symmetry strata (Michel and Zhilinskiĭ, 2001a) and dynamical strata (Efsthathiou, Sadovskii, and Zhilinskiĭ, 2007). The former are well defined and fixed, while the exact definition of the latter may depend, to an extent, on the order of the perturbation theory used in the study. In most cases, but not necessarily, dynamical strata form subsets within symmetry strata. We are interested only in *structurally stable* dynamical strata that persist after the perturbation theory is extended to higher orders.

B. Hamiltonian and parameter space

We can represent the electric and magnetic fields by respective three-vectors $\mathbf{F}=(F_b, F_e, 0)=-\mathbf{E}$ and $\mathbf{G}=(G, 0, 0)=-|e|\mathbf{B}$ with \mathbf{E} the electric field and \mathbf{B} the magnetic flux density, as shown in Fig. 1. Since for any such pair of three-vectors

$$\langle \mathbf{F}, \mathbf{G} \rangle^2 \leq \mathbf{G}^2 \mathbf{F}^2 = G^2 F^2 = G^2 (F_b^2 + F_e^2), \tag{1}$$

the set of all possible mutual orientations of the two fields can be represented in \mathbb{R}^3 with coordinate functions

$$(\xi_1, \xi_2, \xi_3): (\mathbf{F}, \mathbf{G}) \mapsto (\langle \mathbf{F}, \mathbf{G} \rangle, G^2, F^2)$$

as a solid cone $\{\xi_2 \xi_3 \geq \xi_1, \xi_2 \geq 0, \xi_3 \geq 0\}$ drawn in Fig. 2. This representation of the parameter space of the system was given by Michel and Zhilinskiĭ (2001a).

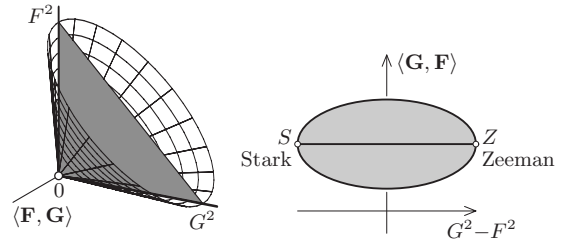


FIG. 2. The set of all distinct mutual configurations of electric (\mathbf{F}) and magnetic (\mathbf{G}) fields is a solid cone C (left): its constant F^2+G^2 section is a disk D (right). The shaded quarterplane ($F^2 \geq 0, G^2 \geq 0$) inside C and bold median line of D represent orthogonal fields; the boundaries $\partial C \setminus \{\langle \mathbf{G}, \mathbf{F} \rangle = 0\}$ and $\partial D \setminus \{S, Z\}$ without exceptional points representing single fields and no fields correspond to parallel symmetry stratum; other points represent generic configurations.

Assuming infinite proton mass and neglecting spin and relativistic corrections the Hamiltonian of our system is (in atomic units)

$$H_{3D} = \frac{1}{2} \mathbf{P}^2 - \frac{1}{|\mathbf{Q}|} + F_e Q_2 + F_b Q_1 + \frac{1}{2} G(Q_2 P_3 - Q_3 P_2) + \frac{1}{8} G^2(Q_2^2 + Q_3^2) = E, \tag{2}$$

where (\mathbf{Q}, \mathbf{P}) are standard canonical coordinates on $T^*\mathbb{R}^3$ and $\frac{1}{2} \mathbf{P}^2 - |\mathbf{Q}|^{-1}$ corresponds to the unperturbed two-body Hamiltonian. For this specific perturbation of the Kepler system, we study sufficiently large negative physical energies E at which the classical motion remains bound in a domain of sufficiently small $|\mathbf{Q}| > 0$. Since H_{3D} is singular in $|\mathbf{Q}| = 0$, the phase space of our system is $(\mathbb{R}^3 \setminus \{0\}) \times \mathbb{R}^3$ which will be denoted \mathbb{R}_*^6 .

The Hamiltonian (2) has an approximate first integral N which becomes exact after normalization.² N is called the Keplerian action; it Poisson commutes with the unperturbed Hamiltonian. The value³ $n \geq 0$ of N can be used to define the n -scaled field amplitudes

$$g = Gn^2, \quad (f_e, f_b) = 3(F_e, F_b)n^3. \tag{3}$$

Rewriting inequality (1) in terms of such amplitudes,

$$(gf_b)^2 \leq g^2 f_e^2, \tag{4a}$$

we define the n -shell parameter space C . In coordinates (gf_b, g^2, f_e^2) , it is a right-angle cone, identical to that in Fig. 2, left. Next we introduce parameters

$$s = \sqrt{g^2 + f_b^2 + f_e^2} \geq 0, \quad a^2 = \frac{g^2}{s^2}, \quad d = \frac{gf_b}{s^2}, \tag{4b}$$

where s is the combined field strength which serves as a universal perturbation scale parameter and should remain small. It is natural to consider constant- s sections

²See Sec. IV.A.1 for details and explicit definition of N .

³See Sec. VII for the action quantization of N and the relation of n to the principal quantum number.

D of C . Since for each fixed $s > 0$ the dimensionless parameters a^2 and d satisfy

$$d^2 \leq (1 - a^2)a^2, \quad (4c)$$

D is a disk in the parameter plane (d, a^2) . So for $s > 0$ the parameter space $C \setminus 0$ is a solid cylinder $\mathbb{R}_{>0} \times D$.

The uniform n scaling (3) and its energy equivalent

$$\tilde{g} = G(2/\Omega)^2, \quad (\tilde{f}_e, \tilde{f}_b) = 3(F_e, F_b)(2/\Omega)^3, \quad (5)$$

with

$$\Omega = \sqrt{-8E}, \quad (6)$$

were introduced by Sadovskii *et al.* (1996) and Sadovskii and Zhilinskiĭ (1998). Cushman and Sadovskii (1999, 2000), Efsthathiou, Cushman, and Sadovskii (2004), and Efsthathiou, Sadovskii, and Zhilinskiĭ (2007) relied on E scaling⁴ (5) which may seem more natural in classical mechanics where we work within a constant E level set. All our essential results, such as possible qualitative types of systems, dynamical strata, etc., do not depend on the choice of scaling, but the quantitative correspondence may be quite involved. The n scaling (Efsthathiou *et al.*, 2009) is more suited in quantum mechanics. It simplifies comparison to quantum energies and to other work (Schleif and Delos, 2007, 2008).

C. Historical overview and perspective

We point here to the milestones in the global analysis of perturbation (2); Sec. VIII gives a more substantial discussion of the literature. Pauli (1926) set up the problem and used the first order of the perturbation theory. On the example of the quadratic Zeeman effect, Herrick (1982) and Solov'ev (1982, 1983) demonstrated the importance of the second order for the qualitative understanding of these systems.

After numerous studies of concrete field configurations, significant progress was made by Cushman and Sadovskii (1999, 2000), who showed that all orthogonal field perturbations were of three basic generic types. Of these, systems near the Zeeman and Stark limits are similar to the ones studied by Herrick (1982) and Solov'ev (1982, 1983), while systems of the third kind had monodromy. This work opened the way to classify all perturbations with the Hamiltonian (2) and thus to complete the study initiated by Pauli (1926).

Michel and Zhilinskiĭ (2001a) described all symmetry strata in the parameter space C ; Efsthathiou, Sadovskii, and Zhilinskiĭ (2007) conjectured that this space was further stratified into *zones* of resonant $k_1:k_2$ approximations. The resonances themselves were analyzed by Karasev and Novikova (2005). A complete description of the near and exactly orthogonal field configurations which correspond to the 1:1 zone was given by Efsthathiou, Sadovskii, and Zhilinskiĭ (2007), Schleif and

Delos (2007, 2008), and Efsthathiou *et al.* (2009). For other resonances, it is not even known how large their zones are in the parameter space and how stable they may be in the presence of nonintegrability. At the level of common physical intuition, it seems that the size and the stability of a zone decrease with the order of the resonance. This makes the 1:1 zone the largest and the most important and the 1:2 zone the second largest and stable. The structure of the 1:2 zone and of higher zones is not established. Known examples of the 1:2 systems (Efsthathiou, Sadovskii, and Zhilinskiĭ, 2007; Efsthathiou *et al.*, 2008) suggest that a relatively small subset of them may have fractional monodromy.

D. Structure of the paper

Careful definition of our subject and scope (cf. Sec. VIII.B) results in a field which continues to be important both to the particular family of fundamental physical system (2) and beyond it and which remains large and rich in substance. Understanding the ideas and results of the global analysis requires certain concretization of tools and constructions involved, which we discuss with a concrete example. With regard to these techniques, two aspects are notable: their necessity for the analysis of the concrete system and their universality within a broader context of dynamical systems.

Thus normalization and reduction of the Keplerian S^1 symmetry is in many ways similar to those in the study of molecular vibrations where n -shells of the hydrogen atom correspond to the so-called *polyads*. Furthermore, resonances and related techniques that we encounter here (Secs. IV and V) are commonly found in molecules. All these aspects are intricately connected to concepts of dynamical symmetry which were developed extensively for the hydrogen atom and its perturbations (cf. Sec. VIII.C.4). In the presence of typically nonfree actions of the dynamical symmetries associated to the resonance(s) and of the exact given symmetries, singular reduction and required invariant theory (Sec. IV) is the most universal single method discussed in this review. Its importance goes far beyond our examples. Furthermore, the geometry of the reduced phase spaces of our system is by far not exceptional. The range of systems with the (reduced) phase space $S^2 \times S^2$ goes from systems with several coupled angular momenta [cf. Sadovskii and Zhilinskiĭ (1999); Hansen *et al.* (2007)] to systems of interacting laser beams in nonlinear optics (Sugny *et al.*, 2009). Finally, many of our examples have Hamiltonian monodromy, a basic global nontrivial property found in many different systems. Even though it is crucial to any qualitative description, monodromy is not widely known and understanding its potential as a physical phenomenon is only beginning (Delos *et al.*, 2008, 2009; Lagrange *et al.*, 2010). A detailed explanation of various basic and advanced examples of monodromy in Secs. II.D and VI should be greatly beneficial.

In Sec. II we continue with a review of the mathematical concepts and tools required for our study. We illustrate them using the results on the stratification of the

⁴Efsthathiou, Sadovskii, and Zhilinskiĭ (2007) denoted the E -scaled fields as (f_e, f_b, g) .

1:1 zone (Efsthathiou, Sadovskii, and Zhilinskiĭ, 2007; Schleif and Delos, 2007; Efsthathiou *et al.*, 2009) and the properties of the different types of systems in this zone in Sec. III.

In Sec. IV we detail the standard two-stage normalization and reduction procedure. At the first stage, after the Keplerian reduction, we uncover resonances and introduce zones. At the second stage, we reduce Pauliean symmetry and construct the second-order integrable approximation to the original system. Again the 1:1 zone is used as an example.

In Sec. V we analyze our integrable approximation for the 1:1 zone systems. We consider the energy-momentum map for different parameters a^2 and d , describe the respective fibration, and find all qualitatively different bifurcation diagrams. Following Efsthathiou, Sadovskii, and Zhilinskiĭ (2007) and Efsthathiou *et al.* (2009), this provides a classification of all perturbed systems under consideration (Sec. III). We discuss and compute monodromy, a specific aspect of this classification, in Sec. VI.

In Sec. VII we consider how to use the integrable approximation in order to compute the (approximate) joint quantum spectra of our system and construct lattices representing quantum states within the regular domain of classical energy-momentum values. We relate the resulting lattices to the 1:1 zone classification of Efsthathiou *et al.* (2009).

The literature on the subject is reviewed in two ways. The most relevant references are cited immediately in the text. A broader discussion of the literature is given in Sec. VIII. The notation used is summarized in the List of Symbols.

II. BASIC MATHEMATICAL CONCEPTS

Looking back at the rich history of the subject (see Sec. VIII), it is most natural to ask why a basic global description of this fundamental system is being developed at such a late stage. This seems to happen not due to the absence of interest—at least not in the mid-1980s and 1990s, when the perturbation theory of this system was the subject of intense research—but to an extent due to the lack of an appropriate and timely combination of mathematical tools and ideas.

Here, along with providing further details of the description of our system, we give an informal introduction to the basic concepts from the theory of Hamiltonian dynamical systems used throughout the study, notably the geometry of the reduction of Lie symmetries, and the elementary topology of toric fiber bundles.

A. Regularization, first integrals, and their flows

Working directly with the original 3-DOF system with the Hamiltonian (2) is inconvenient due to the $1/r$ singularity, and it is quite common to regularize it first by lifting to a 4-DOF system. To this end, we apply the Kustaanheimo-Stiefel (KS) map as explained in Sec. IV.A.1. The regularized 4-DOF system possesses an ad-

ditional strict integral ζ . The construction of a completely integrable approximation to the perturbed system is detailed in Sec. IV. In addition to the energy \mathcal{H} and the KS integral ζ , the integrable approximation has two more first integrals N and μ .

The integrals (N, μ, ζ) and energy \mathcal{H} are Hamiltonian functions on the phase space \mathbb{R}^8 of the regularized system, and we can study the Hamiltonian flows of the respective vector fields. The flows of (N, μ, ζ) are periodic with period 2π and define three different S^1 symmetry actions on \mathbb{R}^8 . The symmetries corresponding to N and ζ are called Keplerian and KS symmetries, respectively, while the symmetry defined by μ will be called Pauliean (see Secs. II.B.2 and IV.D). Following the established terminology in the theory of integrable Hamiltonian systems we call integrals such as (N, μ, ζ) with periodic flows of constant period, *momenta*, or *actions*. Their S^1 orbits serve to establish three *global* angle coordinates on all regular Liouville tori T^4 in \mathbb{R}^8 . The fourth angle coordinate on these tori is, in general, defined only *locally* on and in a sufficiently small open neighborhood of a given torus (see Sec. VI). In other words, (N, μ, ζ) are global actions, while the fourth action can only be defined locally.

We can always reduce the S^1 orbits of (N, μ, ζ) to the original phase space \mathbb{R}^6 using the KS regularization map. In that way, we construct S^1 orbits of actions on \mathbb{R}^6 associated with N and μ , while the ζ orbits become points in \mathbb{R}^6 . The nonperiodic Hamiltonian flow associated with \mathcal{H} can be studied similarly.

B. Geometry of the reduction map

1. First or Keplerian reduction

The integrable approximation to our system and the reduced energy \mathcal{H} are obtained in two steps. The first step, at which Keplerian symmetry is reduced, is common to all perturbed two-body systems and its geometry was understood quite well due to a combined effort of mathematicians and physicists.⁵ For finite energies $E < 0$, the Keplerian symmetry action associated to N is free, all its orbits are circles S^1 , and any point on the first reduced phase space $S^2 \times S^2$ lifts to one such circular orbit. This is regular reduction. The 2-DOF first reduced system on the phase space $S^2 \times S^2$ (for $N=n>0$) is described using six invariants (see Sec. IV.C),

$$\mathbf{x} = (x_1, x_2, x_3)^T \quad \text{and} \quad \mathbf{y} = (y_1, y_2, y_3)^T,$$

of the Keplerian symmetry action satisfying two relations,

⁵See, e.g., Guillemin and Sternberg (1990), Cushman (1992), and Cordani (2003).

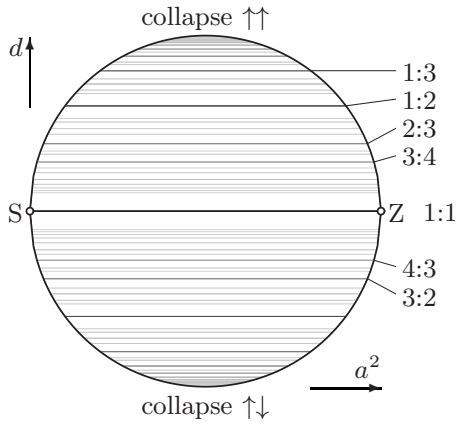


FIG. 3. $k_-:k_+$ resonant systems in the constant- s nonzero section D_s of the set of all possible perturbations [Eq. (2)] of the hydrogen atom by small static electric and magnetic fields \mathbf{F} and \mathbf{G} .

$$\mathbf{x}^2 = x_1^2 + x_2^2 + x_3^2 = \mathbf{y}^2 = y_1^2 + y_2^2 + y_3^2 = (n/2)^2. \quad (7)$$

(\mathbf{x}, \mathbf{y}) are appropriately rotated Fock vectors $\frac{1}{2}(\mathbf{K} \pm \mathbf{L})$, where \mathbf{K} is the eccentricity (or Laplace-Runge-Lenz⁶) vector and \mathbf{L} is the angular momentum. They generate a Lie-Poisson algebra with the standard $\mathfrak{so}(3) \times \mathfrak{so}(3) = \mathfrak{so}(4)$ structure: for any functions ξ and χ of (\mathbf{x}, \mathbf{y}) we have the Poisson bracket

$$\{\xi, \chi\}_{\mathbf{x}, \mathbf{y}} = \mathbf{x} \cdot [\nabla_{\mathbf{x}} \xi \times \nabla_{\mathbf{x}} \chi] + \mathbf{y} \cdot [\nabla_{\mathbf{y}} \xi \times \nabla_{\mathbf{y}} \chi]. \quad (8)$$

2. Resonant Pauliean symmetry S^1 and zones

For any (\mathbf{Q}, \mathbf{P}) -polynomial perturbation of the fixed center Kepler system and in particular for the one in Eq. (2), the lowest nontrivial term in the first reduced Hamiltonian defines a linear flow on $S^2 \times S^2$. This has been implied already by Pauli (1926). Specifically, to the lowest nontrivial order, the first reduced energy is

$$\Delta E^{(1)} = \omega_- x_1 + \omega_+ y_1, \quad (9)$$

where for our system we show in Sec. IV.C that

$$\omega_{\pm} = \sqrt{(g \pm f_b)^2 + f_e^2} = s \sqrt{1 \pm 2d}. \quad (10)$$

The Hamiltonian flow generated by $\Delta E^{(1)}$ on $S^2 \times S^2$ is a simultaneous rotation of the \mathbf{x} and \mathbf{y} spheres around axes x_1 and y_1 with respective frequencies ω_- and ω_+ . In the fixed- s parameter disk D_s (see Fig. 3), systems with frequency ratio

$$\frac{\omega_-}{\omega_+} = \sqrt{\frac{1-2d}{1+2d}} \quad (11)$$

are represented by a constant- d (horizontal) segment.

⁶One can probably attach several more names to the eccentricity vector \mathbf{K} [see p. 400 of Cushman and Bates (1997), and also Goldstein (1975, 1976) and Guillemin and Sternberg (1990)].

We come to the central point of the analysis. Assuming that ω_- and ω_+ are incommensurate, we may normalize our system completely with respect to $\Delta E^{(1)}$. Then the momenta x_1 and y_1 become two first integrals of the system and we can use them as actions and so have global action-angle coordinates. However, there are *resonances*. Thus for orthogonal fields (line SZ in Fig. 3) we have $d=0$ and the ratio is 1:1. Furthermore, it is clear that near resonances a blind complete normalization would be useless for understanding the dynamics because it discards the effects of the nearby resonance. We come to the concept of a resonance zone (Efsthathiou, Sadovskii, and Zhilinskiĭ, 2007).

Suppose that frequencies ω_- and ω_+ are close to a $k_-:k_+$ resonance of order⁷ k_-+k_+ , where k_- and k_+ are positive integers with $\gcd(k_-, k_+) = 1$; then

$$\omega_- k_+ - \omega_+ k_- \approx 0. \quad (12)$$

Introducing momenta

$$\mu = k_- x_1 + k_+ y_1 \quad \text{and} \quad \nu = k_- x_1 - k_+ y_1, \quad (13)$$

which define two periodic flows on $S^2 \times S^2$, we rewrite

$$\Delta E^{(1)} = \frac{1}{2} \left(\frac{\omega_-}{k_-} + \frac{\omega_+}{k_+} \right) \mu + \frac{1}{2} \left(\frac{\omega_-}{k_-} - \frac{\omega_+}{k_+} \right) \nu := \omega(\mu + \delta\nu), \quad (14)$$

where $\delta \ll 1$ is called *detuning* and ω is the frequency of the Pauliean motion. In particular, for the 1:1 resonance we have $\mu = x_1 + y_1$ and

$$\frac{\omega}{s} = 1 - \frac{d^2}{2} + O(d^4), \quad \delta = d + O(d^3),$$

$$\omega_{\pm} = 1 \pm d + O(d^2).$$

The principal term $\omega\mu$ in $\Delta E^{(1)}$ defines a periodic Hamiltonian flow. We call its S^1 action on $S^2 \times S^2$ the resonant Pauliean symmetry.

The main proposition of Efsthathiou, Sadovskii, and Zhilinskiĭ (2007) is that all systems within a $k_-:k_+$ zone (and not only those with exact $k_-:k_+$ resonance) should be normalized with respect to such S^1 symmetry. The width of the zone $\delta_{\max} > 0$ is the maximum value of $|\delta|$ for which the $k_-:k_+$ resonant approximation to the dynamics is regarded to be meaningful.

Note that it is possible that resonances of the linear (Pauliean) approximation, or at least the 1:1 resonance, were known before but remained ignored. Recently the resonances and respective quantum algebras were studied comprehensively by Karasev and Novikova (2005). Efsthathiou, Sadovskii, and Zhilinskiĭ (2007) added the zone concept. The main advantage of the zones is that systems within each zone are described on the basis of the same resonant approximation and can be considered and classified as a family. It may be possible to cover a

⁷The order of a nonreducible rational k_1/k_2 is $|k_1| + |k_2|$. Because k_{\pm} are positive [cf. Eqs. (10) and (12)] and mutually prime, the order of the $k_-:k_+$ resonance equals $k_- + k_+$.

large part of the parameter space by a small number of zones, i.e., a number of such families. The width of a zone is likely to decrease with the order (see footnote 7) of the resonance, so the 1:1 zone, which represents nearly orthogonal fields, is the largest. This zone is centered on the ZS line with $d=0$ (Fig. 3) and its width is given by $d_{\max} > 0$.

3. Singular reduction of Pauliean symmetry

Because the second reduction depends on the concrete form of the perturbation (2), it was studied largely by atomic physicists who relied in their classical mechanical analysis on action-angle-like coordinates⁸ and corresponding normalization techniques widely used in applied dynamical systems of the time, especially in astronomy. As the standard example of the asymmetric Euler top⁹ shows, action-angle variables are not optimal for the global description of all possible motions in the system, while they may be quite appropriate for local results, such as small planetary orbit corrections. As shown in Sec. IV.D.2, the second reduced 1-DOF system with the Hamiltonian \mathcal{H} is topologically similar to an Euler top (see footnote 9). Hence its global analysis requires the use of Euler-Poisson techniques and invariant theory (Cushman and Bates, 1997; Efsthathiou and Sadovskii, 2005). Although physicists uncovered the Euler top analogy (Sec. VIII.C.5) the adaptation of the corresponding techniques did not follow, and the main casualty was geometry.

Any Pauliean S^1 symmetry action is *not free*. This can be seen most simply for the axial spatial symmetry $SO(2)$ of the Zeeman limit (Michel and Zhilinskiĭ, 2001a). Such action has four fixed points on $S^2 \times S^2$ (Sadovskii *et al.*, 1996; Sadovskii and Zhilinskiĭ, 1998; Michel and Zhilinskiĭ, 2001a). A nonfree action requires singular reduction.¹⁰ The geometry of the resulting reduced spaces depends on the properties of the specific Pauliean S^1 symmetry action that we reduce and in particular on the specific resonance. For each resonance, the family of reduced spaces is parametrized by the values m of μ . These spaces are not all the same; some may be different topologically, while others may be singular.

Our second reduced phase spaces $P_{n,m}$ (for $n > 0$), i.e., the spaces of orbits of the combined T^2 action associated

⁸See, e.g., Delos *et al.* (1983a, 1983b, 1984) as well as Deprit *et al.* (1996); Main *et al.* (1998); Salas *et al.* (1998); Salas and Lanchares (1998); and Berglund and Uzer (2001).

⁹A Euler top (rotor) is a freely rotating rigid body. It is called asymmetric when its three moments of inertia differ; its reduced phase space is a smooth S^2 equipped with a Lie-Poisson algebra $\mathfrak{so}(3)$ generated by the components of angular momentum. Using action-angle variables for this system (Kozlov, 1974; Postell and Uzer, 1990; Fassò, 1996) requires several charts in order to cover the whole phase space.

¹⁰Singular reduction, as an extension of the regular case of free actions by Marsden *et al.* (1990), was introduced by Arms (1986, 1988), Arms *et al.* (1990, 1991), and Cushman and Sjamaar (1991) [see also Cushman and Bates (1997), Ortega and Ratiu (1998), and Efsthathiou and Sadovskii (2005)].

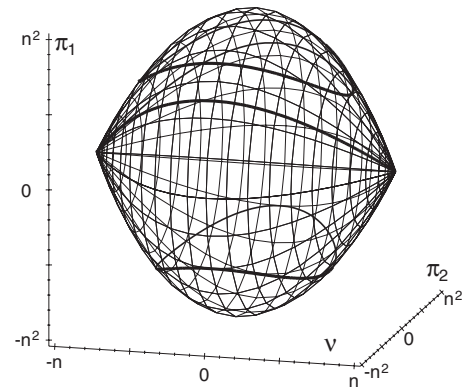


FIG. 4. Second reduced phase space $P_{n,0}$ with $n > 0$ of the 1:1 systems is a two-sphere with two isolated conical singular points. Adapted from Cushman and Sadovskii, 2000.

with momenta N and μ , are single points for $|m|=m_{\max}$ and have S^2 topology for $|m| < m_{\max}$. This makes the second reduced system with $|m| < m_{\max}$ similar to the Euler top (see footnote 9). However, under the Pauliean reduction map, two of the four fixed points become $P_{n,\pm m_{\max}}$, while the images of the other two end up on spaces $P_{n,\pm m_{\text{crit}}}$ with $m_{\text{crit}} < m_{\max}$ which are not smooth as a result.

Thus for the 1:1 systems, $m_{\max}=n$ and $m_{\text{crit}}=0$, and the two fixed points map to two isolated conical singularities of the singular space $P_{n,m=0}$ (see Fig. 4), while all other spaces with $0 < |m| < n$ are smooth (see Fig. 5). Understanding this geometry and the specifics of the $m=0$ space was achieved by Cushman and Sadovskii (1999, 2000).

C. The study of the integrable fibration

Two constructions, the energy-momentum map \mathcal{EM} and the bifurcation diagram \mathcal{BD} , are indispensable to any global analysis (Cushman and Bates, 1997; Efsthathiou and Sadovskii, 2005). We explain them below.

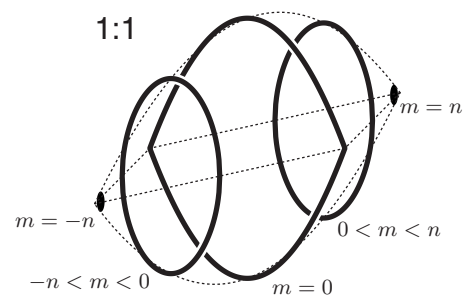


FIG. 5. Successive constant- m sections of the orbit space of the action of the 1:1 resonant Pauliean symmetry S^1 on the reduced phase space $S^2 \times S^2$ for fixed Keplerian action $n > 0$; each section represents a projection of a reduced phase space $P_{n,m}$. Such orbit spaces are discussed in detail by Michel and Zhilinskiĭ (2001a) [see also Sadovskii *et al.* (1996) and Cushman and Sadovskii (2000)].

1. Energy-momentum map \mathcal{EM}

First integrals (N, μ, \mathcal{H}) take values (n, m, h) with $n \geq 0$ and $|m| \leq \frac{1}{2}(k_+ + k_-)n$, while the KS integral ζ is always 0. We define the energy-momentum map¹¹

$$\begin{aligned} \mathcal{EM}: \mathbb{R}^8|_{\zeta=0} &\rightarrow \mathbb{R}^3: (q, p) \mapsto (N(q, p), \mu(q, p), \mathcal{H}(q, p)) \\ &= (n, m, h), \end{aligned} \tag{15a}$$

which maps invariant manifolds (in the KS space restricted to $\zeta=0$) of the integrable approximation to points in \mathbb{R}^3 . We also use the n -shell map,

$$\mathcal{EM}_n: \mathbb{S}^2 \times \mathbb{S}^2 \rightarrow \mathbb{R}^2: (\mathbf{x}, \mathbf{y}) \mapsto (\mu(\mathbf{x}, \mathbf{y}), \mathcal{H}(\mathbf{x}, \mathbf{y})) = (m, h), \tag{15b}$$

which maps invariant manifolds in the first reduced phase space $\mathbb{S}^2 \times \mathbb{S}^2$ (on which $N=n>0$ is fixed) to points in \mathbb{R}^2 . Images of \mathcal{EM}_n are constant- n sections of the \mathcal{EM} image. Furthermore, we can pull back the \mathcal{EM} map (15a) to the original phase space \mathbb{R}_*^6 and define

$$\mathcal{EM}_{3D}(\mathbf{Q}, \mathbf{P}) = \mathcal{EM}(q, p) \tag{15c}$$

for any (q, p) such that $\text{KS}(q, p) = (\mathbf{Q}, \mathbf{P})$.

2. Critical points of \mathcal{EM}

At regular points (q, p) , the Jacobian of map \mathcal{EM} (15a) has rank 3 (maximal); the rank cannot vanish on $\mathbb{R}^8 \setminus \{0\}$ because the Keplerian symmetry acts freely on $\mathbb{R}^8 \setminus \{0\}$ and this implies that the Hamiltonian vector field X_N corresponding to N and also dN do not vanish there. So we can have critical points $(q, p)_{\text{crit}} \neq 0$, i.e., for $n > 0$, at which the rank drops to either 2 or 1 and which we call points of rank 2 or 1. Linearizing at $(q, p)_{\text{crit}}$ we can analyze their stability. This analysis can be done either in the full phase space or after successive reduction of symmetries in Sec. IV. We make a few basic observations here and in the next section.

a. Critical points of rank 2

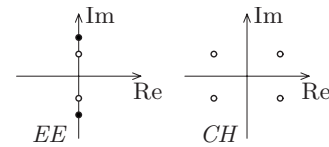
When the rank of the Jacobian of the \mathcal{EM} map at $(q, p)_{\text{crit}}$ is 2, the Hamiltonian vector field X_H is a linear combination of X_N and X_μ . Thus X_H is tangent to the \mathbb{T}^2 orbit of X_N and X_μ that goes through $(q, p)_{\text{crit}}$. This \mathbb{T}^2 orbit is a dynamically invariant set and all points on it are rank 2 critical points. Its stability in the normal direction is determined by an appropriately selected 2×2 block of the Hamiltonian matrix of the linearized equations of motion. Alternatively, the normal stability can be determined by reducing the \mathbb{T}^2 symmetry generated by X_N and X_μ , thus descending to $P_{n,m}$ where the \mathbb{T}^2 orbit becomes an equilibrium and we can study the 2×2 Hamiltonian matrix of the linearized equations of motion. Its eigenvalues $\pm\lambda$ may be imaginary or real,

depending on whether the equilibrium is elliptic or hyperbolic. Since we have two other symplectic two-planes and two respective parameters (n, m) , such \mathbb{T}^2 orbits of rank 2 critical points form typically two-parameter families. They look like two-surfaces in the image of \mathcal{EM} and thus become one-dimensional curves in the image of \mathcal{EM}_n .

b. Critical points of rank 1

At these points the vector fields X_H, X_N , and X_μ are collinear. Thus X_H is tangent to the \mathbb{S}^1 orbit of X_N that goes through $(q, p)_{\text{crit}}$. This \mathbb{S}^1 orbit is a dynamically invariant set and all points on it are rank 1 critical points. Such \mathbb{S}^1 orbits form typically one-parameter families. Their stability in the normal direction is determined by an appropriately selected 4×4 block of the Hamiltonian matrix of the linearized equations of motion. Alternatively, the normal stability can be determined by reducing the \mathbb{S}^1 symmetry generated by X_N , thus descending to $\mathbb{S}^2 \times \mathbb{S}^2$ where the \mathbb{S}^1 orbit becomes an equilibrium and we can study the 4×4 Hamiltonian matrix of the linearized equations of motion.

Linear stability is determined by the four eigenvalues of this matrix. In 2-DOF systems, four typical arrangements of the eigenvalues¹² occur: elliptic-elliptic (EE) and complex hyperbolic (CH) whose eigenvalues are illustrated below



as well as hyperbolic-hyperbolic and elliptic-hyperbolic.

Nondegenerate¹³ equilibria o of integrable 2-DOF Hamiltonian systems with the Hamiltonian H and first integral J can be classified in terms of the respective linearly independent quadratic parts of the linearization at o ,

$$\begin{pmatrix} H^{(2)} \\ J^{(2)} \end{pmatrix} = \begin{pmatrix} a & b \\ c & d \end{pmatrix} \begin{pmatrix} A \\ B \end{pmatrix} \quad \text{with } \det \begin{pmatrix} a & b \\ c & d \end{pmatrix} \neq 0,$$

where (A, B) can be of one of the following four types (see footnote 13)

Equilibrium type	A	B
Elliptic-elliptic (EE)	$(p_1^2 + q_1^2)/2$	$(p_2^2 + q_2^2)/2$
Elliptic-hyperbolic (EH)	$(p_1^2 + q_1^2)/2$	$p_2 q_2$
Hyperbolic-hyperbolic (HH)	$p_1 q_1$	$p_2 q_2$
Focus-focus (FF)	$p_1 q_1 + p_2 q_2$	$p_1 q_2 - p_2 q_1$

in appropriate symplectic coordinates (q_1, p_1, q_2, p_2) . For

¹¹The historical convention for the name ‘‘energy-momentum’’ is opposite to that for the value, which has the momentum value m before that of energy h , so that m follows the abscissa.

¹²See classification of symplectic matrices by Williamson (1936).

¹³Definition of nondegeneracy and complete linear classification of equilibria can be found in Bolsinov and Fomenko (2004).

all types except FF the type of o corresponds to that given by the eigenvalues of the Hamiltonian matrix at o . For nonzero $a, b \in \mathbb{R} \setminus \{0\}$, the FF case corresponds to CH; this is always the case in our system.¹⁴

Only EE and FF equilibria occur in our system. Because their matrix factorizes in two 2×2 blocks, the EE families (as well as HH and EH) are typically intersections of respective two-parameter families of rank 2 critical values. In the range of \mathcal{EM} , a critical set of type EE is a line of intersection of two critical two-surfaces representing rank 2 elliptic critical points. In the constant- n section, i.e., in the range of \mathcal{EM}_n , this gives a point of intersection of two lines. The FF family forms a thread in the image of \mathcal{EM} that is (excluding its possible endpoints) *isolated*. In the image of \mathcal{EM}_n this gives an isolated point.

c. Restrictions due to symmetry and topology

Let H be a Morse-type Hamiltonian function on $S^2 \times S^2$. Four is the minimum number of stationary points (equilibria) such H can have (Sadovskii and Zhilinskiĭ, 1998; Michel and Zhilinskiĭ, 2001a; Symington, 2003). On the other hand, we have a specific Pauliean symmetry S^1 , which brings drastic simplification into the system: if H , like the second normalized Hamiltonian \mathcal{H} , is invariant with respect to this S^1 symmetry, the equilibria must be located at the fixed points of the S^1 action. The number of fixed points is again four. It follows that our system has on $S^2 \times S^2$ exactly four nondegenerated equilibria.

Morse theory also restricts the indices of the four equilibria (Sadovskii and Zhilinskiĭ, 1998) to 4, 2, 2, and 0. Points of index 4 and 0 (or Hessian signature ++++ or ----) are necessarily of type EE. They correspond to a maximum and a minimum¹⁵ and, as can be seen from Eq. (14), to maximal and minimal values $m = \pm n$ of momentum μ . Index 2 points can be either EE (with frequencies of opposite signs and signature +-+-) or CH. For the 1:1 resonance, they correspond to $m=0$.

The reason why EH and HH points cannot exist is again due to the Pauliean symmetry. EH does not have the correct index. To exclude HH, consider the specific S^1 action induced by the Pauliean symmetry on the symplectic $\mathbb{R}_x^2 \times \mathbb{R}_y^2$ neighborhood of the fixed point on $S^2 \times S^2$. The action is diagonal (see Sec. IV.D.1) and in each symplectic \mathbb{R}^2 plane it is a rotation about the origin which permits only elliptic-elliptic or focus-focus points.

3. Fibers of the energy-momentum map \mathcal{EM}

Fibers $\mathcal{EM}^{-1}(n, m, h)$ of \mathcal{EM} will be denoted $\Lambda_{n,m,h}$. If Λ has several connected components, the latter will be

¹⁴If $b=c=0$, the eigenvalues are $(\pm a, \pm a)$ and the FF equilibrium is not CH. This may happen in the presence of symmetries, as in the example of the spherical pendulum (Efsthathiou, 2005).

¹⁵In most configurations except near the collapse (Fig. 3), these elliptic equilibria are global maximum and minimum.

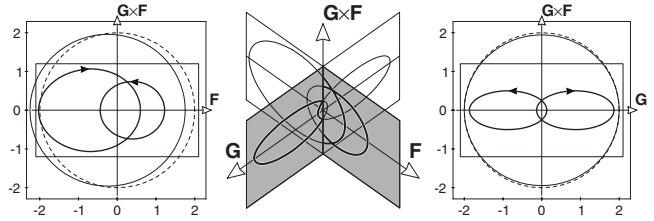


FIG. 6. Kepler ellipses for $a^2 = \frac{3}{4}$, $d=0$ (orthogonal fields), $s \approx 0.2$, and $n \approx 1$ projected in the physical space \mathbb{R}^3 . Rectangles set the scale of the center plot; dashed and solid circles mark limits of the unperturbed and full potential; arrows on the orbits indicate Keplerian flow. From Sadovskii and Zhilinskiĭ, 1998.

distinguished as Λ' , Λ'' , etc. A regular fiber of \mathcal{EM} or \mathcal{EM}_{3D} is a union of regular tori T^4 or T^3 , respectively. A critical fiber $\mathcal{EM}^{-1}(c)$ over a critical value c contains at least one critical point $(q, p)_{\text{crit}}$. Such a fiber has at least one connected component Λ_c which is not a regular torus, except in certain degenerate cases where the critical value c appears at the boundary of the bifurcation diagram \mathcal{BD} and $\mathcal{EM}^{-1}(c)$ differs from the nearby fibers in the number of connected components. When describing fibers, we drop their Keplerian and KS cycles associated with integrals n and ζ and describe only fibers of \mathcal{EM}_n (15b) in $S^2 \times S^2$ from which fibers in the original phase space \mathbb{R}_*^6 or in the KS space $\mathbb{R}^8|_{\zeta=0}$ can be obtained by taking into account the respective S^1 or T^2 orbits over each point in $S^2 \times S^2$. In most cases this means taking the Cartesian product of the \mathcal{EM}_n fibers with S^1 or T^2 , respectively. In this section, we describe what kinds of fibers are to be found. These are basic types for a 2-DOF system.

a. Relative equilibria (RE)

Lower dimensional (non-Lagrangian) tori that are purely group orbits of the Lie symmetries of the system are its relative equilibria.¹⁶ After reduction of these symmetries, RE become equilibria of the reduced system.

When Λ_c consists of elliptic critical points of rank 2, it is a T^2 Keplerian-Pauliean RE in \mathbb{R}_*^6 , i.e., a T^2 defined entirely by the combined periodic flows of Hamiltonian vector fields X_N and X_μ of momenta N and μ . On $S^2 \times S^2$, such RE is represented as an S^1 Pauliean orbit, and on $P_{n,m}$ it is a regular point which is an equilibrium of the second reduced system. They form families with two parameters n and m .

When Λ_c consists of EE critical points of rank 1, it is a purely Keplerian RE S^1 in \mathbb{R}_*^6 called Kepler ellipse (Flöthmann et al., 1994; Sadovskii and Zhilinskiĭ, 1998). There are four families of such ellipses, each parametrized by n (see Fig. 6); on $S^2 \times S^2$, we have four equi-

¹⁶For a standard definition of RE, see Appendix 5C of Arnol'd (1989) and Chap. 3.3 of Arnol'd, Kozlov, and Neishtadt (1988).

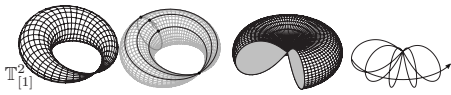


FIG. 7. Two \mathbb{R}^3 embeddings of a singly pinched torus $\mathbb{T}^2_{[1]}$.

librium points.

b. Singular fibers

If Λ_c contains hyperbolic points of rank 2 or CH points of rank 1, it is typically (excluding degenerate cases) a *singular* three-dimensional variety in \mathbb{R}^6 . It includes both critical and regular points. The former constitute an unstable RE, while the latter belong to the stable and unstable manifolds of that RE. Reducing the Keplerian symmetry, we obtain two-dimensional singular varieties in $\mathbb{S}^2 \times \mathbb{S}^2$ shown in Figs. 7 and 8.

A singly pinched torus $\mathbb{T}^2_{[1]}$ is a torus with one fundamental loop contracted to a point which is a FF equilibrium. In a space \mathbb{R}^3 it can be represented in two different ways (Fig. 7) which are the same in \mathbb{R}^4 . A doubly pinched torus $\mathbb{T}^2_{[2]}$ (Fig. 8, left) is a degenerated singular fiber which contains two FF points, i.e., has two pinches. A curled torus $\mathbb{T}^2_{[1/2]}$ and bitorus \mathbb{T}^2_{bi} are the two simplest hyperbolic two-dimensional singular varieties which can be obtained as a cylinder on a figure eight whose ends are glued with or without a twist, respectively. Both contain hyperbolic points of rank 1 which form a Pauliean \mathbb{S}^1 RE on $\mathbb{S}^2 \times \mathbb{S}^2$.

4. \mathcal{BD} as stratified unfolded \mathcal{EM} image

In order to uncover the topology of an integrable fibration we go through a number of steps: we find the base of the fibration, reconstruct individual fibers, and establish connections between them. The combined result of the first two steps can be represented in the form of the stratified image of the \mathcal{EM} map (Efsthathiou, Sadovskii, and Zhilinskiĭ, 2007; Efsthathiou *et al.*, 2009), which is otherwise called bifurcation diagram¹⁷ (Bolsinov and Fomenko, 2004), critical locus (Cushman and Bates, 1997), or base diagram (Symington, 2003) and which will be denoted \mathcal{BD} . In comparison the new element in our concept of \mathcal{BD} is that we consider it as a multisheeted covering surface, similar to a Riemann surface. This construction is essential to our study and we give more detail.

The base of the fibration is, of course, the image of the \mathcal{EM} map in Eqs. (15). It is a domain in \mathbb{R}^3 . Within the base, we distinguish regular and critical values. The set of all regular values or regular stratum is a union of open domains in \mathbb{R}^3 , whose closure consists of critical values. The latter are further distinguished by the type of connected components of their preimages and form

¹⁷A bifurcation diagram shows how the topology of the fibers changes as their image moves in the range of the \mathcal{EM} map.

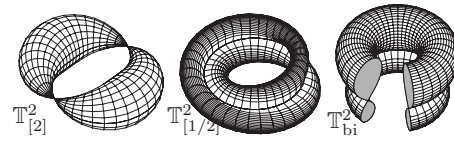


FIG. 8. Possible \mathbb{R}^3 representations of singular fibers (left to right): doubly pinched torus, curled torus, and bitorus.

critical strata. We focus on the topology of critical and regular strata.

We first look for the \mathcal{EM} values which lift to fibers with $k > 1$ connected components, and if they exist, we construct an unfolding or covering surface S of the base. As a simple example, consider the case of a 2-DOF system with \mathcal{EM} values (m, h) shown in Fig. 9, right, where the set of all regular values (left side projection) is shaded gray, and within it, values with $k=2$ and $k=1$ are distinguished by dark and light shades. The corresponding unfolded surface S (bottom projection) consists of a single regular sheet. Within it, the set of all regular values is an open two-ball whose points lift to single regular tori \mathbb{T}^2 . The upper boundary of the $k=2$ subset is made up of critical values c such that $\mathcal{EM}^{-1}(c)$ consists of a single regular torus; such a boundary is called a caustic (Efsthathiou, Sadovskii, and Zhilinskiĭ, 2007). Caustics can be structurally stable in the presence of a symmetry that forbids specific resonances, e.g., for parallel fields.

A different 2-DOF example is given in Fig. 10. In this case, the unfolded \mathcal{EM} image S consists of several open regular domains, which are glued along a common boundary whose points c lift to bitori \mathbb{T}^2_{bi} . This example illustrates the concepts of cells and walls.¹⁸

We work normally with unfolded lower cells, called cells for brevity. Such a cell is defined as the closure of a connected domain of regular values of the unfolding surface S ; it intersects other cells only along a common boundary in S , such as the line of critical values c . Any common boundary of several cells is a wall. In the 1:1 zone, we encounter only walls of this kind. For 1:2 and higher resonances, Nekhoroshev *et al.* (2006) discovered walls of a different kind, called passable. Such walls are formed by lines of “weakly” critical values c which lift to a hyperbolic singular fiber called a curled torus. They exist in the 1:2 zone (Efsthathiou, Sadovskii, and Zhilinskiĭ, 2007).

D. Global action-angle variables and monodromy

So far we have focused on covering the set of regular \mathcal{EM} values by disconnected regular interiors of several cells. This is the basic consequence of the presence of hyperbolic fibers called bitori. For each cell, we want to describe all Liouville tori in the preimage $\mathcal{EM}^{-1}(\mathbb{R})$ of its regular interior \mathbb{R} using one set of smooth action-angle

¹⁸Nekhoroshev *et al.* (2006) distinguished upper and lower cells situated in the full space and the base of the fibration, respectively [see also Bolsinov and Fomenko (2004)].

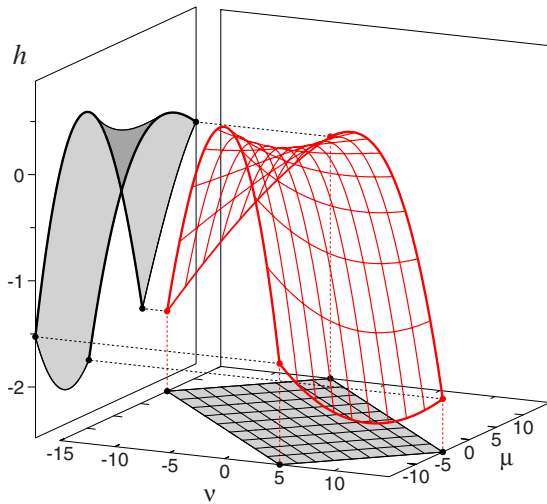


FIG. 9. (Color online) Example of a self-overlapping \mathcal{BD} with a caustic from Efsthathiou, Sadovskii, and Zhilinskiĭ (2007): the \mathcal{EM} map image is shown projected on the left vertical plane with coordinates (m, h) .

coordinates. Physicists prefer such coordinates because they make quantization simple (see Sec. II.E), give a unified description of large groups of states, and are at the foundation of many perturbation theory variants, notably the methods by Birkhoff. Simple systems with global actions, such as a nonresonant harmonic oscillator, are used widely as models. Unfortunately, the study of the domain of such coordinates (in \mathbb{R}^6) is often ignored. Aggravated by the complexity of the coordinates in use, this is admittedly far from trivial.

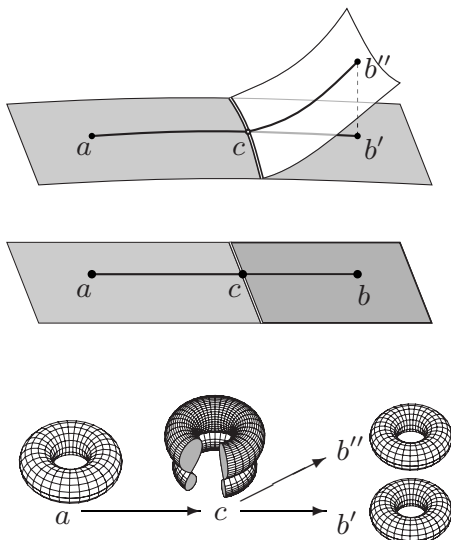


FIG. 10. Overlapping lower cells in the \mathcal{EM} image (middle) and their unfolding surface (top). Double line marks branching boundary; bold solid line shows a path, which corresponds to the change in the topology of the fiber illustrated on the bottom. Points a , b' , b'' , and c lift each to a single connected component; b' and b'' correspond to the same \mathcal{EM} value b ; the graph $a \rightarrow c \rightarrow (b', b'')$ is what Bolsinov and Fomenko (2004) called the “B atom.” From Sadovskii and Zhilinskiĭ, 2007.

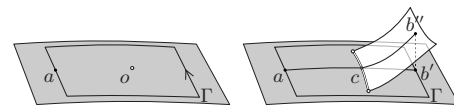


FIG. 11. Nonsimply connected cells: the preimage of the isolated critical value o (left) is a pinched torus; the nontrivial path Γ is used to study monodromy: other points and paths are similar to those in Fig. 10. From Efsthathiou, Sadovskii, and Zhilinskiĭ, 2007.

The task can be systematized by pulling actions $I(q, p)$ back to \mathbb{R} , i.e., by considering them as functions $\mathcal{I}(m, h)$. If global actions exist, then $\mathcal{I}(m, h)$ can be defined as smooth single valued functions on the entire \mathbb{R} . It is clear that a nontrivial topology of \mathbb{R} and in particular the situation when \mathbb{R} is not simply connected should be a first alert. We consider this in detail.

The important specific of action-angle coordinates is that they are only guaranteed (under certain general conditions by the Arnol’d-Liouville theorem¹⁹) to exist locally in a neighborhood of a regular torus. This was well understood by mathematicians, who searched systematically for conditions under which these coordinates can be extended (Nekhoroshev, 1969, 1972). Duistermaat (1980) turned the question around and defined the simplest topological obstruction to global action-angle variables which he called Hamiltonian monodromy and which we call monodromy²⁰ for brevity.

1. Basic case of Hamiltonian monodromy

In the simplest case (Duistermaat, 1980), which has many concrete physical realizations,²¹ monodromy occurs in a 2-DOF system with a nondegenerate FF equilibrium. As explained in Sec. II.C.3 and shown in Fig. 11, left, such equilibrium is typically isolated; it is the singular point of the singly pinched torus $\mathbb{T}_{[1]}^2$ which is represented as an isolated critical \mathcal{EM} value o . The set of regular values \mathbb{R} is a punctured open two-ball $B_*^2 = B^2 \setminus o$. To uncover monodromy, consider a closed directed path Γ in \mathbb{R} which encircles o and the regular torus bundle over Γ . Using local action-angle coordinates, regular tori in this bundle can be connected, i.e., we can give a continuous map from a torus to its neigh-

¹⁹See Arnol’d, Kozlov, and Neishtadt (1988), and Arnol’d (1989). As usual, several other names may be added to this theorem: Nekhoroshev (1994) suggested Poincaré and Lyapunov, while Vũ Ngọc and Nguyễn Tiên pointed to a similar statement by Mineur (1937).

²⁰Monodromy describes what happens after we go once ($\mu\acute{o}\nu\omicron$) around a path ($\delta\rho\acute{\omicron}\mu\omicron$). It appears in the topology of fiber bundles, complex analysis, Poincaré maps, and other contexts. Symington (2003) considered topological and affine monodromy, which are what we use here for the classical system (Sec. VI) and for its quantum analog (Secs. II.E and VII), respectively.

²¹See Cushman and Bates (1997) and discussion in Sec. VIII.D.

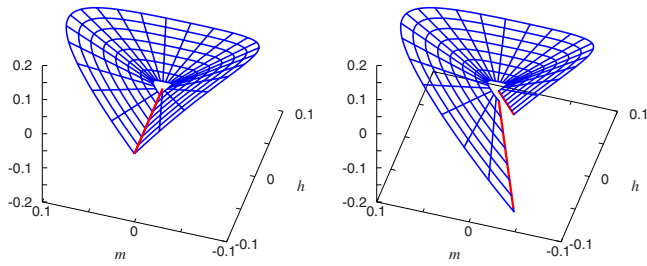


FIG. 12. (Color online) Different possible choices of the leaves of the multivalued part $m \arg(h+im)$ of the second action $\mathcal{I}_2(m,h)$ near $(0,0)$. In the special case (left), $\mathcal{I}_2(m,h)$ is C^0 smooth, while in a more general case (right), $\mathcal{I}_2(m,h)$ is discontinuous.

bor. It turns out²² that the bundle is nontrivial, i.e., it is not a direct product $S^1 \times T^2$ and these tori cannot be described by one set of action-angle coordinates.²³ We discuss this phenomenon and its consequences further in Sec. VI.

2. Specifics of monodromy

Monodromy is a topological property. It does not depend on the particular contour Γ chosen for its computation but on the homotopy class $[\Gamma]$ of the fundamental group $\pi_1(\mathbb{R})$ of \mathbb{R} . So it extends to the whole of \mathbb{R} and, consequently, the system has no global action $\mathcal{I}(m,h)$ on \mathbb{R} . Monodromy is a property of the bundle (see footnote 23). Considering each fiber individually does not uncover it. The key is in establishing an additional structure which is a global connection on the bundle and which describes how regular tori “fit together” in the total space. The specifics of this phenomenon is that despite its seemingly humble local origins, “just” an isolated singular fiber and “just” one isolated value o , its topological consequences are global. This made monodromy so difficult to uncover and to explain in physics and at the same time so interesting. Cushman was first to appreciate monodromy fully as a potential physical phenomenon (see footnote 21).

3. Multivalued action functions

In the presence of monodromy, at least one of the action functions $\mathcal{I}(m,h)$ is a multivalued real function on the set \mathbb{R} of regular \mathcal{EM} values (m,h) . In the simplest situation of Sec. II.D.1, such an action \mathcal{I}_2 has near $(m,h)=0$ a universal form (Vũ Ngọc, 2000)

²²As follows most directly from the so-called geometric monodromy theorem, see Sec. VI.B.5.

²³The nontriviality of the bundle is the principal aspect. Thus in some “exotic” situations when o corresponds to 12 elementary FF points (Nguyễn Tiên, 1995; Cushman and Zhilinskiĭ, 2002; Zhilinskiĭ, 2005), monodromy along a non-null-homotopic path Γ , can be trivial but the bundle over the part of \mathbb{R} encircled by Γ remains highly nontrivial.

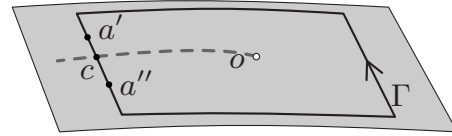


FIG. 13. The \mathcal{BD} of a system with fractional monodromy (cf. Fig. 11, left). The passable wall (dashes) is a line of weakly critical values that lift to curled tori; a' and a'' are regular values on different sides of the wall; o is an isolated strongly critical value. The path Γ encircles o and crosses the wall transversely at c .

$$2\pi\mathcal{I}_2(m,h) \approx m \arg(h+im) + \dots$$

As can be seen from Fig. 12, this makes a global action in the regular neighborhood of o impossible: for any single valued choice of $\mathcal{I}_2(m,h)$, going once around Γ results in a different $\partial\mathcal{I}_2/\partial(m,h)$ or in a different value of \mathcal{I}_2 itself. Note that for an isolated FF singularity, two continuous choices are possible²⁴ and have been popular in applications,²⁵ but they are by no means the only possibility and cannot be equated with monodromy itself.

4. Generalized or fractional monodromy

As pointed out in Sec. II.C.3, the bitorus is by far not the only possible hyperbolic fiber with rank 2 (corank 1) critical points. So the 1:2 zone systems may have families of curled tori $T_{[1/2]}^2$ with parameters (n,m) . Nekhoroshev *et al.* (2006) called them “weakly singular” fibers because, contrary to bitori, they do not separate different upper cells or form boundaries and because we can connect regular tori along a path crossing them.

Within a \mathcal{BD}_n , a family of $T_{[1/2]}^2$ is represented as a line called a passable wall (see Fig. 13). Considering a path Γ across such wall, Nekhoroshev *et al.* (2002, 2006) defined a mapping between two index 2 subgroups of first homologies $H_1(\Lambda_{a'})$ and $H_1(\Lambda_{a''})$ of tori $\Lambda_{a'}$ and $\Lambda_{a''}$ on the opposite sides of the wall. This formal mathematical construction is shown in Fig. 14 which shows the evolution of a specific basis cycle²⁶ of H_1 . It can be seen that a single cycle breaks and does not survive the passage, while a double cycle can be continued. Note that for a regular K -torus Λ , its first homology H_1 and its fundamental group π_1 are isomorphic and are both equivalent to a Z^K lattice. However, it is the index 2 subgroup of

²⁴This agrees with a general statement by Symington (2003).

²⁵Notably by Bates (1991), Child (1998, 2001, 2007), Child *et al.* (1999), and Winnewisser *et al.* (2006) for the champagne bottle or Mexican hat potential and its analogs.

²⁶Cycles of H_1 can be defined using local actions and the latter can be continued along Γ . This is the most common way to establish the connection on the tori and to compute monodromy. For fractional monodromy it was implemented by Efsthathiou, Cushman, and Sadovskii (2007); a different proof was given by Sugny *et al.* (2008). Nekhoroshev *et al.* (2006) and Nekhoroshev (2007, 2008) defined cycles in a more general geometric nondynamical way that underlines the topological nature of monodromy.

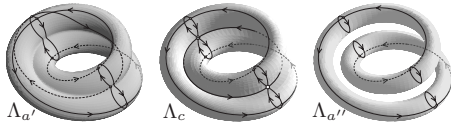


FIG. 14. Deformation of cycles of regular fibers $\Lambda_{a'}$ and $\Lambda_{a''}$ as we go from a' to a'' on Γ in Fig. 13. From Nekhoroshev *et al.*, 2006.

$H_1(\Lambda)$ that can be continued across passable walls (Giacobbe, 2008). In the situation when a passable wall has an open end terminated by an isolated critical value o (see Fig. 13), the path Γ can be chosen so that it encircles o crossing the wall only once. The preimage of such an o is a pinched torus and the system has monodromy. Because we deal with a subgroup of H_1 , this generalized monodromy is also called fractional. A more formal reason for such terminology is given in the next section.

5. Monodromy map and its matrix

Monodromy is a mapping \mathfrak{M} that for each class $[\Gamma]$ of closed directed paths $\Gamma \in \mathbb{R}$ supplies an automorphism $\mathfrak{M}_{[\Gamma]}$ of the first homology group $H_1(\Lambda_a)$, a transformation of the affine coordinates on the regular torus Λ_a with $a \in \Gamma$. For orientable \mathbb{R} and for a given initial cycle basis in $H_1(\Lambda_a)$, the automorphism $\mathfrak{M}_{[\Gamma]}$ can be represented by a matrix M in $SL(K, \mathbb{Z})$,²⁷ the rows of M correspond to the new basis elements expressed in terms of the initial basis. Since the group of orientation preserving automorphisms (see footnote 27) of $H_1(\Lambda_a)$ is $SL(K, \mathbb{Z})$, M is defined up to conjugation in $SL(K, \mathbb{Z})$.

For a concrete construction, recall that cycles of $H_1(\Lambda_a)$ are coordinate “axes” on Λ_a . In an integrable Hamiltonian dynamical system, these cycles can be defined using commuting periodic Hamiltonian flows on Λ_a corresponding to local actions I , and in that case conjugate angles ϕ serve as affine coordinates. This leads to an identification of a K -torus Λ_a with a lattice \mathbb{Z}^K , which Duistermaat (1980) called the period lattice. Matrices M define transformations of the basis vectors of this lattice. See more in Sec. VI.

For the most basic monodromy in Sec. II.D.1, the standard form of the monodromy matrix is

$$M(1) = \begin{pmatrix} 1 & 0 \\ -1 & 1 \end{pmatrix}.$$

In other words, on all tori in a saturated neighborhood of the singly pinched torus we can always choose one “fixed” cycle²⁸ γ_1 which $\mathfrak{M}_{[\Gamma]}$ leaves unchanged, while the second cycle γ_2 transforms under $\mathfrak{M}_{[\Gamma]}$ into $\gamma_2 - \gamma_1$.

²⁷ $SL(K, \mathbb{Z})$ is the group of integer $K \times K$ matrices M with $\det M = +1$. It is used for all systems described or mentioned. If \mathbb{R} is not orientable, e.g., a Möbius strip (or if the regular fibers are not tori and are not orientable), we should allow for improper changes of the directions (signs) of cycles and use a larger group $GL(K, \mathbb{Z})$ where $\det M = \pm 1$.

²⁸Called vanishing cycle in the Picard-Lefschetz theory.

The fixed cycle is normally associated with a momentum of an S^1 action, which in simple cases, including our system, is defined globally.

When $k > 1$ FF points combine in a degenerated singular fiber²⁹ known as torus with k pinches, the standard matrix is

$$M(k) = \begin{pmatrix} 1 & 0 \\ -k & 1 \end{pmatrix}.$$

For fractional monodromy³⁰ this matrix can formally be written as $M(\frac{1}{2})$, while the actual cycle transformation is defined only for the index 2 subgroup with basis $(\gamma_1, 2\gamma_2)$ which transforms according to matrix $M(1)$.

E. Quantum-classical correspondence

Duistermaat (1980) introduced monodromy as a property of the regular toric bundle that originates in the topology of its base \mathbb{R} . Furthermore, we have seen that monodromy can be uncovered without studying the fibers if we introduce an additional structure on \mathbb{R} defined by $\mathcal{I}(m, h)$ (local actions pulled back to \mathbb{R}). In 2-DOF (see Secs. II.E.1 and II.E.2), in a sufficiently small regular neighborhood of every regular point $(m, h) \in \mathbb{R}$, the functions $\mathcal{I}(m, h)$ define two unit vectors $(u_1, u_2) = u(m, h)$ along the directions in \mathbb{R} which correspond to the individual increase of actions \mathcal{I}_1 and \mathcal{I}_2 , i.e., to the columns of the inverse of the Jacobian matrix $\partial(\mathcal{I}_1, \mathcal{I}_2) / \partial(m, h)$. It is said that (u_1, u_2) define an affine structure on \mathbb{R} (Symington, 2003; Vũ Ngọc, 2007). Monodromy is related to this structure and not to $\mathcal{I}(m, h)$ itself.

1. Quantum joint spectrum lattice

For us the interest in the above affine structure is due to its direct relation to quantum mechanics. According to the Einstein-Brillouin-Keller (EBK) quantization principle, also known as torus or action quantization, allowed quantum (m, h) are those for which $\mathcal{I}_1, \mathcal{I}_2$ are integer values (times \hbar and plus a small constant correction). It follows that quantum (m, h) form in \mathbb{R} a two-dimensional discrete lattice of points whose two translation operations are given locally by $u(m, h)$. Since at all regular (m, h) the Jacobian $\partial\mathcal{I} / \partial(m, h)$ is nondegenerate, the local structure of the lattice (for 2-DOF) is \mathbb{Z}^2 .

In practice, the lattice can be computed directly as the joint spectrum of mutually commuting operators $\hat{\mu}$ and $\hat{\mathcal{H}}$ which correspond to the first integrals, momentum μ , and energy \mathcal{H} . At any regular node, the spectrum can be described by local quantum numbers (n_1, n_2) which increase by 1 in the directions given by (u_1, u_2) and which can be thus extended consistently to neighboring nodes.

²⁹See Bates and Zou (1993), Matveev (1996), and Nguyễn Tiên (2002).

³⁰See Nekhoroshev *et al.* (2002, 2006), Efsthathiou, Cushman, and Sadovskii (2007), and Sugny *et al.* (2008).

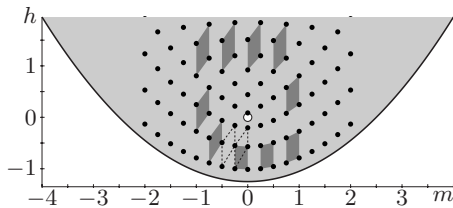


FIG. 15. Lattice of the joint energy-momentum spectrum for the 1:-1 resonant oscillator. Dark quadrangles show parallel transport of an elementary cell around the lattice defect at $o = (0,0)$, which is the critical value of the classical \mathcal{EM} map similar to that in Fig. 16, left. From Nekhoroshev *et al.*, 2002.

In a system with several cells, we consider several quantum lattices within the regular interiors R of each cell that may overlap in the \mathcal{EM} range.³¹

2. Quantum monodromy

In the presence of monodromy, the locally trivial regular toric bundle is nontrivial globally. Similarly, the corresponding affine locally regular \mathbb{Z}_2 lattice has a defect³² which prevents extending the \mathbb{Z}_2 structure to the whole lattice. In other words, it prevents choosing a fixed unique basis (u_1, u_2) or, equivalently, it prevents choosing global quantum numbers. This phenomenon has become known as quantum (Sadovskii and Zhilinskiĭ, 1999; Vū Ngoc, 1999) or affine (Symington, 2003) monodromy. It can be most clearly uncovered from an elementary cell diagram (Cushman and Duistermaat, 1988; Sadovskii and Zhilinskiĭ, 1999), such as the one in Fig. 15. At the initial point (m, h) on the nontrivial path $\Gamma \subset R$, we choose a basis $u(m, h)$ which defines an elementary cell. Moving along Γ we redefine continuously the vectors (u_1, u_2) and the cell. We come back with a different cell. The resulting change of the elementary cell is described by the matrix which relates the initial vectors (u_1, u_2) and the final vectors (w_1, w_2) . Considering the transformation properties of $\partial\mathcal{I}/\partial(m, h)$, we can verify (Vū Ngoc, 1999; Nekhoroshev *et al.*, 2006) that this matrix is the inverse transpose $(M^{-1})^T$ of the classical monodromy matrix M .

3. Generalizations

For integrable systems with $K > 2$ DOF we proceed similarly. For the original system with the Hamiltonian (2), K is 3 and, after normalizing and introducing first integrals N and μ , we study three-dimensional lattices with local \mathbb{Z}^3 structure (see Sec. VII).

In order to apply the same approach in the presence of weak singularities, for example, to study quantum fractional monodromy, we should transport multiple el-

ementary cells (Nekhoroshev *et al.*, 2002, 2006; Zhilinskiĭ, 2005). Thus double cells are used in the 1:2 zone.

F. Main conjecture of the global classification

Reconstruction starting from the bifurcation diagram \mathcal{BD} (stratified unfolded image of the \mathcal{EM} map) is at the heart of our analysis. We obtain six dimensions (initial physical phase space) from eight (KS space), eight from four (reduced space $S^2 \times S^2$), and—as in the title of Symington (2003)—four from two (bifurcation diagram \mathcal{BD}). The main conjecture (Efsthathiou, Sadovskii, and Zhilinskiĭ, 2007) is that our global dynamical classification can be given in terms of \mathcal{BD} topology. Two groups of problems have to be cleared in order to make this into a more rigorous statement: we should (i) extend the results deriving the topology and symplectic geometry of the integrable fibration from its \mathcal{BD} and (ii) understand the reliability of the integrable approximation.

1. Toric fibrations and their \mathcal{BD}

A K -DOF integrable system with a toric fibration, i.e., a trivial fibration whose every regular fiber is a single torus \mathbb{T}^K and whose only critical fibers are non-Lagrangian tori $\mathbb{T}^{K'}$ with $K' < K$, has global action-angle variables. In other words, the system has K first integrals in involution which are momenta, i.e., which define periodic Hamiltonian flows, and the \mathcal{EM} map is equivalent to a global momentum map J . In particular, the images of \mathcal{EM} and J are diffeomorphic. The diffeomorphism is given by the expression for energy in terms of momenta.

Furthermore, if additionally the phase space is closed, then after replacing \mathcal{EM} by J (cf. Fig. 9) the \mathcal{BD} of this system becomes a solid convex polytope (with some additional characteristics) and the set of regular values within it is an open K -ball B^K with piecewise linear boundary ∂B^K (Atiyah, 1982, 1983; Guillemin and Sternberg, 1982, 1984). The set of all regular tori is a trivial regular toric bundle $B^K \times \mathbb{T}^K$. The inverse is also true (Delzant, 1988): a \mathcal{BD} diffeomorphic to the one described above together with an effective³³ torus action on the total space define completely a toric fibration of the latter. These statements extend to more general phase spaces if the \mathcal{EM} map is proper,³⁴ and all fibers are connected.

The phase space $S^2 \times S^2$ of the first reduced system allows a regular toric fibration (Symington, 2003) and the family of integrable approximations to system (2) includes systems with such fibration. In the 1:1 zone they are called A_0 (Efsthathiou, Sadovskii, and Zhilinskiĭ, 2007; Efsthathiou *et al.*, 2009), and their constant- n \mathcal{BD}_n is a rectangle-like two-ball whose boundary has four cone singular points. The latter correspond, of course, to Keplerian RE.

³¹See Joyeux *et al.* (2003) and Efsthathiou, Joyeux, and Sadovskii (2004) for an early example and Sec. VII.

³²See Cushman and Duistermaat (1988), Sadovskii and Zhilinskiĭ (1999), Zhilinskiĭ (2005), and Nekhoroshev *et al.* (2006).

³³We work with effective torus actions in Sec. VI.A.2.

³⁴Under a proper map, the inverse image of any compact space remains compact.

2. Recovering topology of singular fibrations from their \mathcal{BD}

Results for integrable fibrations with singular fibers were obtained primarily in 2-DOF. Symington (2003) and Vũ Ngọc (2007) studied “almost” toric fibrations or fibrations, which can only have pinched tori (Fig. 8, left and center) as their singular fibers and therefore are defined by an \mathcal{EM} map with either elliptic or focus-focus critical points. In this case, the topology of the fibration and the total space follows from that of the \mathcal{BD} . Symington also proved that $S^2 \times S^2$ can have an almost toric fibration. Such systems exist in our family; in the 1:1 zone, they are called A_1 , A_2 , and $A_{1,1}$ (Efsthathiou, Sadovskii, and Zhilinskiĭ, 2007; Efsthathiou *et al.*, 2009). These systems have one, two on the same fiber, and two on distinct fibers focus-focus equilibria, respectively, and all of them possess nontrivial monodromy. What is particularly interesting from Symington (2003) and Vũ Ngọc (2007) is that their extension of Delzant (1988) to almost toric fibrations relies on an additional affine integral structure instead of an assumption of an existing torus action (in the total space) [see Sec. II.E and, for an interesting parallel, Kontsevich and Soibelman (2006)]. The geometric monodromy theorem (Nguyễn Tiên, 1997; Cushman and Duistermaat, 2001), discussed in Sec. II.D, fits in the same context. The difference from Symington (2003) and Vũ Ngọc (2007) is that the statement is more local. It does not attempt to consider the whole \mathcal{BD} and to recover the whole fibration from it, as can be done for a compact or properly compactified total space and almost toric fibration.

3. Extending to systems with hyperbolic singular fibers

Alas, when the mathematical theory in the preceding section meets physical reality, we realize that the former is far from satisfactory. In our system, hyperbolic fibers appear regularly. In the 1:1 zone, the fiber is a bitorus (Fig. 8, right), and systems which possess it are called B type. In the 1:2 zone we can also have curled tori, and both fibers appear typically following the disintegration of a caustic (Efsthathiou, Sadovskii, and Zhilinskiĭ, 2007). So we have to deal with the situation.

In Sec. II.C.4 we saw that bitori are related to the existence of several unfolded cells in the \mathcal{BD} . In 2-DOF bitori appear typically as a one-dimensional family \mathcal{C} , so that their images c form a \mathcal{C} segment of critical values within the \mathcal{BD} , which forms a wall between the cells. We detach the cells, ignore the \mathcal{C} segments, and consider each cell individually as a base of an almost toric fibration. This divides the whole integrable fibration into several subfibrations fitting in the same total space. Although it might be possible to connect these fibrations between themselves, i.e., “across” the bitorus walls, we will not attempt that presently for the lack of reliable theory [see, however, Bartsch *et al.* (2007) and compare to the phenomenon of bidromy in Sec. III.C.1]. In quantum mechanics, such construction corresponds to several overlapping joint spectrum lattices within one energy-momentum domain.

With regard to all kinds of possible arrangements of hyperbolic singularities in a 2-DOF system (Bolsinov and Fomenko, 2004), the fibrations considered here can be called almost toric with trivial families of hyperbolic singularities or trivially singular. Basically, this means that (in 2-DOF) we do not have HH critical points (Dullin and Vũ Ngọc, 2007), whose existence complicates significantly the unfolding of the stratified \mathcal{EM} image into a \mathcal{BD} . In our systems, different one-dimensional families \mathcal{C} of bitori do not come out of a neighborhood of the same singular fiber (i.e., their \mathcal{EM} images do not “intersect”) and this makes unfolding straightforward.

Another kind of Bott-type hyperbolic singular fibers that we encounter in our systems with resonances 1:2 and higher is curled tori. These are weakly singular, meaning that \mathcal{EM} images of their families \mathcal{C} constitute passable walls within the same cell. The example in Sec. III.C.2 shows that families of curled tori and bitori can join. In $k_-:k_+$ resonant systems with both $k_- > 1$ and $k_+ > 1$, families of different curled tori exist and can exceptionally join at the same singular fiber (Nekhoroshev, 2007; Giacobbe, 2008; Sugny *et al.*, 2008).

4. Extending to nearly integrable systems

The conjecture that monodromy can apply not only to integrable systems but also to systems with a reliable integrable approximation was made “out of necessity” by Cushman and Sadovskii (2000). It was later confirmed by Rink (2004) and Broer *et al.* (2007) who established a connection on the Cantor set of KAM tori along a path crossing these tori in the total space. This involves interpolation of the first homologies along the path. We can also envisage interpolating local actions and reproducing the affine structure of the integrable approximation. This can be quite naturally done in quantum mechanics by computing average values of approximate integrals (see Sec. VII for more details).

III. RESULTS: QUALITATIVE TYPES OF PERTURBATIONS

The first complete global second-order description of perturbations [Eq. (2)] was given by Cushman and Sadovskii (1999, 2000) for the one-parameter subfamily with perpendicular fields. In the same spirit, integrable approximations to other perturbations [Eq. (2)] can be constructed using second-order normalization and going to higher orders if necessary. For each approximation, we study the fibration of the phase space defined by its first integrals. The topological properties of the fibration and in particular monodromy give comprehensive qualitative characteristics of the original perturbed nonintegrable system.

A. Symmetry strata and their stabilizers

Depending on the configuration of fields \mathbf{G} and \mathbf{F} , systems with the Hamiltonian (2) have different isotropy symmetries and have been classified by Michel and Zhi-

TABLE I. Symmetry strata of the constant s section D_s of the parameter space of the family of perturbations of the hydrogen atom with the Hamiltonian equation (2); see Sec. III.A and Michel and Zhilinskiĭ (2001a) and Efsthathiou *et al.* (2009).

Stratum	Dimension	Symmetry	Definition [cf. Fig. 16 and Eq. (4b)]	Comment
S	0	$C_{\infty v} \times \mathcal{T}$	$a=0$	One point
Z	0	$C_{\infty h} \wedge \mathcal{T}_s$	$a=1$	One point
\parallel	1	$C_{\infty} \wedge \mathcal{T}_s$	$d^2 = a^2(1-a^2), a^2 \in (0,1)$	Two open semicircles
(SZ) or \perp	1	$Z_2 \times \mathcal{T}_s$	$d=0, a^2 \in (0,1)$	Open interval
Generic	2	\mathcal{T}_s	$0 < d^2 < a^2(1-a^2), a^2 \in (0,1)$	Two open half-disks

linskiĭ (2001a). We list all possible configurations and respective isotropies in Table I and give the action of these groups on the phase space \mathbb{R}^6 . The order 2 group $\mathcal{T} = \{1, T\}$ includes the (time) reversal operation

$$T: (\mathbf{Q}, \mathbf{P}) \mapsto (\mathbf{Q}, -\mathbf{P});$$

the group $\mathcal{T}_s = \{1, T_s\}$ includes a combination $T_s = T \circ \sigma$ of T and reflection in the plane of vectors \mathbf{F} and \mathbf{G} ,

$$\sigma: (\mathbf{Q}, \mathbf{P}) \mapsto (Q_1, Q_2, -Q_3, P_1, P_2, -P_3)$$

(see Fig. 1); the discrete order 4 group $Z_2 \times \mathcal{T}_s$ of \perp configurations includes the group $Z_2 = \{1, \sigma_h\}$ of reflections in the plane orthogonal to \mathbf{G} [cf. Sadovskii and Zhilinskiĭ (1998)]. Single fields \mathbf{G} and \mathbf{F} and parallel fields $\mathbf{G} \parallel \mathbf{F}$ have Lie symmetry $SO(2)$ with the axis C_{∞} aligned with the field vector: we use axis Q_1 for \mathbf{G} and $\mathbf{G} \parallel \mathbf{F}$ and axis Q_2 for \mathbf{F} . The groups $C_{\infty v}$ and $C_{\infty h}$ are standard spatial extensions of the two respective C_{∞} groups.

Note that symmetry strata do not depend on the integrable approximation and persist for the nonintegrable case. On the other hand (albeit for a differently oriented axis), the action of the approximate S^1 symmetry of any system in the 1:1 zone is equivalent to that of C_{∞} . After normalization, such systems have isotropy symmetry $S^1 \wedge \mathcal{T}_s \sim C_{\infty} \wedge \mathcal{T}_s$. This makes the analysis and results of Michel and Zhilinskiĭ (2001a) closely related to our analysis of 1:1 systems.

Michel and Zhilinskiĭ (2001a) used invariant theory to reduce the spatiotemporal symmetries in Table I and de-

scend to the orbit space \mathcal{O} that they call *orbifold*. For all cases with $SO(2)$ isotropy, this space is similar to the one in Fig. 5—a pillowlike closed three-ball with four conical corners on its surface. Subsequently, they studied possible reduced Hamiltonians as functions $\mathcal{H}: \mathcal{O} \rightarrow \mathbb{R}$. Qualitatively different \mathcal{H} are distinguished by the set of their critical levels. In comparison to this approach, we go into more detail by considering combined levels of momentum μ and energy \mathcal{H} on \mathcal{O} . This allows us to reconstruct fibers of the \mathcal{EM} map. We make similar emphasis on the critical levels.

B. Classification of systems in the 1:1 zone

Within the n -shell parameter space D_n [see Fig. 3 and Eq. (4c)], the 1:1 zone is a strip

$$\{(a^2, d) \in D_n, |d| < d_{\max} \ll \frac{1}{2}\} \tag{16}$$

divided by the $[SZ]$ segment. The structurally identical halves of the zone correspond to slightly acute ($\langle \mathbf{G}, \mathbf{F} \rangle > 0$) and obtuse ($\langle \mathbf{G}, \mathbf{F} \rangle < 0$) angles between \mathbf{F} and \mathbf{G} . So assuming $\langle \mathbf{G}, \mathbf{F} \rangle > 0$ suffices. The size of the 1:1 zone is given by d_{\max} . Different criteria for this value are possible. We can look for the closest sufficiently low-order resonance, e.g., 4:3 used in Fig. 16, which cannot be ignored at time scales comparable to that of the second-order average. We can also follow structures specific to the particular resonance, e.g., gray shaded areas and triangular regions near S and Z limits in Fig. 16, and assume that they vanish at the periphery of the zone.³⁵

As shown in Fig. 16, the 1:1 zone includes the \perp symmetry stratum (SZ) , S , Z , and part of the \parallel stratum near S and Z . Cushman and Sadovskii (1999, 2000) showed that SZ itself is stratified into three dynamical strata. Systems in the central stratum have monodromy. Later Efsthathiou, Cushman, and Sadovskii (2004) related transitions from and to this central region to Hamiltonian Hopf bifurcations. Recently Efsthathiou, Sadovskii, and Zhilinskiĭ (2007) and Schleif and Delos (2007) showed that near orthogonal configurations are deformations of

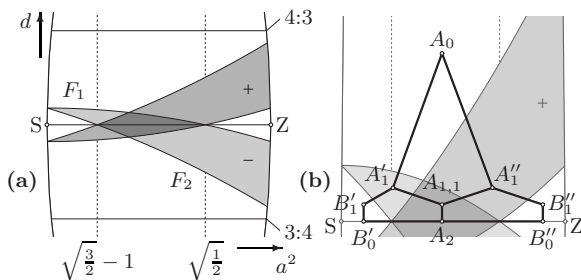
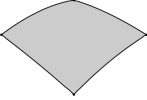
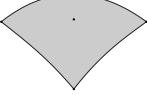
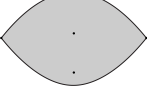
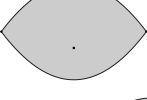
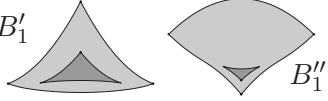
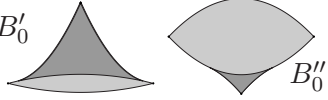




FIG. 16. Structure of the 1:1 zone (Efsthathiou, Sadovskii, and Zhilinskiĭ, 2007; Efsthathiou *et al.*, 2009). Different dynamical strata of the zone (a) correspond to vertices of the genealogy graph (b); vertical edges of the graph represent bifurcations with broken symmetry of order 2, and other edges correspond to Hamiltonian Hopf bifurcations.

³⁵Consistent mathematical zone width estimates which may reproduce the above criteria can probably be given by adapting Nekhoroshev stability theory to parametric isochronous systems (Fassò, 2008).

TABLE II. Qualitatively different systems in the 1:1 zone (Efsthathiou *et al.*, 2009). For each system, constant- n sections \mathcal{BD}_n of bifurcation diagrams \mathcal{BD} in coordinates m (horizontal) and h (vertical) are displayed in the second column.

Type	\mathcal{BD}	Monodromy	Additional description of the \mathcal{BD}
A_0 generic, \parallel		Trivial	The single cell \mathcal{BD}
A_1 generic, \parallel		Nontrivial $M(1)$ (cf. Sec. II.D.1)	Contains an isolated critical value o that corresponds to a singly pinched torus $\mathbb{T}_{[1]}^2$
$A_{1,1}$ generic		Nontrivial $M(1)$ or $M(2)$	Contains two isolated critical values o^-, o^+ that correspond to different singly pinched tori
A_2 (SZ)		Nontrivial $M(2)$	Contains an isolated degenerated critical value o that lifts to a doubly pinched torus $\mathbb{T}_{[2]}^2$
B_1 generic, \parallel		Nontrivial $M(1)$	Two partially overlapping cells glued along a bitorus line. Both \mathcal{BD} 's are equivalent and appear in the dynamical strata B'_1 near the Stark limit and B''_1 and $\parallel B'_1$ near the Zeeman limit
B_0 (SZ), Z		Trivial	Three cells glued along a line; two of the cells overlap completely (dark shade). Both \mathcal{BD} 's are equivalent and appear in the B'_0 and B''_0 dynamical strata near the Stark and Zeeman limits, respectively
A_0^* \parallel near S		Trivial	Single unfolded cell that partially overlaps itself; upon unfolding, becomes a type A_0 \mathcal{BD}
S		Trivial	Single unfolded cell that overlaps itself, a special case of A_0^* with additional \mathbb{Z}_2 symmetry

the strictly orthogonal ones breaking the specific \mathbb{Z}_2 symmetry of the latter. Classification of these systems was finalized by Schleif and Delos (2008) and Efsthathiou *et al.* (2009).

Table II lists qualitatively different structurally stable 1:1 systems. The B systems may have regular fibers consisting of two components (tori); all regular fibers of A systems are single tori. The \mathcal{BD} 's of B systems consist of several cells (cf. Figs. 10 and 11, right) or may consist of one folded cell (cf. Fig. 9); the latter case is called A^* . Plain single cell \mathcal{BD} 's are of type A . Nonsimply connected cells (cf. Fig. 11), i.e., cells with nontrivial fundamental group $\pi_1(\mathbb{R})$ of their regular interior \mathbb{R} , are further characterized using monodromy. This characteristic is reflected in the subscripts $k=0,1,2$, each corresponding to a cycle of $\pi_1(\mathbb{R})$ and to the respective class of monodromy matrices $M(k)$ in Sec. II.D.5.

The structure of the zone is described completely by specifying how the types in Table II fit within the parameter strip (16). This structure is shown in Fig. 16 using the results of Efsthathiou *et al.* (2009) who computed analytically the parametric boundaries of all dynamical strata within the second-order approximation. We can

now pick a structurally stable traversal path that starts on the SZ axis and describe the topology of the zone by specifying the types of systems we may encounter. As can be seen from Fig. 16, there are two such paths, $B_0B_1A_1A_0$ and $A_2A_{1,1}A_1A_0$.

C. Systems in the 1:2 zone

The characteristic feature of any 1:2 resonance is that the respective symmetry action has special “short” S^1 orbits with isotropy \mathbb{Z}_2 . Their period is half that of generic orbits. The Pauliean 1:2 symmetry action on $S^2 \times S^2$ has such critical orbits in addition to the four fixed points common to any Pauliean symmetry (Sec. II.C.2). In the total space \mathbb{R}_{*}^6 , the former lift to “short” T^2 RE, whose Pauliean cycle is half the period of the Keplerian cycle, while the latter correspond to the four Keplerian ellipse RE. Among these four Keplerian RE, two have again the maximum absolute values $|m|=m_{\max}=3n/2$ of the Pauliean momentum μ , while two others have intermediate nonzero values $|m|=m_{\text{crit}}=n/2$; the boundaries of the \mathcal{BD} are formed by the images of both short and

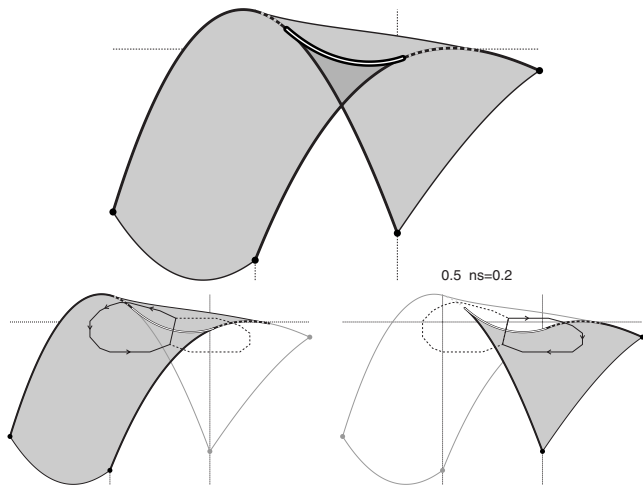


FIG. 17. Most typical single-cell \mathcal{BD} of 1:2 resonant systems. Dashed and double lines mark images of curled tori and bitori, respectively; four black dots represent Keplerian S^1 RE, bold and regular boundaries correspond to short and regular T^2 RE; and energy scale is adjusted. In the upper plot, dark gray shade represents values with two-component preimages. Lower plots show two parts of the cell which join (with an overlap) along the bitorus line \mathcal{C} and the respective parts of the bipath (two merged thin solid and dotted loops) used to uncover fractional bidromy. Upper plot, from Efstathiou, Sadovskii, and Zhilinskiĭ, 2007.

regular T^2 RE (see Figs. 17 and 18). Typical singular fibers are curled tori and bitori.

1. Most typical 1:2 structure

For the exact 1:2 resonance, the most typical \mathcal{BD} is shown in Fig. 17. It consists of a single unfolded cell. In the range of the \mathcal{EM} map, this cell partly overlaps itself (in the region shaded dark gray in Fig. 17, top). It can be disassembled in two overlapping sheets which are glued together along the bitorus wall \mathcal{C} . Comparing to Fig. 9, we notice that \mathcal{C} comes from a disintegrated caustic. Comparing to Figs. 10 and 11, right, we see a different situation: here a path starting “above” \mathcal{C} at point a can reach “below” \mathcal{C} in two different ways by entering the overlap region either from the left or from the right and arriving at respective b' or b'' , which correspond to the same \mathcal{EM} value b . Except for crossing passable walls (dashed lines in Fig. 17, top, representing families of curled tori), such path remains in the regular interior \mathbb{R} of the same cell and the coordinates on the two regular torus components $\Lambda_{b'}$ and $\Lambda_{b''}$ of fiber $\mathcal{EM}^{-1}(b)$ can be related. Therefore, the system has global actions.³⁶

³⁶Except for the passable walls associated with the 1:2 resonance, the \mathcal{BD}_n in Fig. 17 resembles the case with bidromy, a nontrivial topological characteristics proposed by Sadovskii and Zhilinskiĭ (2007). Further study is required to understand whether these systems do indeed have bidromy.

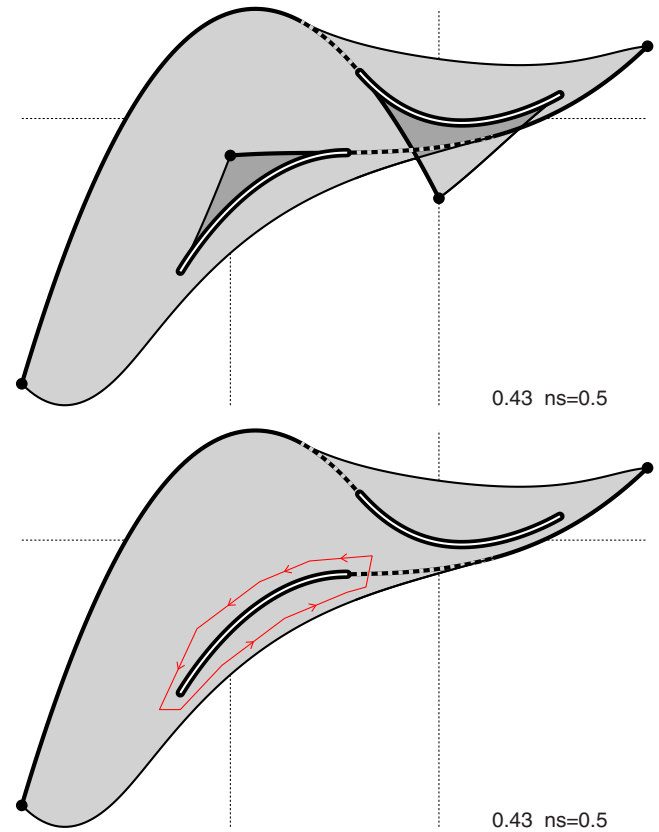


FIG. 18. (Color online) \mathcal{BD} of a 1:2 resonant system with fractional monodromy (top) and its main cell (bottom), compare to Fig. 17. The energy scale is adjusted arbitrarily. The closed path Γ encircling the segment of bitorus images and intersecting the line of curled torus images results in fractional monodromy. From Efstathiou, Sadovskii, and Zhilinskiĭ, 2007.

2. Fractional monodromy

A more rare (but stable within a small interval of parameter a^2) is the three-cell \mathcal{BD} in Fig. 18. Each of its two small “triangular” cells or “kites”³⁷ has (at its tip) the image of a Keplerian RE with intermediate momentum $m = \pm m_{\text{crit}}$. They are attached to the large main cell in Fig. 18, bottom, along two respective segments (walls) of critical values (double line) corresponding to bitori. Each segment continues with a “string” (passable wall) of weakly critical values (dashed line) corresponding to curled tori; the strings merge with the boundary when curled tori contract to their short singular circle.

Except for the strings, the situation is similar to the B_1 systems in the 1:1 zone. Each kite represents a stable local deformation of an ideal system with fractional monodromy studied by Nekhoroshev *et al.* (2002, 2006), Efstathiou, Cushman, and Sadovskii (2007), and Sugny *et al.* (2008). In other words, the kite can be obtained continuously from the germ pinched torus which includes the Keplerian equilibrium and whose image is an endpoint of a string of curled torus images. Therefore, the system has fractional monodromy for each of the

³⁷We employ the terminology of Waalkens *et al.* (2004).

two paths in the main cell which encircle the bitorus segments as shown in Fig. 18, bottom.

D. Higher-order resonance zones

All zones with $k_- + k_+ > 3$ remain completely unexplored. It should be understood that studying a $k_- : k_+$ resonant zone requires going to at least order $k_- + k_+$ of the normal form \mathcal{H} . Technical difficulties of such computations apart, the size of the zone, and its structural stability with regard to the nonintegrable component of the dynamics decrease exponentially with growing order. So before we attempt to study higher resonances seriously, the theory of zones may require quantitative development (see footnote 35).

Another aspect of $k_- + k_+ > 2$ zones is the role of “non-resonant” terms $\mathcal{H}^{(k)}$ of orders $k < k_- + k_+$. Specific $k_- : k_+$ systems, notably those with $k_- : k_+$ fractional monodromy,³⁸ would exist only if $\mathcal{H}^{(k)}$ becomes insignificant. This seems to be possible for 1:2 but may no longer be so for higher resonances. Indeed, the 1:2 systems with fractional monodromy (Sec. III.C.2) are already rather exceptional: they exist in a relatively small interval of a^2 , where nonresonant terms in $\mathcal{H}^{(2)}$ nearly vanish and require large values of ns to make the resonant term $\mathcal{H}^{(3)}$ sufficiently important. For $k_- + k_+ > 3$ such arrangements may be even more problematic in our three-parameter family, and we are more likely to encounter structures similar to that in Sec. III.C.1.

Nevertheless, even if the $\mathcal{H}^{(k_- + k_+)}$ resonance term can be made dominant, we should not expect to find (families of) $k_- : k_+$ curled tori because unlike $\mathbb{T}_{[1/2]}^2$ such singular fibers are structurally unstable. Instead, in the image of the \mathcal{EM} map, we may typically find small passable “corridors” for which “fuzzy” monodromy can be defined (Nekhoroshev, 2008).

E. Systems with additional Lie symmetry

Finally, systems with (approximate) additional Lie symmetries may require special attention: if such symmetries are incompatible with the S^1 symmetry of the resonant part of the linearized first reduced Hamiltonian on $S^2 \times S^2$, then we may have to consider constructing and analyzing a superintegrable approximation system. Such systems lie near the boundary ∂D of the parameter space D in Fig. 3 which includes the \parallel stratum, S , and Z (see Table I) and where we should select additionally two collapse points with $a^2 = 1/2$ and $d = \pm 1/2$.

It can be shown that for $a^2 > 1/2$, i.e., on the Z side of ∂D , the action of the axial symmetry C_∞ coincides with the resonant S^1 action and therefore, the \parallel stratum and Z can be analyzed as integral parts of resonant zones. On the S side of ∂D , we need to consider a special \parallel zone with $a^2 \leq 1/2$ and d close to $a^2(1 - a^2)$, within which reso-

nances result in different superintegrable approximations. Of these, only S and, to some extent, the collapse points (Sadovskii *et al.*, 1996) have been studied.

IV. THE INTEGRABLE APPROXIMATION

As outlined in Sec. II, the first step in the construction of an integrable approximation to the system with the Hamiltonian (2) is the Kustaanheimo-Stiefel (KS) regularization through which the system is described as a perturbation of a 4-DOF isotropic harmonic oscillator. It is followed by the Keplerian normalization of the regularized system (cf. Sec. II.B.1) with respect to the approximate dynamical oscillator symmetry S^1 associated with the approximate first integral N . After the subsequent reduction, we obtain a 2-DOF Hamiltonian system on the first reduced phase space $S^2 \times S^2$. The final step is the construction of an integrable 1-DOF Hamiltonian system by a second normalization and reduction of the 2-DOF system on $S^2 \times S^2$ (cf. Sec. II.B.3). We go through these steps in detail.

Up to the final step, the procedure is common to all resonance zones. It has been refined throughout a number of papers, started with Reinhardt and Farrelly (1982), Johnson *et al.* (1983), Robnik and Schrüfer (1985), and Kuwata *et al.* (1990), and continued by Farrelly *et al.* (1992) for parallel fields and Gourlay *et al.* (1993) for orthogonal fields, where the KS transformation becomes essential; we follow closely Sadovskii and Zhilinskiĭ (1998), Cushman and Sadovskii (2000), Efstathiou, Cushman, and Sadovskii (2004), and Efstathiou *et al.* (2009). The second reduction is specific to each zone and we mostly focus on the 1:1 case, which embraces all of the above cited work and is the only one for which the complete stratification of the resonance zone is presently obtained.

Before describing the consequent stages of normalization and reduction, we describe our notation. Coordinates on the original phase space $\mathbb{R}_*^6 = (\mathbb{R}^3 \setminus \{0\}) \times \mathbb{R}^3$ are given by three-vectors (\mathbf{Q}, \mathbf{P}) . Similarly, coordinates on the KS phase space \mathbb{R}^8 are given by four-vectors q and p ; q^2, p^2 will denote their respective scalar squares. We also identify \mathbb{R}^8 with \mathbb{C}^4 where we use complex coordinates

$$z = (z_1, z_2, z_3, z_4)^T, \quad z_j = q_j + ip_j \quad \text{for } j = 1, \dots, 4.$$

Our subsequent analysis in Sec. V is based on the second reduced energy correction obtained in Sec. IV.D.2.f. This quantity is our main objective here. It will be denoted by $\Delta\mathcal{E}$ and it will have two dynamical parameters $n \geq 0$ and m that are the values of the momenta N and μ , respectively. Recall from Sec. I.B that N is called Keplerian integral and that n is the classical equivalent of the principal quantum number. Subtracting “scalar” terms that depend only on (n, m) , we obtain the Hamiltonian function \mathcal{H} whose value will be called h . It plays the role of “energy” in our \mathcal{EM} maps (15a) and (15b) and our \mathcal{BD} (Table II and elsewhere).

³⁸See Zhilinskiĭ (2005), Nekhoroshev (2007, 2008), Giacobbe (2008), and Sugny *et al.* (2008).

A. Keplerian normalization and reduction

1. KS regularization

The KS method is a standard procedure to regularize the Keplerian vector field. The first step is time rescaling: fixing an energy level $E < 0$ (negative, since we are only interested in classically bound motion), we introduce the new time scale $dt \mapsto dt/|\mathbf{Q}|$. Equation (2) becomes

$$1 = \frac{1}{2}(\mathbf{P}^2 - 2E)\mathbf{Q} + F_e Q_2 \mathbf{Q} + F_b Q_1 \mathbf{Q} + \frac{G}{2}(Q_2 P_3 - Q_3 P_2)\mathbf{Q} + \frac{G^2}{8}(Q_2^2 + Q_3^2)\mathbf{Q}, \quad (17)$$

where $\frac{1}{2}(\mathbf{P}^2 - 2E)|\mathbf{Q}|$ is the unperturbed Hamiltonian.

The subsequent KS transformation (Kustaanheimo, 1964; Kustaanheimo and Stiefel, 1965; Stiefel, 1970; Stiefel and Scheifele, 1971) maps $\mathbb{R}_*^8 = (\mathbb{R}^4 \setminus \{0\}) \times \mathbb{R}^4$ onto the original phase space \mathbb{R}_*^6 ,

$$\text{KS}: (q, p) \mapsto \left(M_{\text{KS}}(q)q, \frac{1}{q^2} M_{\text{KS}}(q)p \right) = \left(\mathbf{Q}, \mathbf{0}, \mathbf{P}, -\frac{2\zeta}{q^2} \right), \quad (18)$$

where $M_{\text{KS}}(q)$ is the 4×4 matrix,

$$M_{\text{KS}}(q) = \begin{pmatrix} q_1 & -q_2 & -q_3 & q_4 \\ q_2 & q_1 & -q_4 & -q_3 \\ q_3 & q_4 & q_1 & q_2 \\ q_4 & -q_3 & q_2 & -q_1 \end{pmatrix}. \quad (19)$$

Note that the quadratic Hamiltonian function

$$\zeta = \frac{1}{2}(q_1 p_4 - q_2 p_3 + q_3 p_2 - q_4 p_1), \quad (20)$$

which appears in Eq. (18), generates on \mathbb{R}^8 an S^1 action called the KS symmetry. Since, as can be computed straightforwardly, all Poisson brackets of ζ with any of the coordinates (\mathbf{Q}, \mathbf{P}) expressed in terms of (q, p) are zero, ζ Poisson commutes with any function H_{KS} defined on \mathbb{R}^8 as the KS transform $H \circ \text{KS}$ of a function H on \mathbb{R}_*^6 . Moreover, since the Kepler system corresponds to $\zeta=0$, we can treat ζ as a constant of motion identically equal to 0, i.e., restrict to $\mathbb{R}^8|_{\zeta=0}$. So the KS map (18) and the space \mathbb{R}_*^6 can be seen as a singular reduction map for the KS symmetry and its space of orbits with $\zeta=0$, respectively.

After further successive coordinate and time rescalings

$$(q, p) \mapsto (q/\sqrt{\Omega}, p\sqrt{\Omega}), \quad t \mapsto \Omega t,$$

the KS transformed Hamiltonian becomes

$$H_{\text{KS}} = \frac{1}{2}(p^2 + q^2) + \frac{1}{3}\tilde{f}_e(q_1 q_2 - q_3 q_4)q^2 + \frac{1}{6}\tilde{f}_b(q_1^2 - q_2^2 - q_3^2 + q_4^2)q^2 + \frac{1}{2}\tilde{g}(q_2 p_3 - q_3 p_2)q^2 + \frac{1}{8}\tilde{g}^2(q_1^2 + q_4^2) \times (q_2^2 + q_3^2)q^2 = 4\Omega^{-1}, \quad (21)$$

where \tilde{g} , $(\tilde{f}_e, \tilde{f}_b)$, and Ω are defined in Eqs. (5) and (6) in Sec. I.B. H_{KS} is a perturbation of

$$2N = \frac{1}{2}(p_1^2 + q_1^2 + p_2^2 + q_2^2 + p_3^2 + q_3^2 + p_4^2 + q_4^2), \quad (22)$$

which describes a 4-DOF harmonic oscillator in 1:1:1:1 resonance.

For our purposes it is convenient to make one more symplectic and orthogonal (in \mathbb{R}^8) change of coordinates,

$$(q_1, q_4, p_1, p_4)^T \mapsto A \cdot (q_1, q_4, p_1, p_4)^T, \quad (23a)$$

$$(q_2, q_3, p_2, p_3)^T \mapsto A \cdot (q_2, q_3, p_2, p_3)^T, \quad (23b)$$

given by the matrix

$$A = \frac{1}{\sqrt{2}} \begin{pmatrix} 0 & 0 & -1 & -1 \\ 1 & -1 & 0 & 0 \\ 1 & 1 & 0 & 0 \\ 0 & 0 & 1 & -1 \end{pmatrix}. \quad (23c)$$

After this change of coordinates, the KS integral ζ in Eq. (20) becomes diagonal,

$$\zeta = \frac{1}{4}(-p_1^2 - q_1^2 - p_3^2 - q_3^2 + p_2^2 + q_2^2 + p_4^2 + q_4^2). \quad (24)$$

At the same time, since the transformation in Eqs. (23) is orthogonal, the expression for N remains unchanged. From now on we work with coordinates (q, p) defined by Eqs. (23).

2. Normalization of the Keplerian symmetry

We normalize the KS Hamiltonian H_{KS} in Eq. (21) with respect to its unperturbed part $2N = \frac{1}{2}(q^2 + p^2)$. The normalization is done most naturally using the standard Lie series algorithm of Gröbner (1960, 1967), Deprit (1969), Deprit *et al.* (1969), Henrard (1970), and Meyer and Hall (1992). In this algorithm, H_{KS} and its normal form \bar{H}_{KS} are manipulated as formal series in (q, p) with uniform smallness parameter \tilde{s} in Eq. (4b) tracing the order k of terms in the series. We obtain

$$\bar{H}_{\text{KS}} = \bar{H}_{\text{KS}}^{(0)} + \bar{H}_{\text{KS}}^{(1)} + \bar{H}_{\text{KS}}^{(2)} + \dots, \quad (25)$$

where $\bar{H}_{\text{KS}}^{(0)} = 2N$ and each term $\bar{H}_{\text{KS}}^{(k)}$ of order $O(\tilde{s}^k)$ is a homogeneous polynomial in (q, p) of degree $2k+2$. For the 1:1 systems, we can truncate Eq. (25) at terms of degree 6 in (q, p) ; for a $k_- : k_+$ resonance, we should normalize to order $k = k_+ + k_-$. Expressions for $\bar{H}_{\text{KS}}^{(1)}$ and $\bar{H}_{\text{KS}}^{(2)}$ can be obtained from those for the reduced Hamiltonian which we give in Eqs. (30a) and (30b) and in Table III. Since normalization preserves the KS symmetry, \bar{H}_{KS} Poisson commutes with both N and ζ .

3. Reduction of the Keplerian symmetry

Each of the integrals $2N$ and 2ζ is an action for \bar{H}_{KS} because their respective flows $S^1 \times \mathbb{C}^4 \rightarrow \mathbb{C}^4$ given by

$$t, z \mapsto \varphi_{2N}^t(z) = (z_1 e^{it}, z_2 e^{it}, z_3 e^{it}, z_4 e^{it}) \quad (26a)$$

and

TABLE III. Second order of the Keplerian (first) normal form \bar{H}_{KS} in Eq. (25) and the energy correction ΔE in Eqs. (32).

Terms in $72n^{-1}\bar{H}_{\text{KS}}^{(2)}$	Terms in $72\Delta E^{(2)}$
$(27\tilde{g}^2 - 17\tilde{f}_b^2 - 17\tilde{f}_e^2)n^2$ $-6\tilde{f}_b^2(7X_1^2 + 7Y_1^2 - 20X_1Y_1) - 6\tilde{f}_e^2(7X_2^2 + 7Y_2^2 - 20X_2Y_2)$ $+12\tilde{f}_e\tilde{f}_b(-7X_1X_2 + 10X_1Y_2 + 10X_2Y_1 - 7Y_1Y_2)$ $+24\tilde{f}_e\tilde{g}(3X_1X_2 + 4Y_1X_2 - 4X_1Y_2 - 3Y_1Y_2)$ $+72\tilde{f}_b\tilde{g}(X_1^2 - Y_1^2) - 9\tilde{g}^2(6X_1^2 + 6Y_1^2 + 8X_2Y_2 + 8X_3Y_3)$	$(9g^2 - 17f_e^2 - 17f_b^2)n^2$ $+12f_b^2(X_1^2 + Y_1^2 + X_1Y_1) + 12f_e^2(X_2^2 + Y_2^2 + X_2Y_2)$ $+12f_e\tilde{f}_b(2X_1X_2 + X_1Y_2 + X_2Y_1 + 2Y_1Y_2)$ $+24f_e\tilde{g}(X_2Y_1 - X_1Y_2)$ $+36g^2[X_1Y_1 + (X_2 - Y_2)^2 + (X_3 - Y_3)^2]$

$$t, z \mapsto \varphi_{2\zeta}^t(z) = (z_1 e^{-it}, z_2 e^{it}, z_3 e^{-it}, z_4 e^{it}) \quad (26b)$$

are periodic (with period 2π); here $S^1 = \mathbb{R}/2\pi\mathbb{Z}$. The Cartesian product of these two S^1 actions is a T^2 symmetry action in \mathbb{R}^8 . This action is not effective because the non-trivial element (π, π) in T^2 acts trivially on \mathbb{C}^4 . Indeed, $\varphi_{2N}^\pi \circ \varphi_{2\zeta}^\pi(z) = z$ for all $z \in \mathbb{C}^4$.

Modifying the older approach of Cushman and Sadovskii (2000) and Efstathiou, Cushman and Sadovskii (2004), we consider first momenta $\eta_+ = N + \zeta$ and $\eta_- = N - \zeta$ which generate an S^1 symmetry action on the respective \mathbb{C}^2 subspaces (z_2, z_4) and (z_1, z_3) of \mathbb{C}^4 . The Cartesian product of these actions is an effective symmetry action $T^2 \times \mathbb{C}^4 \rightarrow \mathbb{C}^4 \sim \mathbb{R}^8$ given by

$$(t_+, t_-), z \mapsto (z_1 e^{it_-}, z_2 e^{it_+}, z_3 e^{it_-}, z_4 e^{it_+}). \quad (27)$$

When reducing this T^2 symmetry, we notice that the S^1 symmetry actions on $\mathbb{C}^2 \sim \mathbb{R}^4$ generated by η_\pm are 1:1 resonant. The reduction map of such actions defines the Hopf fibration [see, e.g., Cushman and Bates (1997)]. Therefore, we face a Cartesian product of two Hopf fibrations.

Our reduction relies on algebraic invariant theory: we give a set of T^2 invariant polynomials such that any smooth T^2 invariant function can be expressed as a smooth function of these polynomials. The ring of all T^2 invariant polynomials is generated by

$$\begin{aligned} X_1 &= \frac{1}{4}(-p_1^2 - q_1^2 + p_3^2 + q_3^2), \\ X_2 &= \frac{1}{2}(-p_1 p_3 - q_1 q_3), \\ X_3 &= \frac{1}{2}(p_3 q_1 - p_1 q_3), \\ Y_1 &= \frac{1}{4}(-p_2^2 - q_2^2 + p_4^2 + q_4^2), \\ Y_2 &= \frac{1}{2}(p_2 p_4 + q_2 q_4), \\ Y_3 &= \frac{1}{2}(-p_4 q_2 + p_2 q_4), \\ N &= \frac{1}{4}(p_1^2 + p_2^2 + p_3^2 + p_4^2 + q_1^2 + q_2^2 + q_3^2 + q_4^2), \\ \zeta &= \frac{1}{4}(-p_1^2 + p_2^2 - p_3^2 + p_4^2 - q_1^2 + q_2^2 - q_3^2 + q_4^2). \end{aligned} \quad (28)$$

Vectors $\mathbf{X} = (X_1, X_2, X_3)^T$ and $\mathbf{Y} = (Y_1, Y_2, Y_3)^T$ satisfy

$$\mathbf{X}^2 = \mathbf{Y}^2 = \left(\frac{N - \zeta}{2}\right)^2 = \left(\frac{n}{2}\right)^2, \quad (29)$$

where after reduction we set $N = n$ and $\zeta = 0$. Equation (29) shows that the reduced phase space is $S^2 \times S^2$. Like \mathbf{x} and \mathbf{y} in Eq. (8), the invariants \mathbf{X} and \mathbf{Y} span the Poisson algebra which has the standard structure of $\mathfrak{so}(3) \times \mathfrak{so}(3) = \mathfrak{so}(4)$. Note that $\mathbf{L} = \mathbf{X} + \mathbf{Y}$ and $\mathbf{K} = \mathbf{X} - \mathbf{Y}$ are the KS transformed angular momentum and eccentricity (see footnote 6) vectors, respectively.

We can now reduce the T^2 action (27). Expressing the normalized Hamiltonian \bar{H}_{KS} in Eq. (25) in terms of the invariant polynomials (28) and setting, subsequently, $\zeta = 0$ and $N = n$, we obtain

$$\bar{H}_{\text{KS}}^{(0)} = 2n \quad (30a)$$

and

$$\bar{H}_{\text{KS}}^{(1)} = n[(-\tilde{f}_b + \tilde{g})X_1 - \tilde{f}_e X_2 + (\tilde{f}_b + \tilde{g})Y_1 + \tilde{f}_e Y_2]. \quad (30b)$$

The coefficients in $\bar{H}_{\text{KS}}^{(2)}$ are given in Table III.

B. Energy correction

The first reduced Hamiltonian \bar{H}_{KS} is a conserved quantity parametrized using $\Omega(E)$ -scaled fields $\tilde{f}_e, \tilde{f}_b, \tilde{g}$ in Eq. (5) but its value is related to the physical energy E of the system in a complicated way. It is adequate if we work at one constant value of E . At the same time, an approximation to E itself is essential for comparisons to other methods of normalization, to quantum computations [see, e.g., Schleif and Delos (2007, 2008)] and to experimental applications. Derivation of such approximation was already used by Robnik and Schrüfer (1985); it is described by Sadovskii and Zhilinskiĭ (1998) and Cushman and Sadovskii (2000).

Equations (5) and (21) define E implicitly. Similarly, for the first normal form we have

$$\bar{H}_{\text{KS}}(\mathbf{X}, \mathbf{Y}; \tilde{f}_e, \tilde{f}_b, \tilde{g}) = 4\Omega^{-1} := 4\varepsilon. \quad (31)$$

We rewrite Eq. (31) substituting $(\tilde{f}_e, \tilde{f}_b, \tilde{g})$ and Ω by their explicit definitions in Eq. (5) and ε . The small parameters are the strengths of the fields (F_e, F_b, G) . In order to track the orders of terms, we make the change

$(F_e, F_b, G) \rightarrow \lambda(F_e, F_b, G)$ implying $0 < \lambda \ll 1$. In this way \bar{H}_{KS} in Eq. (31) becomes a power series in λ truncated at degree $k=3$. We can now obtain from Eq. (31) a power series

$$\varepsilon(\mathbf{X}, \mathbf{Y}; \lambda) = \frac{n}{2} + \lambda \varepsilon_1(\mathbf{X}, \mathbf{Y}) + \lambda^2 \varepsilon_2(\mathbf{X}, \mathbf{Y}) + O(\lambda)^3,$$

where we compute ε_1 and ε_2 by comparing to the \bar{H}_{KS} terms in Eq. (31) of the same order in λ . Then the energy E of the system can be computed by Taylor expanding

$$E = -1/(8\varepsilon^2)$$

[which follows from Eqs. (6) and (31)] to the same order in λ , to which the normal form was obtained initially, i.e., second in our case. Finally, we undo the λ scaling and obtain the energy in the form

$$E(\mathbf{X}, \mathbf{Y}) = -\frac{1}{2n^2}[1 - \Delta E(\mathbf{X}, \mathbf{Y})], \quad (32a)$$

where

$$\Delta E = \Delta E^{(1)} + \Delta E^{(2)} + \dots, \quad (32b)$$

and each $\Delta E^{(k)}$ contains terms of order k in (F_e, F_b, G) .

Further simplification of Eqs. (32) can be achieved by substituting the n -scaled fields (f_e, f_b, g) defined in Eq. (3). This makes each term $\Delta E^{(k)}$ an order- k homogeneous polynomial in the variables $(n, \mathbf{X}, \mathbf{Y})$. We compute

$$\Delta E^{(1)} = (-f_b + g)X_1 - f_e X_2 + (f_b + g)Y_1 + f_e Y_2, \quad (33)$$

which is, up to replacing the energy scaled parameters $(\tilde{f}_e, \tilde{f}_b, \tilde{g})$ by the n -scaled parameters (f_e, f_b, g) and an overall scaling factor of n , identical to the principal order of \bar{H}_{KS} in Eq. (30b). The second-order term $\Delta E^{(2)}$ is given in Table III.

The function $\Delta E(\mathbf{X}, \mathbf{Y})$ is called energy correction; it is a Hamiltonian function defined on $S^2 \times S^2$ which can be used to study our system for fixed n and different values of E . In order to do this, we normalize ΔE again and obtain the second normal form energy correction $\Delta \mathcal{E}$.

C. Standard form of the linear term and resonances

In order to simplify the first-order energy correction $\Delta E^{(1)}$ in Eq. (33) further, we rotate $S^2 \times S^2$ so that

$$\mathbf{X} \mapsto A_-^{-1} \mathbf{x}, \quad \mathbf{Y} \mapsto A_+^{-1} \mathbf{y}, \quad (34a)$$

with matrices

$$A_{\pm} = \text{diag} \left(\frac{1}{\omega_{\pm}} \begin{pmatrix} g \pm f_b & \pm f_e \\ \mp f_e & \pm g \pm f_b \end{pmatrix}, 1 \right) \quad (34b)$$

and ω_{\pm} in Eq. (10). As a result, $\Delta E^{(1)}$ becomes a linear combination of the new coordinates x_1 and y_1 only [see Eq. (9)]. Note that all $\Delta E^{(k)}$ are homogeneous polynomials of degree k in $(n, \mathbf{x}, \mathbf{y})$ and also in the parameters (f_e, f_b, g) .

Rotations in Eqs. (34) preserve the Poisson structure and furthermore, due to the particular form of this transformation, the invariants (\mathbf{x}, \mathbf{y}) satisfy automatically Eq. (7) and generate the $\text{so}(3) \times \text{so}(3)$ Poisson algebra in Eq. (8). We obtain $\Delta E(\mathbf{x}, \mathbf{y}) = \Delta E^{(1)} + \Delta E^{(2)}$, where $\Delta E^{(1)}$ is given by Eq. (9) and $\Delta E^{(2)}$ can be computed from Table III.

On $S^2 \times S^2$, $\Delta E^{(1)}$ generates a linear Hamiltonian flow

$$t, (x, y) \mapsto (R(\omega_- t)x, R(\omega_+ t)y), \quad (35a)$$

where

$$R(t) = \text{diag} \left(1, \begin{pmatrix} \cos t & \sin t \\ -\sin t & \cos t \end{pmatrix} \right), \quad (35b)$$

which is a simultaneous rotation of each of the two spheres with frequency ratio in Eq. (11). Recall that in Sec. II.B.2 we called this residual approximate dynamical symmetry of the system Pauliean.

D. Normalization and reduction of the Pauliean symmetry

In the previous sections we constructed an approximation to the original Hamiltonian system for which the Keplerian action N is an exact first integral. In order to have a completely integrable approximation, we need one more integral, and for this reason we normalize a second time. This is possible because, as discussed in Sec. II.B.2 and as follows from Eqs. (35), the Hamiltonian vector field defined on the first reduced phase space $S^2 \times S^2$ by the lowest-order term $\Delta E^{(1)}$ of ΔE has a linear flow and we can normalize with respect to this flow.

Note that in an arbitrary 3-DOF system such second normalization may not be always possible and thus perturbed Keplerian systems such as the Hamiltonian in Eq. (2) are a special case. Indeed, we can see from Eqs. (17) and (21) that the regularized perturbation terms in the Kustaanheimo-Stiefel regularized Hamiltonian H_{KS} have a common factor of $|\mathbf{Q}| = q^2$. The latter results in a common factor of n in the normalized KS Hamiltonian H_{KS} and this leads to a common factor of $(2n^2)^{-1}$ in $E(\mathbf{X}, \mathbf{Y})$ given by Eqs. (32) with each term $\Delta E^{(k)}$ being of degree k in (\mathbf{X}, \mathbf{Y}) . Thus the linear-in- (\mathbf{X}, \mathbf{Y}) term $\Delta E^{(1)}$ has necessarily a linear flow. It appears (Valent, 2003) that Pauli (1926) relied implicitly on this property of the Hamiltonian (2) in his linear level theory and we acknowledge this in the name of the symmetry action in Eqs. (35).

1. Resonances, zones, and second normalization

When the frequency ratio ω_-/ω_+ in Eq. (11) is irrational, the flow in Eqs. (35) generated by $\Delta E^{(1)}$ defines an \mathbb{R}^1 action. If we normalize with respect to \mathbb{R}^1 , the normal form $\Delta \mathcal{E}$ will be a function only of x_1 and y_1 . The latter will become two additional global actions, and the torus bundle of the integrable approximation will be trivial. An example of the result of such trivialization is shown in Fig. 9, where the bottom projection represents the

image of the momentum map in the plane (x_1, y_1) . From the topological point of view, all such systems are the same. In Table II, we call this type of system A_0 .

If ω_-/ω_+ is rational, the flow in Eqs. (35) is periodic and hence defines an S^1 action on $S^2 \times S^2$ which we called resonant Pauliean symmetry in Sec. II.B.2. Normalizing ΔE with respect to this symmetry gives different results. The resonant normal form $\Delta \mathcal{E}$ contains resonant terms that appear in $\Delta \mathcal{E}^{(2)}$ and higher-order terms of $\Delta \mathcal{E}$ and has only one additional conserved momentum μ defined in Eq. (13); its other first integral is $\Delta \mathcal{E}$. By the usual small denominator argument, it is clear that resonant terms, especially for low-order (see footnote 7) resonances, are important even when we detune the resonance, i.e., for small $\delta(k_-, k_+) \neq 0$ in Eq. (14). Following Efsthathiou, Sadovskii, and Zhilinskiĭ (2007) we consider a $k_-:k_+$ zone in the parameter space where all systems are normalized with regard to the same $k_-:k_+$ resonant Pauliean symmetry S^1 . For a slightly detuned system, i.e., within the zone, such normalization will preserve more adequately the qualitative properties of the original nonintegrable system.

Resonances $k_-:k_+$ occur for certain angles between the electric and magnetic fields \mathbf{F} and \mathbf{G} . The condition

$$k_-/k_+ = |\mathbf{G} - 3n\mathbf{F}|/|\mathbf{G} + 3n\mathbf{F}|$$

follows from Eqs. (3), (4b), (11), and (12). For strictly orthogonal fields $d=0$, we have $\omega_+ = \omega_- = s$, and the resonance is 1:1. As a detailed example, we discuss approximate 1:1 resonances which correspond to near orthogonal fields with $d \approx 0$. These systems form the 1:1 zone. Recall from Fig. 3 that, in any fixed $s > 0$ section of the parameter space, the strictly orthogonal fields correspond to the $d=0$ segment (SZ) and the 1:1 zone is a strip with (SZ) in the middle.

The Hamiltonian $\Delta E(\mathbf{x}, \mathbf{y})$ in Eq. (32b) describes a 2-DOF system on $S^2 \times S^2$, which in general has no other exact first integrals. Pulled back to the original KS space \mathbb{R}^8 with coordinates (q, p) , $\Delta E(\mathbf{x}(q, p), \mathbf{y}(q, p))$ defines a 4-DOF system in \mathbb{R}^8 with three exact integrals N , ζ , and ΔE .

We normalize ΔE with respect to the generator μ in Eq. (13) of the exact $k_-:k_+$ resonant S^1 symmetry. Truncating the normal form at a certain order, we obtain a 2-DOF Liouville integrable approximation system on $S^2 \times S^2$ with Hamiltonian (or the second normal form),

$$\Delta \mathcal{E} = \Delta \mathcal{E}^{(1)} + \Delta \mathcal{E}^{(2)} + \dots, \quad (36)$$

such that $\{\Delta \mathcal{E}, \mu\} = 0$, i.e., μ and $\Delta \mathcal{E}$ become exact first integrals. The first term in $\Delta \mathcal{E}$ is

$$\Delta \mathcal{E}^{(1)} = \omega_- x_1 + \omega_+ y_1 = \omega(\mu + \delta\nu), \quad (37)$$

where momenta μ and ν are defined in Eq. (13). It equals $\Delta E^{(1)}$ in Eq. (14) because $\{\nu, \mu\} = 0$. Higher-order terms are specific to the particular resonance. For a general $k_-:k_+$ resonance, normalization should be carried out to least order (see footnote 7) $k_- + k_+$ where the lowest-order specific resonant term π_1 appears. Thus for

TABLE IV. Coefficients of the second-order term $\Delta \mathcal{E}^{(2)}$ in the 1:1 second reduced Hamiltonian. To represent invariants μ , ν , and π_1 as functions on the first reduced space $S^2 \times S^2$ or the KS space \mathbb{R}^8 , use Eqs. (47) and (44). The relation of dimensionless parameters a^2 and d , and smallness parameter s to the electric and magnetic field strengths, is given in Eqs. (3) and (4b).

Monomial	Coefficient $\times 24s^{-2}(1-4d^2)^{3/2}$
n^2	$a^{-2}(1-4d^2)^{1/2}[(2a^2+7)a^4-68d^4+(-36a^4+2a^2+17)d^2]$
μ^2	$\{(1-4d^2)^{1/2}[-6a^4+(8d^2+4)a^2+22d^2-7]-10(a^2+2d^2-1)(4d^2-1)\}$
ν^2	$\{10(a^2+2d^2-1)(4d^2-1)+(1-4d^2)^{1/2}[-6a^4+(8d^2+4)a^2+22d^2-7]\}$
$\mu\nu$	$-24d(1-4d^2)^{1/2}(a^4-a^2+5d^2-1)$
π_1	$3[a^2(1-4d^2)^{1/2}+a^2-2d^2](4d^2-1)$

the 1:1 resonance we should go to the second order $\Delta \mathcal{E}^{(2)}$. As an example, terms in $\Delta \mathcal{E}^{(2)}$ of the 1:1 resonant normal form can be obtained from Table IV and Eq. (13).

ΔE can be normalized either in $S^2 \times S^2$ or in \mathbb{R}^8 . We describe both approaches. Note that because of the formal similarity of $\Delta E^{(1)}$ and $\bar{H}_{\text{KS}}^{(1)}$, the following discussion applies also to the second normalization of \bar{H}_{KS} which is useful when working at a constant physical energy level.

The most studied resonance is 1:1. Instead of restricting immediately to this particular case, we give basic formulas for the general $k_+:k_-$ resonance, which can be obtained at no additional cost following the general outline of the 1:1 work. We illustrate these relations further using the 1:1 and 1:2 systems. Analysis of $k_+:k_-$ resonances can also be found in Karasev and Novikova (2005).

a. Second normalization in $S^2 \times S^2$

Normalization on $S^2 \times S^2$ is done most easily in coordinates

$$u_1 = x_1, \quad u_2 = x_2 + ix_3, \quad \bar{u}_2 = x_2 - ix_3, \quad (38)$$

$$w_1 = y_1, \quad w_2 = y_2 + iy_3, \quad \bar{w}_2 = y_2 - iy_3.$$

The Lie operator $\{\mu, \cdot\}$ acts diagonally on the space of monomials in (u, w) and the standard Lie series algorithm³⁹ applies immediately.

b. Second normalization in \mathbb{R}^8

Instead of normalizing on $S^2 \times S^2$, we can reexpress first energy correction ΔE in the KS coordinates (q, p) on \mathbb{R}^8 . Then the lowest-order term $\Delta E^{(1)}$ in Eq. (9) and the momentum μ in Eq. (13) become quadratic functions

³⁹See Gröbner (1960, 1967), Deprit (1969), and Meyer and Hall (1992) for a general introduction. The adaptation for $S^2 \times S^2$ is given by Efsthathiou, Cushman, and Sadovskii (2004) and Efsthathiou (2005).

of (q, p) that can be written, after an appropriate linear change of coordinates $(q, p) \rightarrow (\xi, \eta)$, as respective linear combinations

$$\Delta E^{(1)} = \frac{1}{2}(\omega_- N_1 + \omega_+ N_2 - \omega_- N_3 - \omega_+ N_4) \quad (39)$$

and

$$\mu = \frac{1}{2}(k_- N_1 + k_+ N_2 - k_- N_3 - k_+ N_4) \quad (40)$$

of four terms,

$$N_i = \frac{1}{2}(\eta_i^2 + \xi_i^2) \quad \text{with } i = 1, \dots, 4, \quad (41)$$

representing four one-dimensional harmonic oscillators. Subsequently, ΔE is normalized straightforwardly with respect to the linear diagonal flow generated by the dominant resonant part $\omega \mu$ of $\Delta E^{(1)}$ in Eq. (39). We now give more details. The required change of coordinates,

$$\begin{aligned} (q_1, q_3)^T &\mapsto C(f_b - g, f_e)(\xi_1, \xi_3)^T, \\ (p_1, p_3)^T &\mapsto C(f_b - g, f_e)(\eta_1, \eta_3)^T, \\ (q_2, q_4)^T &\mapsto C(f_b + g, -f_e)(\xi_4, \xi_2)^T, \\ (p_2, p_4)^T &\mapsto C(f_b + g, -f_e)(\eta_4, \eta_2)^T, \end{aligned} \quad (42)$$

is given by the 2×2 matrix,

$$C(a, b) = \frac{1}{\sqrt{2\sigma\sqrt{\sigma-a}}} \begin{pmatrix} -b & \sigma - a \\ a - \sigma & -b \end{pmatrix} \in \text{SO}(2), \quad (43)$$

with $\sigma = (a^2 + b^2)^{1/2}$. This transformation is orthogonal and symplectic. In the new coordinates (ξ, η) we have

$$N = \frac{1}{2}(N_1 + N_2 + N_3 + N_4), \quad (44a)$$

$$\zeta = \frac{1}{2}(-N_1 + N_2 - N_3 + N_4),$$

and

$$\begin{aligned} x_1 &= \frac{1}{2}(N_1 - N_3), & y_1 &= \frac{1}{2}(N_2 - N_4), \\ x_2 &= \frac{1}{2}(\eta_1 \eta_3 + \xi_1 \xi_3), & y_2 &= \frac{1}{2}(\eta_2 \eta_4 + \xi_2 \xi_4), \\ x_3 &= \frac{1}{2}(\eta_3 \xi_1 - \eta_1 \xi_3), & y_3 &= \frac{1}{2}(\eta_4 \xi_2 - \eta_2 \xi_4). \end{aligned} \quad (44b)$$

The lowest order in Eq. (39) represents a harmonic four-oscillator. In the $k_-:k_+$ zone, its frequencies are close to the $k_+:k_-:(-k_+):(-k_-)$ resonance. For the same reasons as in the previous section, we normalize with respect to the exact $k_+:k_-:(-k_+):(-k_-)$ resonance.

For near orthogonal fields, the resonance is 1:1:(-1):(-1) and we normalize with respect to the linear periodic flow defined by the momentum

$$\mu = x_1 + y_1 = \frac{1}{2}(N_1 + N_2 - N_3 - N_4) \quad (45)$$

using again the standard Lie series algorithm. The resulting $\Delta \mathcal{E}^{(2)}(\xi, \eta)$ follows from Table IV and Eqs. (44).

2. Reduction of the Pauliean symmetry

The final step in the construction of the integrable approximation for the system with the Hamiltonian (2) is the reduction of the residual dynamical S^1 symmetry of the second normal form energy correction $\Delta \mathcal{E}$. Since $\{\Delta \mathcal{E}, \mu\} = 0$ by construction, $\Delta \mathcal{E}$ is invariant under the flow of the Hamiltonian vector field X_μ of μ . This remains true no matter if we consider $\Delta \mathcal{E}$ and μ as functions on $S^2 \times S^2$ or \mathbb{R}^8 . For simplicity, and since the reduction map $\mathbb{R}^8 \rightarrow S^2 \times S^2$ is already defined, we start with the second normalized system on $S^2 \times S^2$ and we proceed with its final reduction by constructing the second reduced space $P_{n,m}$ and the second reduced Hamiltonian \mathcal{H} on it. We give details of the 1:1 case.⁴⁰

a. Invariants of the $k_-:k_+$ resonant S^1 action

The $k_-:k_+$ momentum μ generates an S^1 action on $S^2 \times S^2$,

$$\varphi_\mu^t: [t, (x, y)] \mapsto [R(k_- t)x, R(k_+ t)y], \quad (46)$$

where the rotation matrix $R(t)$ is defined in Eq. (35b). The algebra of polynomials in (x, y) invariant under the S^1 action in Eq. (46) is generated by the invariants

$$\begin{aligned} \mu &= k_- x_1 + k_+ y_1, & \nu &= k_- x_1 - k_+ y_1, \\ \pi_1 &= \text{Re } \mathfrak{p}, & \pi_2 &= \text{Im } \mathfrak{p}, \end{aligned} \quad (47)$$

$$\pi_3 = 4(x_2^2 + x_3^2) \geq 0, \quad \pi_4 = 4(y_2^2 + y_3^2) \geq 0,$$

where in coordinates $z_i = \xi_i - i\eta_i$ or (u_2, w_2) from Eq. (38),

$$\mathfrak{p} = (z_1 \bar{z}_3)^{k_+} (z_2 \bar{z}_4)^{k_-} = 2^{k_- + k_+} u_2^{k_+} \bar{w}_2^{k_-}.$$

From Eq. (7) we obtain immediately that

$$\begin{aligned} \pi_3 &= 4N_1 N_3 = n^2 - (\nu + \mu)^2 / k_-^2, \\ (48a) \end{aligned}$$

$$\pi_4 = 4N_2 N_4 = n^2 - (\nu - \mu)^2 / k_+^2.$$

Furthermore, our invariants satisfy

$$\pi_1^2 + \pi_2^2 = \pi_3^{k_+} \pi_4^{k_-} = \rho_{k_-:k_+}(n, \mu, \nu)^2, \quad (48b)$$

where $\rho_{k_-:k_+} \geq 0$ is a function of (n, μ, ν) .

b. Pauliean orbit space \mathcal{O}_n

Orbits of a symmetry action are distinguished by the values of invariants (Michel and Zhilinskiĭ, 2001b). For a fixed value $n > 0$ of the Keplerian action, we can choose μ , ν , and π_1 as three principal invariants labeling continuously the orbits of the Pauliean S_1 symmetry up to an additional discrete label that may be given by (the sign of) the auxiliary invariant π_2 . We can see from Eqs. (48) that all such orbits form a closed ball \mathcal{O}_n which can be embedded in \mathbb{R}^3 with coordinates (μ, ν, π_1) . This orbit

⁴⁰For the 1:1 systems, we follow Cushman and Sadovskii (2000) with some changes in notation: their invariants (π_1, \dots, π_6) are denoted here by $(\nu, \pi_1, \pi_2, \mu, \pi_3, \pi_4)$.

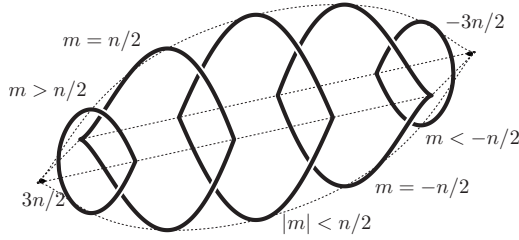


FIG. 19. Characteristic intersections (thick solid lines) of the orbit space $\mathcal{O}_n^{1:2}$ for the 1:2 resonance with constant- m planes. Each intersection also represents the projection of the second reduced phase spaces $P_{n,m}^{1:2}$ with the plane $\{\pi_2=0\}$. We show intersections for seven different values of m starting at $m=m_{\max}=3n/2$ and ending at $m=-m_{\max}$.

space is shown in Figs. 5 and 19 for the 1:1 and 1:2 resonances, respectively. Points of $\partial\mathcal{O}_n$ represent orbits with $\pi_2=0$, while interior points represent pairs of orbits distinguished by the sign of π_2 . Orbits with $\pi_2>0$ and $\pi_2<0$ are mapped into each other by the residual discrete symmetry operation T_s (see Sec. III.A and Table I) which acts as

$$T_s: (\mu, \nu, \pi_1, \pi_2) \mapsto (\mu, \nu, \pi_1, -\pi_2). \quad (49)$$

Immersing in \mathbb{R}^3 reflects the geometry of \mathcal{O}_n . The general orbit space $\mathcal{O}_n^{k_-:k_+}$ looks like a ‘‘pillow.’’ For $\pi_1=\pi_2=0$, it has four singular points and may have line singularities. More specifically, we can see from Eq. (48b) that $\partial\mathcal{O}_n^{k_-:k_+} \cap \{\pi_1=0\}$ is a rectangle with corners at $m=\pm m_{\text{crit}}$ and $m=\pm m_{\max}$, where

$$m_{\max} = \frac{k_+ + k_-}{2}n \quad \text{and} \quad m_{\text{crit}} = \frac{|k_+ - k_-|}{2}n. \quad (50)$$

The corners represent Keplerian ellipses (Sec. II.C.3.a). For $\mathcal{O}_n^{1:1}$ they are conical and are the only singularities; for $\mathcal{O}_n^{1:2}$, the $m=\pm m_{\text{crit}}=\pm n/2$ corners become cusplike and there are also two singular lines. Points on these lines represent short \mathbb{T}^2 orbits. For $k_{\pm}>3$ all sides of the rectangle represent two different families of short \mathbb{T}^2 orbits.

Michel and Zhilinskii (2001a) considered the second reduced Hamiltonian \mathcal{H} as a function on \mathcal{O}_n . Such study enables one to distinguish certain possible qualitatively different systems. The analysis on the reduced phase space $P_{n,m}$ makes the classification more substantial.

c. Second reduced phase space $P_{n,m}$

Fixing $\mu=m$ in Eqs. (48), we obtain the second reduced phase space $P_{n,m}$ as a semialgebraic variety defined by Eq. (48b) with

$$n \geq 0, \quad |m| \leq m_{\max}, \quad \nu \in [\nu_{\min}, \nu_{\max}], \quad (51)$$

where

$$\nu_{\min} = \max(-nk_- - m, -nk_+ + m),$$

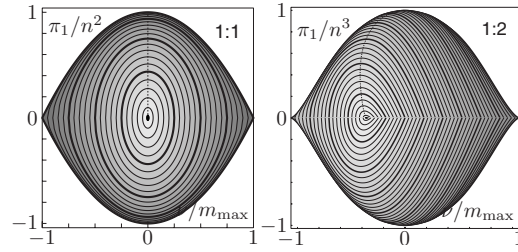


FIG. 20. Projections of the reduced phase spaces $P_{n,m}^{1:1}$ and $P_{n,m}^{1:2}$ on the $\pi_2=0$ plane with coordinates (ν, π_1) . For $P_{n,m}^{1:1}$ we see $m=0$ (outmost boundary), $0<|m|<n$ (intermediate smooth boundaries), and $m=\pm n$ (point 0) (cf. Figs. 4 and 5); for $P_{n,m}^{1:2}$ we see boundaries entirely for sufficiently large $m \leq m_{\max}$ and partially for $m > -m_{\text{crit}}$ (cf. Fig. 19).

$$\nu_{\max} = \min(nk_- - m, nk_+ + m).$$

For all m , $P_{n,m}$ can be immersed in the ambient space \mathbb{R}^3 with coordinates (ν, π_1, π_2) as a surface of revolution around axis ν . So it suffices to consider the projection of $P_{n,m}$ on the plane $\{\pi_2=0\}$ with coordinates (ν, π_1) , as shown in Fig. 20 for the 1:1 resonance. Such a projection is compatible with the T_s symmetry (49) of the system and is nothing but a constant- m section of \mathcal{O}_n (cf. Fig. 5). We can see that the spaces $P_{n,\pm n}$ consist of one point and that $P_{n,m}$ with $|m|<n$ has topology S^2 .

d. Second reduced phase spaces $P_{n,m}^{1:1}$ and $P_{n,m}^{1:2}$

In the 1:1 case, the spaces $P_{n,m}^{1:1}$ and $P_{n,-m}^{1:1}$ have the same representation and $P_{n,m}^{1:1}$ is invariant under

$$\mathbb{Z}_2: (\mu, \nu, \pi_1, \pi_2) \mapsto (\mu, -\nu, \pi_1, \pi_2), \quad (52)$$

which is the additional discrete symmetry of $\mathbf{G} \perp \mathbf{F}$ [i.e., exact 1:1 resonant systems with $d=0$ (see Sec. III.A)]. Furthermore, the space $P_{n,m=0}^{1:1}$ has two conical singular points at $(\nu, \pi_1)=(\pm n, 0)$ (see Fig. 4), while $P_{n,m \neq 0}^{1:1}$ is diffeomorphic to a smooth sphere. Each smooth point on $P_{n,m}^{1:1}$ lifts to a circle S^1 in $S^2 \times S^2$ and subsequently to a \mathbb{T}^3 in \mathbb{R}^8 and a \mathbb{T}^2 in \mathbb{R}^6 . Two singular points of $P_{n,0}^{1:1}$ and two single point spaces $P_{n,\pm n}^{1:1}$ lift to four points on $S^2 \times S^2$ and to four Keplerian ellipses S^1 in \mathbb{R}^6 . In the 1:2 case, all spaces $P_{n,m < m_{\max}}^{1:2}$ are nonsmooth S^2 . For $|m| < m_{\text{crit}}$, they have two conical singularities similar to $P_{n,0}^{1:1}$ (a ‘‘lemon’’; see Fig. 4) and have one such singularity for $m_{\max} > |m| > m_{\text{crit}}$ (a ‘‘turnip’’; see Fig. 19).

e. Spherical deformation of $P_{n,m}^{k_-:k_+}$

Since the space $P_{n,m}^{k_-:k_+}$ for $|m| < m_{\max}$ has the topology of S^2 , it is possible to map⁴¹ $P_{n,m}^{k_-:k_+}$ explicitly to a smooth-

⁴¹For 1:1 systems, spherical-like coordinates for the second reduced system were quite popular. However, their singularities impeded the analysis of the geometry and the dynamics on $P_{n,m}^{1:1}$. See Secs. VIII.C.2 and Uzer (1990), Farrelly et al. (1992), Gourlay et al. (1993), and von Milczewski and Uzer (1997a), discussed in Sec. VIII.C.5, as well as Main et al. (1998) and Berglund and Uzer (2001).

sphere. This map should be singular at the isolated singular points of $P_{n,m}^{k_-:k_+}$. Because $P_{n,m}^{k_-:k_+}$ is a surface of revolution, the map can be defined relatively easily. We now give more details.

Taking the components of (\mathbf{x}, \mathbf{y}) or, equivalently, the canonical four-oscillator coordinates in Sec. IV.D.1.b, which we may rewrite as

$$(\xi_i, \eta_i) = \sqrt{2N_i}(\sin \phi_i, \cos \phi_i) \quad \text{with } i = 1, \dots, 4,$$

using canonical angle variables ϕ_i conjugate to oscillator actions N_i , we can define⁴² conjugate canonical angle

$$\varphi = k_-(\phi_1 - \phi_3) - k_+(\phi_2 - \phi_4) \quad (53)$$

and action

$$\frac{\nu}{k_- + k_+} = \frac{k_-(N_1 - N_3)}{2(k_- + k_+)} - \frac{k_+(N_2 - N_4)}{2(k_- + k_+)}, \quad (54)$$

which are action-angle variables of the lowest-order second reduced system whose Hamiltonian $\Delta\mathcal{E}_{n,m}^{(1)}$ depends only on ν and dynamical parameters n and m . Furthermore, the two other Pauliean invariants π_1 and π_2 can be now rewritten as

$$(\pi_1, \pi_2) = \rho_{k_-:k_+}(n, m, \nu)(\cos \varphi, \sin \varphi).$$

As in the 1:1 case, one can go further and define the longitude angle $\theta \in [0, \pi]$ such that

$$\nu = \sigma m_{\text{crit}} + j \cos \theta, \quad j = m_{\text{max}} - m, \quad m \geq m_{\text{crit}},$$

$$\nu = -\sigma m + j \cos \theta, \quad j = m_{\text{max}} - m_{\text{crit}}, \quad |m| \leq m_{\text{crit}},$$

$$\nu = -\sigma m_{\text{crit}} + j \cos \theta, \quad j = m_{\text{max}} + m, \quad m \leq -m_{\text{crit}},$$

where $\sigma = \text{sgn}(k_- - k_+)$ and the algebraic relation (48b) becomes

$$\pi_1^2 + \pi_2^2 = \rho_{k_-:k_+}^2 = \chi_{k_-:k_+}^2 j^2 \sin^2 \theta,$$

where the function $\chi_{k_-:k_+} \geq 0$ of (n, m, ν) is obtained by combining the above formulas with Eqs. (48).

f. Second reduced energy correction on $P_{n,m}$

Expressing the second normalized energy correction $\Delta\mathcal{E}$ in Eq. (36) in terms of (ν, π_1, π_2) and $\mu = m$ gives the second reduced energy correction

$$\Delta\mathcal{E} = \Delta\mathcal{E}^{(1)} + \Delta\mathcal{E}^{(2)} + \dots \quad (55)$$

on $P_{n,m}$, where

$$\Delta\mathcal{E}^{(1)} = \frac{1}{2}(\omega_- + \omega_+)m + \frac{1}{2}(\omega_- - \omega_+)\nu. \quad (56)$$

Table IV gives $\Delta\mathcal{E}^{(2)}$ for the 1:1 resonance. Because of the \mathcal{T}_s symmetry (49), $\Delta\mathcal{E}$ is a function of (ν, π_1) , dynamical parameters (n, m) , and external parameters (s, d, a^2)

only, i.e., it does not depend on π_2 . Furthermore, it is convenient to remove from $\Delta\mathcal{E}$ terms that do not depend on (ν, π_1) and are thus constant on $P_{n,m}$. This gives the Hamiltonian

$$\mathcal{H}(\nu, \pi_1) = \Delta\mathcal{E}(\nu, \pi_1) - \Delta\mathcal{E}(0, 0). \quad (57)$$

Note that up to an extra detuning term $d\nu$ this Hamiltonian is equivalent to the one used by Cushman and Sadovskii (1999, 2000). Using Eq. (47), \mathcal{H} is expressed as function $\mathcal{H}(\mathbf{x}, \mathbf{y})$ on $S^2 \times S^2$; using Eqs. (34) and (28), \mathcal{H} can be expressed in terms of the (q, p) coordinates on the KS space \mathbb{R}^8 .

g. Reduced dynamics and trajectories on $P_{n,m}$

The second reduced space $P_{n,m}$ is a symplectic leaf of $S^2 \times S^2$ equipped with a nonlinear Poisson structure. In the general $k_-:k_+$ case, the latter is

$$\{\nu, \pi_1\} = 2k_-k_+\pi_2,$$

$$\{\nu, \pi_2\} = -2k_-k_+\pi_1, \quad (58)$$

$$\{\pi_1, \pi_2\} = -k_-k_+\partial\rho_{k_-:k_+}^2(n, m, \nu)/\partial\nu$$

[see also Karasev and Novikova (2005)]. The algebras are deformations of $\mathfrak{so}(3)$: the Poisson algebra generated by

$$(J_1, J_2, J_3) = (2k_-k_+)^{-1}(\pi_1\chi_{k_-:k_+}^{-1}, \pi_2\chi_{k_-:k_+}^{-1}, j \cos \theta)$$

has the structure of $\mathfrak{so}(3)$. The reduced dynamics on $P_{n,m}$ is defined by the Euler-Poisson equations $\dot{\nu} = \{\nu, \mathcal{H}\}$, $\dot{\pi}_1 = \{\pi_1, \mathcal{H}\}$, and $\dot{\pi}_2 = \{\pi_2, \mathcal{H}\}$.

For our purposes (see Sec. V) solving these equations is usually unnecessary because we only need to know the topology of the trajectories of the second reduced system for different values h of \mathcal{H} . Since we have a 1-DOF system, trajectories are level sets of \mathcal{H} on $P_{n,m}$. To find them on $P_{n,m}$ immersed in \mathbb{R}^3 , we should simply find intersections

$$\lambda_{n,m,h} = \{\mathcal{H}(\nu, \pi_1) = h\} \cap P_{n,m} \quad (59)$$

in \mathbb{R}^3 of the constant h -level set of \mathcal{H} and $P_{n,m}$. Again due to the above-mentioned symmetry \mathcal{T}_s , it is sufficient to study projections of $\lambda_{n,m,h}$ on the \mathbb{R}^2 plane (ν, π_1) . We obtain our results by studying such projected intersections in Sec. V.

E. Ambiguity of the integrable approximation

Within the framework of the Lie series method (Gröbner, 1960, 1967; Deprit, 1969), the near identity canonical transformation used to put a Hamiltonian $H = H_0 + H_1 + \dots$ in the normal form $\tilde{H} = H_0 + \tilde{H}_1 + \dots$ is given by the time-1 flow of the generator $W = W_1 + W_2$

⁴²Use Eqs. (44) and (13); for 1:1 systems, use the particular form (47) and compare to Cushman and Sadovskii (2000, Sec. 5.4, pp. 189–190). For other resonances, Karasev and Novikova (2005) used similar coordinates to define cylindrical charts of $P_{n,m}$ with singularities at the poles.

$+\dots$ written as a formal series.⁴³ In each order j , the generator W_j can be written as a sum U_j+Z_j such that⁴⁴ $U_j=\{U'_j,H_0\}$ for some U'_j and $\{Z_j,H_0\}=0$, i.e., $Z_j \in \ker \text{ad}_{H_0}$ where $\text{ad}_{H_0}=\{H_0,\cdot\}$. While U_j contributes to the j th order term \tilde{H}_j of the normal form and is defined uniquely by the homological equation, the extra term Z_j remains undetermined. It does not affect \tilde{H}_j but in general it does modify higher-order terms in the normal form.⁴⁵

For systems in the 1:1 zone, going through the construction of the integrable approximation (KS normalization, energy inversion, and Pauliean normalization), one finds that to our order of normalization the only additional modification of the second normalized energy correction $\Delta\mathcal{E}$ may come from the part Z' of Z_1 [of degree 4 in (q,p)] which is involved at the first step of the KS normalization and which Poisson commutes with μ . The resulting modification is the addition to $\Delta\mathcal{E}^{(2)}$ of $\{\Delta\mathcal{E}^{(1)},Z'\}$. It follows (see footnote 43) that $Z'=\alpha\pi_2$ which gives $Z''=-\omega\delta\alpha\pi_1$. So the Keplerian normal forms that appear in the literature⁴⁶ may differ from the KS normal form in Eqs. (32) and Table III due to an appropriate term $Z_1 \in \ker \text{ad}_N$. We have verified this on several examples. At the level of the second 1:1 normal form, the only difference may be due to $\alpha\pi_2$ in W_1 .

The freedom in the construction of the normal form $\Delta\mathcal{E}$ raises the question on whether the results in Sec. III are not an artifact of the particular choice of the generator W . We turn again to the 1:1 example. We first notice that the ambiguity term $-\alpha\omega\delta\pi_1$ vanishes for exactly orthogonal fields where $d=\delta=0$. For nearly orthogonal fields (the 1:1 zone, $|d|\ll 1$), $\Delta\mathcal{E}$ may be modified qualitatively if the π_1 term (Table IV) changes considerably. However, making this term vanish requires $\alpha\sim sa^2/d+O(d)$, which for most 1:1 systems is much larger than the allowed magnitude s of the terms in W_1 . So for these systems the results in Sec. III are structurally stable. The near-Stark 1:1 systems with $a^2\leq|d|\ll 1$ are exceptional. For them, the π_1 term in $\Delta\mathcal{E}^{(2)}$ can be eliminated and higher orders must be considered to complete the analysis.

⁴³Note that in order for $\{W,H\}$ and, consequently, \tilde{H} to retain the reversal T_s symmetry of H (Sec. III.A), the generator W should be antisymmetric with respect to T_s .

⁴⁴Recall that for the KS normalization, $H_0=N$ and that in the second normalization, we use the resonant part μ of H_0 .

⁴⁵Terms Z_j are widely known to cause ambiguity of effective spectroscopic Hamiltonians (Watson, 1967, 1968); it was also suggested to use them for additional simplification of the normal form [see, e.g., Gaeta (1997, 1999, 2001)].

⁴⁶See Solov'ev (1981, 1982, 1983), Grozdanov and Solov'ev (1982), Braun and Solov'ev (1984a, 1984b), Braun (1993), Main et al. (1998), and Schleif and Delos (2007, 2008), and the discussion in Sec. VIII.C.1.

V. DYNAMICAL STRATA IN THE PARAMETER SPACE

Together with Sec. VI this section is the principal workground of our review. We explain how the results announced in Sec. III for the 1:1 zone are obtained from the study of the integrable 1-DOF system with the Hamiltonian \mathcal{H} in Eq. (55) on the reduced space $P_{n,m}$. In order to construct the bifurcation diagrams \mathcal{BD} (Sec. II.C.4) in Table II, we study regular and critical intersections λ in Eq. (59) of the h -level sets of \mathcal{H} and $P_{n,m}$. We specify all critical values of the energy-momentum map \mathcal{EM} and the corresponding critical fibers, i.e., RE and singular fibers (see Sec. II.C.3). Subsequently in Sec. VI, we compute monodromy for nonsimply connected cells of \mathcal{BD} . Results for higher resonances can be obtained by a similar approach.

A. Energy-momentum map \mathcal{EM} and its image \mathcal{BD}

The principal tools in the global study of our system are the maps \mathcal{EM} introduced in Eqs. (15) of Sec. II. They define integrable fibrations with fibers labeled by the values (n,m,h) of the Keplerian action N , the nontrivial part \mathcal{H} of the second reduced energy correction $\Delta\mathcal{E}$ obtained in Sec. IV.D.2.f, and the Pauliean momentum μ defined in Eq. (47), respectively. Depending on the total space of the fibration, both \mathcal{H} and μ are pulled back to \mathbb{R}^8 or to $\mathbb{S}^2\times\mathbb{S}^2$ by the respective reduction maps. Recall from Sec. IV.E that using $\Delta\mathcal{E}$ is qualitatively similar to using the second normal form \tilde{H}_{KS} in the earlier work (Cushman and Sadovskii, 2000; Efsthathiou, Cushman, and Sadovskii, 2004; Efsthathiou, Sadovskii, and Zhilinskii, 2007) but is more convenient for practical comparisons to quantum calculations and possible experiments.

The image (range) of \mathcal{EM} is the base of the fibration; regular \mathcal{EM} values represent generic fibers and lie inside the range. For the \mathcal{EM} in Eq. (15a) the base is a connected domain in \mathbb{R}^3 with coordinates (n,m,h) and connected components of its generic fibers $\mathcal{EM}^{-1}(n,m,h)$ are \mathbb{T}^4 tori in the KS space \mathbb{R}^8 . For the map \mathcal{EM}_n in Eq. (15b), the base is a connected domain in \mathbb{R}^2 with coordinates (m,h) which is a constant n section of the three-dimensional image of \mathcal{EM} . Connected components of the generic fiber $\mathcal{EM}_n^{-1}(m,h)$ are \mathbb{T}^2 tori in $\mathbb{S}^2\times\mathbb{S}^2$. By the inverse KS map, the fiber $\mathcal{EM}^{-1}(n,m,h)$ is related to a \mathbb{T}^3 in the original physical phase space \mathbb{R}^6 .

1. Constant h level sets of the reduced system

In the ambient space \mathbb{R}^3 with coordinate functions (ν,π_1,π_2) , we study intersections $\lambda_{n,m,h}$ in Eq. (59). Since for all $|m|<m_{\text{max}}$ the space $P_{n,m}$ is a two-sphere which may have at most two isolated singular points (Sec. IV) and \mathcal{H} is a smooth function $\mathbb{R}^3\rightarrow\mathbb{R}$, typical connected components of $\lambda_{n,m,h}$ are smooth circles \mathbb{S}^1 . Components of critical intersections can be a single point, a union of two circles sharing a point (a figure 8), or they can be singular circles that include the singular point(s) of $P_{n,m}$. The inverse map \mathcal{EM}^{-1} sends smooth circles to regular

tori, single points to relative equilibria, while nonsmooth circles and figure 8's are lifted to singular fibers. So the analysis of $\lambda_{n,m,h}$ provides the description of the fibers.

Recall that it is sufficient to study the projection of $\lambda_{n,m,h}$ on the plane (ν, π_1) where the level curve $\mathcal{H}=h$ is given by

$$\pi_1 = f_{n,m,h}(\nu). \quad (60a)$$

On the other hand, we can see from Eqs. (48b) and (51) that the projection of $P_{n,m}$ on the plane (ν, π_1) is either a point $(\nu, \pi_1) = (m_{\text{crit}}, 0)$ for $|m| = m_{\text{max}}$ or a disk for $|m| < m_{\text{max}}$ with boundary given by

$$\pi_1 = \pm \rho_{k_-, k_+}(n, m, \nu). \quad (60b)$$

For certain values of m , the latter may have singular points (cf. Fig. 20). The exact form of intersections $\lambda_{n,m,h}$ can be deduced by studying the curves defined by ρ and f . Typically we find that $\lambda_{n,m,h}$ is a curved segment, which becomes a circle S^1 on $P_{n,m}$ or, in some cases, a union of several such disjoint segments. The former situation occurs when for given n, m , and h , either of the two equations

$$f_{n,m,h}(\nu) \pm \rho_{k_-, k_+}(n, m, \nu) = 0 \quad (60c)$$

has two distinct real roots $\nu_{1,2}(n, m, h)$ in $[-m_{\text{max}}, m_{\text{max}}]$; the latter corresponds to the case with more such solutions. This describes all typical intersections.

2. Relative equilibria and other critical fibers

In the trivial case $m = \pm m_{\text{max}}$, the space $P_{n, \pm m_{\text{max}}}$ and the intersection $\lambda_{n, \pm m_{\text{max}}, h}$ are the point $(\nu, \pi_1, \pi_2) = (\pm m_{\text{crit}}, 0, 0)$ at which the critical energy is given by $\mathcal{H}_{n, \pm m_{\text{max}}}(0, 0)$. In the KS space \mathbb{R}^8 , the critical fiber is a \mathbb{T}_n^2 RE; in the original phase space \mathbb{R}_*^6 , it corresponds to the Keplerian S^1 RE (Sec. II.C.3).

Critical intersections $\lambda_{n,m,h}$ with $|m| < m_{\text{max}}$ can typically either include singular points of $P_{n,m}$ or include a tangency of f and one of the ρ curves in Eq. (60b). In the latter case, one of the two equations

$$\pm \frac{\partial \rho_{n,m}}{\partial \nu} = \frac{\partial f_{n,m,h}}{\partial \nu} \quad (61)$$

is satisfied. Solving them for ν at given (n, m) gives critical values $\nu_c^\pm(n, m)$ whose superscript \pm indicates the particular Eq. (61) they satisfy. Substituting $\nu_c^\pm(n, m)$ into Eq. (60c) (with appropriate sign) gives critical $\pi_{1c}(n, m)$. Subsequently, the critical energy $h_c(n, m)$ is obtained as $\mathcal{H}_{n,m}(\nu_c, \pi_{1c})$. When $\nu_c^\pm(n, m)$ is the only possible real root for either of Eq. (60c), h_c gives the energy of a relative equilibrium $S^1 \subset S^2 \times S^2$ (or, equivalently, $\mathbb{T}^2 \subset \mathbb{R}^6$ and $\mathbb{T}^3 \subset \mathbb{R}^8$). If Eq. (60c) has more roots, we should investigate the connectivity of λ_{n,m,h_c} .

3. Bifurcation diagrams

We are now in a position to construct stratified images \mathcal{BD} of the \mathcal{EM} map. To this end, we assemble all pieces of information obtained in the previous section. Specifi-

cally, we find the sets of critical \mathcal{EM} values by finding critical energies $h_c(n, m)$ for all possible $m \in [m', m''] \subseteq [-m_{\text{max}}, m_{\text{max}}]$ as explained in Secs. V.A.1 and V.A.2. Typically $[m', m'']$ is a closed interval and the map $[m', m''] \rightarrow \mathbb{R}^2: m \mapsto (m, h_c(n, m))$ defines smooth curve segments in the range of the \mathcal{EM} map with fixed n . Once for given ns (in the 1:1 resonance zone the product of n and s plays the role of the small perturbation parameter), f , and g , all critical sets are found, we obtain the \mathcal{BD} of the system.

The full \mathcal{BD} is a three-dimensional domain in the (n, m, h) space. One natural possibility is to study first its constant ns slices \mathcal{BD}_n and then consider how they may vary in a small but finite interval of n values for sufficiently small $ns > 0$. Clearly, the only results of general interest are the ones for which the \mathcal{BD} topology does not change qualitatively. Furthermore, qualitative characteristics, such as monodromy, should not change if the analysis is extended to higher orders of the normal form. Results of this kind will be called structurally stable. If, additionally, the slices \mathcal{BD}_n are structurally stable within the whole interval of ns , we can reduce the analysis to two dimensions. This happens in (the most of) the 1:1 zone.

To analyze the dependence of \mathcal{BD}_n on ns , consider rescaling

$$(\mathbf{x}, \mathbf{y}) \mapsto (n\mathbf{x}, n\mathbf{y}),$$

$$(\nu, \pi_1, \pi_2) \mapsto (n\nu, n^2\pi_1, n^2\pi_2),$$

and the resulting expression for the normal form,

$$\tilde{\mathcal{H}} = (ns)\tilde{\mathcal{H}}_1 + (ns)^2\tilde{\mathcal{H}}_2 + (ns)^3\tilde{\mathcal{H}}_3 + \dots, \quad (62)$$

where all dependence on n and s is contained in front factors $(ns)^k$. The rescaled terms $\tilde{\mathcal{H}}_k$ do not change when (ns) is varied, but the relative importance of higher orders increases with (ns) . Note also that the only interesting term in $\tilde{\mathcal{H}}_1$ is the detuning $\delta\nu$ [cf. Eq. (14)], whose magnitude δ is controlled by the additional small parameter $\delta \ll 1$ and is limited by the width of the zone.

B. Energy-momentum map \mathcal{EM} of 1:1 systems

The important specific feature of the 1:1 systems is that in a wide interval of sufficiently large $(ns) \ll 1$ their three-dimensional \mathcal{BD} s are cylinders in ns , i.e., the constant- ns sections \mathcal{BD}_n remain, essentially, qualitatively the same within this interval. The reason for such structural stability is explained in Sec. V.B.3. We make use of it by restricting most of the analysis to typical \mathcal{BD}_n .

1. Constant h level sets of reduced 1:1 systems

We have $m_{\text{max}} = n$ and $m_{\text{crit}} = 0$. So for $|m| \in (0, n)$, the space $P_{n,m}$ is a smooth sphere and $\lambda_{n,m,h}$ are smooth S^1 , while $P_{n,0}$ has two conical singularities and $\lambda_{n,0,h}$ can be singular S^1 . Projection of $P_{n,m}$ in (ν, π_1) is a point ν

$= \pi_1 = 0$ for $P_{n,\pm n}$ or a disk which for $P_{n,0}$ has two singular points on its boundary. Since \mathcal{H} is linear in π_1 and quadratic in ν , the level curve $\mathcal{H} = h$ is given by

$$\pi_1 = f_{n,m,h}(\nu) = a_0 h + (a_1 + a'_1 m) \nu + \frac{1}{2} a_2 \nu^2, \quad (63)$$

where $a_0, a_1, a'_1,$ and a_2 depend only on the parameters (f_e, f_b, g) . When $d=0$, the extra \mathbb{Z}_2 symmetry in Eq. (52) forces $a_1 = a'_1 = 0$, while in all detuned systems $a_1, a'_1 \neq 0$. The number of distinct roots in $[-n, n]$ that Eq. (60c) with f in Eq. (63) can have is 2 or 4 (maximum). Respective regular intersections consist of either one or two segments.

2. Relative equilibria and other critical fibers of 1:1 systems

The critical energy of the Keplerian S^1 RE with $m = \pm n$ equals $\mathcal{H}_{n,\pm n}(0, 0) = 0$. For $|m| \in (0, n)$, critical intersections $\lambda_{n,m,h}$ satisfy Eq. (61) with f in Eq. (63). Computing the derivatives, we obtain

$$\mp 2\nu(n^2 + m^2 - \nu^2)\rho^{-1} = a_2\nu + a_1 + a'_1 m, \quad (64)$$

which do not depend on energy h and which show that Eq. (60c) may have either one or three possible roots $\nu_c^\pm(n, m)$. In the latter case, depending on whether λ_{n,m,h_c} is connected or not, h_c may still give the energy of an RE or that of a bitorus.

For critical intersections $\lambda_{n,0,h_c}$ that do not include singular points $(\nu, \pi_1, \pi_2) = (\pm n, 0, 0)$ of $P_{n,0}$, the analysis is the same as outlined above. If $\lambda_{n,0,h_c}$ contains one or both (ν, π_1, π_2) of $P_{n,0}$, the energy h_\pm is $\mathcal{H}_{\pm n,0}(\pm n, 0)$ and the intersection is necessarily critical. Figure 21 shows two distinct possibilities: (b) and (c) the singular point is an isolated component of $\lambda_{n,0,h_c}$ or (a) $\lambda_{n,0,h_c}$ is a singular circle that includes the point. The latter occurs when

$$|a_1 \pm na_2| = \left| \frac{\partial f_{n,0,h_\pm}(\pm n)}{\partial \nu} \right| < \left| \frac{\partial \rho_{n,0}(\pm n)}{\partial \nu} \right| = 2n. \quad (65)$$

Geometrically, when Eq. (65) holds, the slope of the constant h_\pm level set is such that the set enters inside $P_{n,0}$ as shown in Fig. 21(a). When Eq. (65) does not hold, the set remains outside $P_{n,0}$ near $(\pm n, 0, 0)$ and $\lambda_{n,0,h_\pm}$ either consists only of a singular point $(\pm n, 0, 0)$ [Fig. 21(b)] or is a disjoint union of this point with a circle [Fig. 21(c)]. The latter occurs when the distance between the two roots of $f_{n,0,h_\pm}$ is less than $2n$, i.e., if

$$2|a_1 a_2^{-1} \pm n| < 2n \text{ or } |a_1 a_2^{-1}| < n. \quad (66)$$

Considering possible combinations in Eqs. (65) and (66) for the two singular points $(\pm n, 0)$, we obtain cases $A_0, A_1, A_{1,1}, A_2, B_0,$ and B_1 shown in Fig. 22. The subsequent analysis of each individual case leads to the types of \mathcal{BD} in Table II.

a. Case A_0

In the most simple case with large $|a_2|$ and $|a_1/a_2|$, we have two single point intersections for every m . They occur either as singular points of $P_{n,0}$ for $m=0$ or as tangencies for $m \neq 0$ and lift to relative equilibria $T_n^2 \subset \mathbb{R}^8$

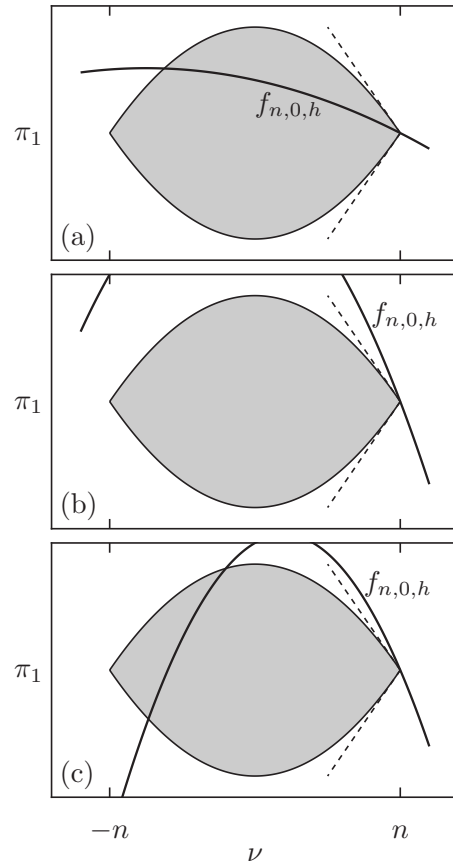


FIG. 21. $\{\pi_2=0\}$ projections of the reduced space $P_{n,0}$ and possible critical intersections $\lambda_{n,0,h_\pm}$ of the level curve $f_{n,0,h_\pm}$ that include the singular point $(n, 0)$ of $P_{n,0}$: (a) a singular circle, (b) a single point, and (c) the union of a single point and a smooth circle. The three types are distinguished by the slope of $f_{n,0,h_\pm}$ at $(n, 0)$ and the distance between the two roots of the equation $f_{n,0,h_\pm} = 0$ [see Eqs. (64) and (65)].

or $T_{n,m}^3 \subset \mathbb{R}^8$, respectively. The reduced energies h of the two single point intersections define the minimum and maximum energies for given n and m .

b. Case $A_{1,1}$

When both $|a_1| \neq 0$ and $|a_2|$ are sufficiently small but $|a_1/a_2|$ is large so that at each of the two singular points, Eq. (65) holds while Eq. (66) does not, intersections $\lambda_{n,m,h}$ are also simple (see Fig. 22). For any m , there are two single point intersections where f and ρ are tangent. At these points h attains its maximum and minimum values for given n and m . The respective fibers are relative equilibria $T_{n,m}^3$. All other intersections are circles. For $m=0$, the circles that go through one of the singular points $(\nu, \pi_1) = (\pm n, 0)$ of $P_{n,0}$ are singular at that point. These are critical levels with energy h_\pm . Each of the fibers $\Lambda_{n,0,h_\pm}$ is the product of T^2 and the two-dimensional simply pinched torus $T_{[1]}^2$ in Fig. 8.

c. Case A_2

Studied first by Cushman and Sadovskii (1999, 2000) for the strictly orthogonal configuration, this case is simi-

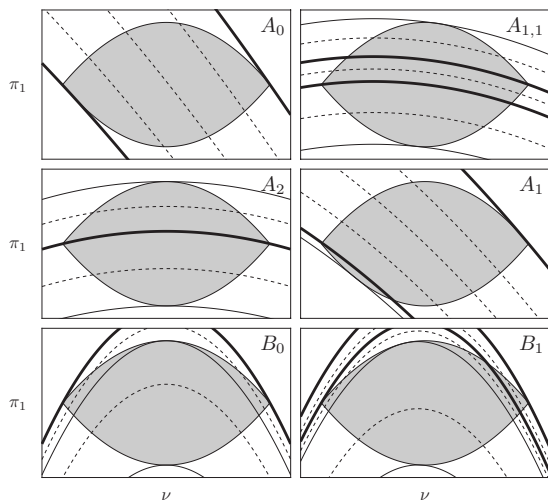


FIG. 22. Different types of intersections $\lambda_{n,0,h}$ of the constant- h level sets of \mathcal{H} with the reduced space $P_{n,0}$ projected on $\{\pi_2=0\}$. Dashed lines represent regular levels whose intersections with $P_{n,0}$ are (a union of) smooth circles; thick black lines represent levels that go through the singular points $(\nu, \pi_1)=(\pm n, 0)$; critical levels that are tangent to $P_{n,0}$ are shown by thin solid curves.

lar to $A_{1,1}$ but due to the additional \mathbb{Z}_2 symmetry of this configuration (52), the coefficient $a_1=0$. As a result, both singular points of $P_{n,0}$ lie on the same critical intersection $\lambda_{n,0,h_c}$. The singular fiber $\Lambda_{n,0,h_c}$ in \mathbb{R}^8 is a \mathbb{T}^2 bundle over a doubly pinched torus $\mathbb{T}_{[2]}^2$ in Fig. 8, center. As we break the \mathbb{Z}_2 symmetry, the double pinched torus separates into two singly pinched tori and we go from A_2 to $A_{1,1}$.

d. Case A_1

This case is intermediate between $A_{1,1}$ and A_0 . It can be obtained by deformation of either A_0 or $A_{1,1}$ and it has one singular circle $\lambda_{n,0,h_c}$ which includes one of the singular points of $P_{n,0}$ while the opposite singular point is a single point intersection. This case has only one singular fiber which is the product of \mathbb{T}^2 and a singly pinched torus $\mathbb{T}_{[1]}^2$.

e. Case B_0

Studied by Cushman and Sadovskii (2000) along with A_2 , this case is qualitatively the same as that of the quadratic Zeeman effect (pure magnetic field, point Z). B_0 systems were studied extensively following Herrick (1982) and Solov'ev (1982). It has large $|a_2|$ and $a_1=0$. As a result, regular intersections $\lambda_{n,m,h}$ can have either one or two smooth circle components lifting to one or two regular tori (see Fig. 22). Furthermore, the two singular points of $P_{n,0}$ are the only components of the same intersection $\lambda_{n,0,h_c}$. They lift to a pair of symmetry equivalent relative equilibria \mathbb{T}_n^2 . Other critical intersections correspond to tangencies of $f_{n,m,h}$ and ρ . They can be of two kinds: a single point or a figure 8. The former lifts to

a $\mathbb{T}_{n,m}^3$ RE, while the latter corresponds to the product of a bitorus \mathbb{T}_{bi}^2 (see Fig. 8) with \mathbb{T}^2 .

f. Case B_1

Unlike B_0 , this case does not have extra \mathbb{Z}_2 symmetry and $a_1 \neq 0$. As a result, critical intersections that go through singularities of $P_{n,0}$ differ: one consists of just one of the singular points, while the other is a disjoint union of the other singular point and a regular circle (see Fig. 21, bottom, and Fig. 22). Other intersections are qualitatively the same as in B_0 .

3. Constant ns bifurcation diagrams \mathcal{BD}_n of 1:1 systems and their structural stability

Using the previous section, we can obtain \mathcal{BD}_n for certain fixed n and s and arrive at the results announced in Sec. III and Table II. We should also verify that the classification of the 1:1 zone systems given in Sec. III is structurally stable for sufficiently small $ns > 0$. For 1:1 systems we work at the second-order level and ns affects the relative importance of rescaled terms $\tilde{\mathcal{H}}_2$ and $\tilde{\mathcal{H}}_1$ in Eq. (62). However, because $d \ll 1$, the 1:1 detuning term $(ns)dv$ in $\tilde{\mathcal{H}}_1$ is *a priori* small and $\tilde{\mathcal{H}}_2$ dominates as long as $(ns)^2 \gg (ns)d$. Under this condition the structure of \mathcal{BD}_n is defined solely by $\tilde{\mathcal{H}}_2$.

For given s and $0 < d_{max} \ll 1$, this gives an interval of n values where our results are stable. Concrete calculations showed that this interval is quite large. Within this interval, the structure of the whole three-dimensional image of the \mathcal{EM} map can be represented as a cylinder in n over one of the two-dimensional images in Table II. This situation is quite specific to the 1:1 zone. It allows us to focus essentially on the two-dimensional analysis.

If we go to higher orders of the normal form, the situation may become more complex. First, attention should be paid to the nongeneric transitional systems which are represented by points of the boundaries of the dynamical strata in Fig. 16. Higher orders become increasingly important as we approach these boundaries. In our second-order treatment, transitional systems often have degenerated critical \mathcal{EM} values which go away at certain higher orders. An example is treated by Efsthathiou, Cushman, and Sadovskii (2004), who studied the boundary between A_2 and B_2 . When the degeneracies are removed, the system and nearby systems in the parameter space may change qualitatively. If this happens, the corresponding part of the boundary between the dynamical strata in Fig. 16 becomes replaced by a small transitional boundary region, so that the transition between our dynamical strata does not happen as a result of a single bifurcation but after a coordinated sequence of bifurcations closely following one another. As ns increases and the included higher order(s) become more important, these complicated regions expand. However, as long as ns remains sufficiently small and the second-order $\tilde{\mathcal{H}}_2$ remains dominating, dynamical strata in Sec. III persist

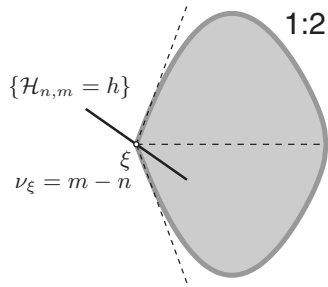


FIG. 23. Critical intersection $\lambda_{n,m,h}$ of the constant- h -level set of $\mathcal{H}_{n,m}$ (bold line) of a 1:2 system and $P_{n,m}^{1:2}$ (gray) with $m_{\text{crit}} < m < m_{\text{max}}$ which corresponds to a curled torus $\mathbb{T}_{[1/2]}^2$.

and occupy most of the parameter space. They can be used for concrete estimates of an admissible interval of the ns values.

C. Analysis of 1:2 systems and higher resonances

To analyze 1:2 resonant systems we normalize (at least) to order 3. Compared to the systems in the 1:1 zone, we should be aware of the following new important aspects. Because now ns controls the rivalry of \mathcal{H}_2 and \mathcal{H}_3 in Eq. (62), the \mathcal{BD}_n of these systems are much less stable and study of the rich three-dimensional \mathcal{BD} in (n, m, h) is imposed. It is generally difficult for \mathcal{H}_3 to dominate because this requires “dangerously” large ns and a fine adjustment of parameter a^2 . So specific 1:2 features such as fractional monodromy may be harder to find.

Another aspect of 1:2 systems is the presence of a new singular fiber, the curled torus $\mathbb{T}_{[1/2]}^2$. It appears, as shown in Fig. 23, under the same geometric conditions as the pinched torus [cf. Fig. 21(a)] but for $|m| < m_{\text{max}}$ and $|m| \neq m_{\text{crit}}$ when the singularity of $P_{n,m}^{1:2}$ corresponds to the short \mathbb{T}^2 RE and not to the Kepler ellipse (Sec. II.C.3.a).

For higher resonances, we should encounter increasing difficulties of the same kind. Furthermore, we should face shrinking zone sizes and require quantitative dynamical justification (cf. footnote 35) of the applicability of the high-order normal form. The higher-order curled tori are rather exceptional singular fibers. Geometrically this can be seen from the fact that singularities of $P_{n,m}^{k_-,k_+}$ with $k_- + k_+ > 3$ are cuspidal and intersections similar to that in Fig. 23 are not typical.

VI. MONODROMY

As pointed out in the Introduction, Sec. III, and Table II, certain systems in the 1:1 zone, namely, A_1 , $A_{1,1}$, A_2 , and B_1 , have nontrivial monodromy of different kinds. We discuss this property in more detail. After introducing the technical concepts of the rotation angle and the first return time and explaining how one can compute monodromy in an integrable system, we recall some general properties of the monodromy map.

First we discuss monodromy in the 2-DOF integrable systems defined on $S^2 \times S^2$. There the form of the mono-

dromy matrix can be easily deduced [up to conjugation in $\text{SL}(2, \mathbb{Z})$] using the geometric monodromy theorem and other general properties of the monodromy map.

Our final aim is to give the monodromy map for the 3-DOF system defined in the original space \mathbb{R}^6 with coordinates (\mathbf{Q}, \mathbf{P}) . In order to do this, we first study the monodromy map in the KS space \mathbb{R}^8 . Then we deduce the monodromy map in \mathbb{R}^6 from the one on $\mathbb{R}^8|_{\xi=0}$ using the properties of the KS map.

Even though the \mathcal{BD} of our 3-DOF system is three dimensional, we only consider constant- n closed paths in the set of regular values of the energy-momentum map, i.e., closed paths that lie on \mathcal{BD}_n . Monodromy for an arbitrary closed path can be deduced from such constant- n paths as long as \mathcal{BD} can be represented within an interval of n values as a cylinder in n . This is certainly the case of the 1:1 systems (Sec. V.B.3). Moreover, it is possible to compare the monodromy map for such closed paths to the monodromy computed for the 2-DOF integrable system. We show that the third dimension (n) enters trivially in the monodromy map.

A. Computation of monodromy

1. Rotation angles in systems with two degrees of freedom

Computation of monodromy in Hamiltonian systems with two degrees of freedom (2-DOF) has been described and used before.⁴⁷ We give a brief outline. In the simplest case, when the system possesses already a globally defined action I_1 , we can use periodic orbits γ_1 generated by the flow of the Hamiltonian vector field X_{I_1} of I_1 to define the first basis element (cycle) $[\gamma_1]$ of the basis of the homology group $H_1(\mathbb{T}^2)$ of a regular torus \mathbb{T}^2 . The second basis cycle $[\gamma_2]$ of $H_1(\mathbb{T}^2)$ is constructed using the integral curve of the nonperiodic flow of the vector field X_H of the Hamiltonian H and an appropriately chosen segment of γ_1 . This is done as follows (see Fig. 24). Consider a regular torus \mathbb{T}^2 corresponding to the values (m, h) of momentum I_1 and energy H and take a point $p \in \mathbb{T}^2$ and the S^1 orbit γ_1 which starts at p . Launch an integral curve of X_H and continue it until it crosses γ_1 first time at point p' . The time T required for the flow of X_H to go from p to p' is called the first return time; the time Θ required for the flow of X_{I_1} to travel from p to p' along γ_1 is called the rotation angle. Construct now the vector field

$$X_{I_2} = (TX_H - \Theta X_{I_1}) / (2\pi),$$

which has a 2π -periodic flow: an orbit γ_2 of this flow started at p comes back to p in time 2π . This orbit represents the second basis cycle of $H_1(\mathbb{T}^2)$.

We can perform the above procedure for any regular torus and thus obtain Θ as a real-valued function on the

⁴⁷See Lerman and Umanskiĭ (1994a, 1994b, 1995), Matveev (1996), Cushman and Bates (1997), Nguyễn Tiên (1997), Cushman and Duistermaat (2001), Efstathiou, Joyeux, and Sadovskii (2004), and Efstathiou (2005).

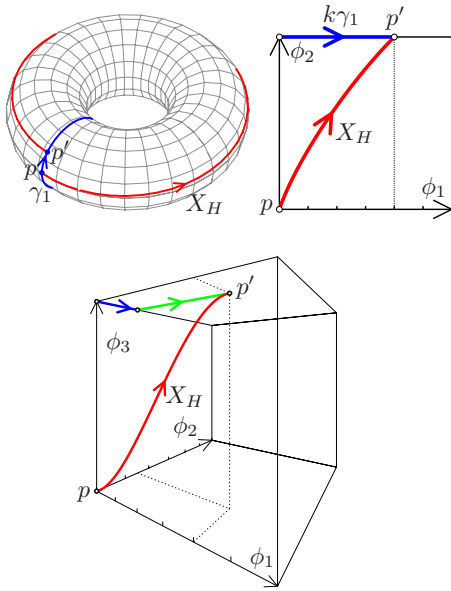


FIG. 24. (Color online) Orbits of the flow of the two Hamilton fields $\{X_{I_j}, j=1, \dots, K-1\}$ of which define $K-1$ diagonal actions on the phase space. Then in some complex coordinates $z = (z_1, \dots, z_K)$, we have $K-1$ commuting flows

image of the energy-momentum map \mathcal{EM} with coordinates (m, h) . In systems with monodromy, $\Theta(m, h)$ is locally smooth and single valued but is globally multivalued: going once around a closed nontrivial path Γ in the set of regular (m, h) values in the counterclockwise direction, the rotation angle increases by an integer multiple of 2π , i.e.,

$$\Theta \mapsto \Theta' = \Theta + 2k\pi, \quad k \in \mathbb{Z}. \tag{67a}$$

This in turn means that the vector field X_{I_2} becomes

$$X_{I_2} \mapsto X'_{I_2} = X_{I_2} - kX_{I_1}, \tag{67b}$$

and, similarly, the respective cycle $[\gamma_2]$ changes to

$$[\gamma_2] \mapsto [\gamma_2] - k[\gamma_1], \tag{67c}$$

while $[\gamma_1]$ remains unchanged. Consequently, $[\gamma_2]$ cannot be defined globally over the whole set of regular (m, h) values. The above transformation of the cycle basis $\{[\gamma_1], [\gamma_2]\}$ is expressed by matrix $M(k)$ in Sec. II.D.5.

To have an idea how Θ is computed, first note that the flow of X_{I_1} defines an S^1 symmetry and that after reducing this symmetry, the period T can be found as the period of the reduced 1-DOF dynamics. At the same time, in many cases it is possible to find coordinates on the total phase space \mathbb{R}^4 , in which the action of I_1 becomes a diagonal simultaneous rotation of two planes (q_1, p_1) and (q_2, p_2) . In complex coordinates $z = (z_1, z_2)$ one has

$$z \mapsto (z_1 \exp(i\omega_1 t), z_2 \exp(i\omega_2 t)).$$

When at $p = (z_1, z_2)$ we launch the orbit of X_H and it comes back to γ_1 after we follow it for time T , we arrive at $p' = (z'_1, z'_2)$. Since $p' \in \gamma_1$ we should have

$$z' = (z_1 \exp(i\omega_1 \Theta), z_2 \exp(i\omega_2 \Theta)),$$

from where, using either of the two equations, we should obtain consistently the rotation angle

$$\Theta = \omega_1^{-1} \arg(z_1/z'_1) = \omega_2^{-1} \arg(z_2/z'_2).$$

Note also that derivatives $d \arg(z_1)/dt$ and $d \arg(z_2)/dt$ can always be expressed as functions on the reduced phase space (Efsthathiou, Cushman, and Sadovskii, 2007) and can be integrated using the reduced dynamics. Furthermore, it is often possible to compute analytically either the integral or at least its variation along the path Γ .

2. Rotation angles in systems with $K > 2$ degrees of freedom and $K-1$ diagonal S^1 actions

The situation is conceptually the same for systems with $K > 2$ degrees of freedom and $K-1$ (globally) defined actions I_j (momenta), $j=1, \dots, K-1$, the vector fields on the phase space. Then in some complex coordinates $z = (z_1, \dots, z_K)$, we have $K-1$ commuting flows

$$\varphi_j: z \mapsto \varphi_j^t(z) = (z_1 \exp(i\omega_1 t), \dots, z_K \exp(i\omega_K t)),$$

which combine into

$$\Phi^{t_1 \dots t_{K-1}}: z \mapsto \varphi_1^{t_1} \circ \dots \circ \varphi_{K-1}^{t_{K-1}}(z).$$

We consider a regular torus \mathbb{T}^K and its homology group $H_1(\mathbb{T}^K) \sim \mathbb{Z}^K$. We can use closed orbits γ_j of the commuting flows φ_j with $j=1, \dots, K-1$ to represent the first $K-1$ basis cycles of $H_1(\mathbb{T}^K)$. This is possible only if the \mathbb{T}^{K-1} action Φ on \mathbb{T}^K is effective.⁴⁸ In the opposite case, there is no cycle γ_K that we can add to the collection of $K-1$ cycles γ_j so that $(\gamma_1, \dots, \gamma_K)$ span the whole $H_1(\mathbb{T}^K)$: no matter how we choose γ_K , only a subgroup $G \subset H_1(\mathbb{T}^K)$ will be spanned. Since the monodromy map is an automorphism of the whole $H_1(\mathbb{T}^K)$, we must ensure effectiveness of the \mathbb{T}^{K-1} action Φ on all regular tori \mathbb{T}^K in order to compute monodromy.

As in the case $K=2$, the K th basis cycle is constructed using the Hamiltonian vector field X_H . Taking a point $p \in \mathbb{T}^K$, we consider in \mathbb{T}^K the orbit of the \mathbb{T}^{K-1} action Φ passing through p . We launch an integral curve of X_H from p and stop when it returns for the first time to the \mathbb{T}^{K-1} orbit at a point p' . The first return time T at which this happens can again be computed beforehand from the 1-DOF reduced dynamics. Since we make sure that the \mathbb{T}^{K-1} action is effective, there is a unique (up to additional integer multiples of 2π) combination of rotation angles $\Theta_1, \dots, \Theta_{K-1}$ such that

$$p' = \Phi^{\Theta_1 \dots \Theta_{K-1}}(p),$$

which implies K linear equations

⁴⁸A group action of a group G on a manifold M is effective if $g \neq \text{id} \in G$ implies that there is some $z \in M$ for which $gz \neq z$.

$$z'_i = z_i \exp\left(i \sum_{j=1}^{K-1} \omega_{ij} \Theta_j\right), \quad i = 1, \dots, K$$

for $K-1$ unknowns $\Theta_1, \dots, \Theta_{K-1}$. (The one extra equation can be used as a consistency check.) We can now define the 2π -periodic vector field,

$$X_{I_K} = \frac{1}{2\pi} \left(TX_H - \sum_{j=1}^{K-1} \Theta_j X_{I_j} \right),$$

and define subsequently the last cycle $[\gamma_K]$.

When we go around a closed circuit Γ in the K -dimensional domain of regular energy-momentum values (m_1, \dots, m_{K-1}, h) , our $K-1$ rotation angles evolve smoothly, and when we complete a tour on Γ , they might change by integer multiples of 2π . We have

$$\Theta_j \mapsto \Theta'_j = \Theta_j + 2\pi k_j, \quad k_j \in \mathbb{Z}.$$

If the system has monodromy and Γ is nontrivial,⁴⁹ then at least one of the integers k_j must be nonzero. The corresponding change in the cycle $[\gamma_K]$ is

$$[\gamma_K] \mapsto [\gamma_K] - (k_1[\gamma_1] + \dots + k_{K-1}[\gamma_{K-1}])$$

or denoting the row vector $\mathbf{k} = (k_1, \dots, k_{K-1})$,

$$[\gamma_K] \mapsto [\gamma_K] - \mathbf{k} \cdot ([\gamma_1], \dots, [\gamma_{K-1}])^T,$$

which gives the $K \times K$ monodromy matrix

$$M(k_1, \dots, k_{K-1}) = \begin{pmatrix} 1 & 0 & \cdots & 0 & 0 \\ 0 & 1 & \cdots & 0 & 0 \\ \vdots & \vdots & \ddots & \vdots & \vdots \\ 0 & 0 & \cdots & 1 & 0 \\ -k_1 & -k_2 & \cdots & -k_{K-1} & 1 \end{pmatrix}. \tag{68}$$

In this particular basis, the monodromy matrix is given solely by its last row. Furthermore, matrices of the kind in Eq. (68) form a subgroup of $SL(K, \mathbb{Z})$ isomorphic to the Abelian group \mathbb{Z}^{K-1} . Indeed we have

$$M(\mathbf{k})^{-1} = M(-\mathbf{k}), \tag{69a}$$

$$M(\mathbf{k}')M(\mathbf{k}'') = M(\mathbf{k}' + \mathbf{k}''). \tag{69b}$$

B. General properties of the monodromy map

We summarize a number of simple general properties of monodromy mappings which are helpful in analyzing particular concrete results discussed later. A monodromy mapping will be denoted m ; the K -dimensional set of regular \mathcal{EM} values of the system will be denoted \mathbb{R} . For each homotopy class $[\Gamma]$ of closed paths Γ in \mathbb{R} , the monodromy mapping m defines an automorphism

$m_{[\Gamma]}$ of the first homology $H_1(\mathbb{T}^K)$. In other words, m is a mapping from the fundamental group π_1 of \mathbb{R} to the group of automorphisms of $H_1(\mathbb{T}^K)$.

1. Monodromy matrix and changes of cycle bases

Since $m_{[\Gamma]}$ is an automorphism of $H_1(\mathbb{T}^K)$, its monodromy matrix M belongs to $SL(K, \mathbb{Z})$, i.e., $\det M = 1$ and all its entries are integer numbers. The matrix M itself is defined up to conjugation in $SL(K, \mathbb{Z})$. Specifically, let $B \in SL(K, \mathbb{Z})$ define a change of the cycle basis in $H_1(\mathbb{T}^K)$. Then in the new basis the monodromy matrix is BMB^{-1} . In other words, for a given monodromy mapping, its matrix M belongs to a given class of $SL(K, \mathbb{Z})$. Describing classes of $SL(K, \mathbb{Z})$, one can come up with a standard form of monodromy matrices. Thus, for k -fold FF singularities in $K=2$ this form is

$$\begin{pmatrix} 1 & 0 \\ k & 1 \end{pmatrix}, \quad k \in \mathbb{Z}.$$

Two further simple aspects should be taken into account with regard to possible monodromy matrices M : one should agree on the choice of the positive direction of circuits $\Gamma \subset \mathbb{R}$ (counterclockwise for $K=2$) and on the orientation of regular tori that defines proper cycle bases. Note that a base can be always made proper by reversing the direction of one of the cycles, such as γ_K in the previous section or more generally by using a matrix \bar{B} over \mathbb{Z} with $\det \bar{B} = -1$.

2. The sum rules

The mapping $m: \pi_1(\mathbb{R}) \rightarrow H_1(\mathbb{T}^K)$ is a homomorphism. This means in particular that for monodromy matrices $M_{[\Gamma]}$ and $M_{-[\Gamma]}$ corresponding to (homotopy classes of) circuits $[\Gamma]$ and $-[\Gamma]$, i.e., to the same class of closed paths taken in opposite directions, we have

$$M_{-[\Gamma]} = M_{[\Gamma]}^{-1}. \tag{70a}$$

Furthermore, consider two (homotopy classes of) circuits $[\Gamma']$ and $[\Gamma'']$ and their combination, $[\Gamma'] + [\Gamma'']$. We have for the respective monodromy matrices [cf. Eq. (69b)]

$$M_{[\Gamma'] + [\Gamma'']} = M_{[\Gamma']} M_{[\Gamma'']}. \tag{70b}$$

3. Deformation principle

Monodromy is a purely topological property. It is insensitive to the particular path $\Gamma \subset \mathbb{R}$ used for its computation and depends solely on the homotopy class $[\Gamma]$ of $\pi_1(\mathbb{R})$. In other words, any continuous deformation of Γ , for which Γ remains in \mathbb{R} , gives the same monodromy $m_{[\Gamma]}$. Furthermore, if we deform the set \mathbb{R} itself by changing the parameters of the system (in our case, field strengths g and f) and the deformation is such that Γ evolves continuously within \mathbb{R} , then the monodromy $m_{[\Gamma]}$ remains the same. Thus $m_{[\Gamma]}$ does not change even if

⁴⁹More generally, see footnote 23.

qualitative changes of the bifurcation diagram occur locally inside the region encircled by Γ or outside that region.

4. The sign of monodromy

The Hamiltonian character of the system imposes further restrictions on the possible monodromy mappings (Cushman and Vũ Ngọc, 2002; Zhilinskiĭ, 2005). Let a system with $K=2$ have an isolated singular fiber Λ_c , which is a k -pinched torus (see Fig. 8, left, for a singly pinched torus). Each “pinch” is a focus-focus equilibrium. There is always an orientable neighborhood B_c of the pinched point c and the orientation in B_c induces an orientation on the fibers $\mathcal{EM}^{-1}(f)$, $f \in B_c$ [see Cushman and Vũ Ngọc (2002)]. Then for all Γ with fixed positive (counterclockwise) direction in B_c which encircle c once, the matrices $M_{[\Gamma]}$ belong in the $SL(2, \mathbb{Z})$ conjugacy class of

$$M(k) = \begin{pmatrix} 1 & 0 \\ -k & 1 \end{pmatrix} \quad \text{with } k \in \mathbb{Z}_{\geq 0}; \quad (71)$$

thus k measures the number of focus-focus equilibria encircled by Γ . The 2×2 matrix $M(k)$ and its inverse $M(-k)$, where $k \in \mathbb{Z}_{>0}$, are not similar in $SL(2, \mathbb{Z})$. Thus fixing the orientation in B_c fixes the class of $M_{[\Gamma]}$ in $SL(2, \mathbb{Z})$ and consequently the sign of k . This justifies the terminology sign of monodromy. When the image of \mathcal{EM} is orientable and the system has a global S^1 action, then a consistent orientation for all critical values of \mathcal{EM} that correspond to pinched tori can be chosen, and the monodromy $M_{[\Gamma]}$ for a path Γ that encircles k focus-focus points is given by Eq. (71).

The term “sign” comes from the above $K=2$ case. More generally, we should consider allowed classes of $SL(K, \mathbb{Z})$. The issue remains open for $K > 2$, but it is quite possible, especially in the special case of maps in Eq. (68), which nontrivial restrictions exist there as well.

5. Geometric monodromy theorem

This theorem (Lerman and Umanskiĭ, 1994a, 1994b, 1995; Matveev, 1996; Nguyễn Tiên, 1997; Cushman and Duistermaat, 2001) states that in a 2-DOF system the monodromy map is completely determined by the number k of focus-focus singularities (or pinches) on the isolated singular fiber called k -pinched torus. With all choices made as described above, the matrix of this monodromy belongs to the class in Eq. (71). Generalizations of this theorem to $K > 2$ are not studied comprehensively. An extension to $K > 2$ can be made readily when the extra degree(s) of freedom correspond to global S^1 actions which act freely so that regular fibers of the $K=2$ case are multiplied by T^{K-2} orbits. But even in this trivial, in some sense, case, we should make certain that we work with effective cycle bases (Dullin *et al.*, 2004; Giacobbe *et al.*, 2004). Generalizations to fractional monodromy (Nekhoroshev *et al.*, 2002, 2006; Efsthathiou, Cushman, and Sadovskii, 2007; Sugny *et al.*, 2008) are not known.

C. Monodromy of systems in the 1:1 zone

1. Monodromy of the n -shell system on $S^2 \times S^2$

We consider first the n -shell energy-momentum map \mathcal{EM}_n in Eq. (15b) for a fixed value of Keplerian action n which is sufficiently small so that the integrable normal form approximation is valid. On the regular components of fibers $\mathcal{EM}_n^{-1}(m, h)$ we can define cycle bases following the outline in Sec. VI.A.1. The momentum μ is a global action and it can be chosen as I_1 ; the corresponding fixed cycle $[\gamma_\mu] = [\gamma_1]$ can be defined on all tori. The stratified image of \mathcal{EM}_n is one of the \mathcal{BD}_n in Table II which is described in Sec. V.B.2. Each \mathcal{BD}_n is a base of a singular toric fibration of $S^2 \times S^2$ for which we can deduce monodromy by finding its singular fibers and applying the geometric monodromy theorem (Sec. VI.B.5) together with deformation arguments (Sec. VI.B.3).

The system has nontrivial monodromy only if the set R_n of regular values of \mathcal{EM}_n is not simply connected. This occurs for types A_2 , $A_{1,1}$, A_1 , and B_1 . In all these cases we can choose a closed path $\Gamma \subset R_n$ which encircles an isolated set of critical values. The monodromy matrix $M_{[\Gamma]}$ has the form (71), so the second basis cycle $[\gamma_2]$ transforms after going once around Γ according to Eq. (67c) with $k > 0$. We say that the system has monodromy k . We can find k from the geometric monodromy theorem (Sec. VI.B.5).

In both cases A_1 and A_2 , the base space consists of one cell with one isolated critical \mathcal{EM}_n value o inside. The set of regular values is not simply connected, and we consider monodromy for a nontrivial closed path Γ that goes once around o (see Fig. 11, left). In the case of A_2 , which was studied originally by Cushman and Sadovskii (2000), o corresponds in $S^2 \times S^2$ to a doubly pinched torus $T_{[2]}^2$. This implies that the A_2 system has nontrivial monodromy with $k=2$. In the case of A_1 , the isolated critical value o , lifts to a singly pinched torus $T_{[1]}^2$ in $S^2 \times S^2$ and the monodromy is 1.

The B_1 systems can be obtained as a deformation of A_1 . The B_1 base space consists of two partially overlapping cells that join along a curved segment \mathcal{C} of critical values. The corresponding cell unfolding surface is shown in Fig. 11, right. The critical segment \mathcal{C} is isolated in the larger cell and is part of the boundary of the smaller cell. The smaller cell can be deformed continuously together with \mathcal{C} into a single isolated critical value of the A_1 system. Under such deformation, the circuit Γ that goes around \mathcal{C} in the set of regular values of the larger cell (Fig. 11, right) transforms continuously into the circuit Γ of the A_1 case (Fig. 11, left). Hence $k=1$: the monodromy of B_1 is the same as that of A_1 .

In the case of the $A_{1,1}$ systems, the base space has two isolated critical values o^- (lower in h) and o^+ (higher in h), each lifting to a singly pinched torus $T_{[1]}^2$ in $S^2 \times S^2$. The two nontrivial cycles $[\Gamma^-]$ and $[\Gamma^+]$ which form a basis of the fundamental group $\pi_1(\mathbb{R})$ of the $A_{1,1}$ base \mathbb{R} are shown in Fig. 25 by closed paths Γ^- and Γ^+ encircling o^- and o^+ , respectively. From the sign theorem (Sec.

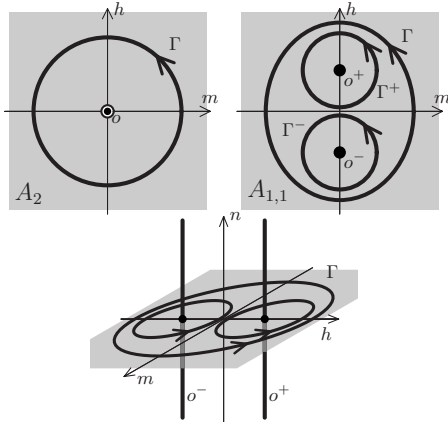


FIG. 25. Energy-momentum map \mathcal{EM} in Eq. (1) defined by first integrals (N, μ, \mathcal{H}) with values (n, m, h) . Top row shows constant- n sections; the three-dimensional image is represented on the bottom; gray shade represents regular \mathcal{EM} values with the same n . Contour Γ goes around the isolated critical value o , which lifts to a doubly pinched torus (top left) of an A_2 system, and around two isolated critical values o^- and o^+ , each lifting to a singly pinched torus (top right) of the $A_{1,1}$ system; contours Γ^- and Γ^+ encircle o^- and o^+ , respectively. In the full image, o , o^- , and o^+ become one-dimensional threads of critical values.

VI.B.4) and the geometric monodromy theorem (Sec. VI.B.5) we obtain that both matrices $M_{[\Gamma^-]}$ and $M_{[\Gamma^+]}$ are of the class $M(1)$ in Eq. (71), i.e., $k^- = k^+ = 1$. Moreover, due to the global S^1 symmetry associated with μ , the fibers $\Lambda^\pm = \mathcal{EM}^{-1}(o^\pm)$ share the same globally defined cycle $[\gamma_1]$, while $[\gamma_2]$ can be chosen so that the respective monodromy matrices have the same standard form $M(1)$. Then by the sum rule (Sec. VI.B.2) in Eq. (70b), the monodromy for the circuit $\Gamma = \Gamma^- + \Gamma^+$ that goes once around both critical values (see Fig. 25) is 2. The latter result follows also immediately once we observe that $A_{1,1}$ systems are a deformation of A_2 (see Figs. 16 and 25 and top left).⁵⁰

In the B_0 case, also studied by Cushman and Sadovskii (2000), the base of the fibration consists of three cells, two of which overlap. The unfolded \mathcal{BD} is shown in Fig. 10. The regular interior of each cell is simply connected. There is no monodromy.

Finally, the simplest case of 1:1 systems is type A_0 . In this case, the detuning d is so large that the specific structure of the 1:1 resonance vanishes. We have one cell with no isolated critical values. The set of regular values is simply connected and the system has no monodromy.

⁵⁰In our case, the deformation merges two singly pinched tori Λ^\pm into one doubly pinched torus Λ . In the case without S^1 symmetry and the respective common fixed cycle $[\gamma_1]$ on Λ^\pm , the two singly pinched tori Λ^\pm would merge instead into a singular sphere S^2 (Gross, 2001, Theorem 1.4). Such a case is reminiscent of the A_2 singularity; not our A_2 system [cf. Bates and Cushman (2005)], but no physical examples are known to date.

As a consequence, A_0 systems have globally defined action-angle coordinates.

2. Monodromy on $\mathbb{R}^8|_{\zeta=0}$

We compute first monodromy for fibers in the KS space \mathbb{R}^8 and we use these results in the next section to compute monodromy in the physical space \mathbb{R}^6 . The energy-momentum map in \mathbb{R}^8 is defined by four first integrals of the second normalized system, the momenta (N, μ, ζ) which induce global diagonal S^1 actions on \mathbb{R}^8 , and energy $\Delta\mathcal{E}$ pulled back to \mathbb{R}^8 . Since we only consider $\zeta=0$, we can consider the \mathcal{EM} map in Eq. (15a). The monodromy along a path Γ in the set of regular values \mathbb{R} of \mathcal{EM} is described by 4×4 monodromy matrices of the kind in Eq. (68) with $K=4$. Furthermore, within a certain interval of the n values, which we study here, any closed path Γ in the three-dimensional set \mathbb{R} of regular values of this \mathcal{EM} is homotopic to a closed constant- n path Γ_n (cf. Sec. VB.3). Consequently, the 4×4 monodromy matrix corresponding to Γ can be always computed using its Γ_n analog.

There are several ways to build an effective \mathbb{T}^3 action out of the three S^1 actions associated with (N, μ, ζ) . One possibility is to use the 2π -periodic Hamiltonian flows of the vector fields of Hamiltonian functions $\mu + \zeta$, $N + \zeta$, and $N - \zeta$. For this choice of actions and for circuits Γ with fixed $N=n$ and $\zeta=0$, we have computed the monodromy matrices for systems of different types in Table II following the outline in Sec. VI.A.2. The matrices always have the form $M(\mathbf{k})$ in Eq. (68) with $K=4$ and

$$\mathbf{k} = (k_{\mu+\zeta}, k_{N+\zeta}, k_{N-\zeta}),$$

where $k_{\mu+\zeta}$, $k_{N+\zeta}$, and $k_{N-\zeta}$ are integers. Concrete values of \mathbf{k} for the 1:1 systems of different types are given in Table V.

To assess the results in Table V, one should verify the monodromy properties in Sec. VI.B. Thus the matrix $M_{A_{1,1}^-}$ for the circuit $\Gamma^- + \Gamma^+$ of the $A_{1,1}$ system (case $A_{1,1}^+$ in Table V) is the same as the matrix M_{A_2} for the A_2 system. This is required by the deformation principle in Sec. VI.B.3 and the already mentioned fact that $A_{1,1}$ is a deformation of A_2 (see Fig. 16). On the other hand, by the sum rule in Sec. VI.B.2, the matrix

$$M_{A_2} = M_{A_{1,1}^-} = M(\mathbf{k}^-)$$

should be the product of matrices

$$M_{A_{1,1}^-} = M_{\Gamma^-} = M(\mathbf{k}^-)$$

and

$$M_{A_{1,1}^+} = M_{\Gamma^+} = M(\mathbf{k}^+).$$

This is indeed true since by Eq. (69b), multiplication of matrices $M(\mathbf{k}^-)$ and $M(\mathbf{k}^+)$ comes down to taking the sum of vectors \mathbf{k}^- and \mathbf{k}^+ , and in Table V we have $\mathbf{k}^- + \mathbf{k}^+ = \mathbf{k}^- + \mathbf{k}^+$.

Furthermore, we note that Γ^- deforms continuously (in the set of regular values \mathbb{R}) as we go from $A_{1,1}$ to-

TABLE V. Monodromy matrix $M(\mathbf{k})$ [see Eq. (68)] for $T^4 \subset R^8$ and for $T^3 \subset R^6$ in systems of different types in Table II. For systems of type $A_{1,1}$ we distinguish additionally monodromy matrices corresponding to the circuits $[\Gamma^+]$, $[\Gamma^-]$, and $[\Gamma^-]+[\Gamma^+]$ which go around the two distinct isolated critical values with $m=0$, the upper o^+ and the lower o^- , and around both values, respectively (see Fig. 25). The three cases are denoted by $A_{1,1}^+$, $A_{1,1}^-$, and $A_{1,1}^{+-}$.

System	Monodromy in R^8			Monodromy in R^6	
	$k_{\mu+\zeta}$	$k_{N+\zeta}$	$k_{N-\zeta}$	k_μ	k_N
$A_2, A_{1,1}^{+-}$	2	1	-1	2	0
$A_{1,1}^+, A_1', B_1'$	1	1	-1	1	0
$A_{1,1}^-, A_1'', B_1''$	1	0	0	1	0

wards the Zeeman limit (see Fig. 16, bottom), enter A_1'' and, subsequently, B_1'' because during this deformation the upper critical value o^+ disappears while o^- persists in A_1'' and then becomes a one-dimensional isolated segment of critical values in B_1'' (cf. Fig. 11). Consequently, we must have

$$M_{A_{1,1}^-} = M_{A_1''} = M_{B_1''},$$

and by the similar argument (closer to the Stark limit),

$$M_{A_{1,1}^+} = M_{A_1'} = M_{B_1'},$$

as given in Table V.

It should also be noted that all matrices in Table V (in R^8) are similar: changing to an appropriate basis, they can be brought to the same standard form $\text{diag}(1, 1, M(1))$ where the 2×2 block $M(1)$ is given by Eq. (71) with $k=1$. The basis choices are given below.

Matrix standard cycle basis

$$M_{A_2} = M_{A_{1,1}^{+-}}(\gamma_{N+\zeta}, \gamma_{N+\mu}, -\gamma_{2\mu}, \gamma_4)$$

$$M_{A_1'} = M_{A_{1,1}^+}(\gamma_{N+\zeta}, \gamma_{N-\zeta}, \gamma_{\mu+\zeta}, \gamma_4)$$

$$M_{A_1''} = M_{A_{1,1}^-}(\gamma_{N+\zeta}, \gamma_{N-\zeta}, \gamma_{\mu-\zeta}, \gamma_4)$$

All three matrices belong in the same class of $SL(4, Z)$. This seems to be an extension of the sign theorem (Sec. VI.B.4). However, contrary to the two-dimensional case, the corresponding inverse matrices also belong to the same class.

Finally we should understand how the matrices in Table V are related to the 2×2 matrices $M(k)$ obtained from the analysis of the reduced system on $S^2 \times S^2$ (Sec. VI.C.1). This can be readily achieved once we recall that the map $R^8|_{\zeta=0} \rightarrow S^2 \times S^2$ is a reduction of a T^2 symmetry acting freely on $R^8|_{\zeta=0}$. Over each point of $S^2 \times S^2$, we have a T^2 orbit $T_{n,\zeta=0}^2$ of the combined 2π -periodic flows of vector fields X_{2N} (Keplerian) and $X_{2\zeta}$ (KS symmetry). So identifying a regular torus $\Lambda_{m,h} = T^2 \subset S^2 \times S^2$, with its preimage T^4 in the KS phase space R^8 at the level of first homologies, we have

$$H_1(T^4) \rightarrow H_1(\Lambda_{m,h}),$$

$$(\gamma_{\mu+\zeta}, \gamma_{N+\zeta}, \gamma_{N-\zeta}, \gamma_4) \rightarrow (\gamma_\mu + 0, 0, 0, \gamma_4) = (\gamma_\mu, \gamma_2).$$

Since under the monodromy map

$$\gamma_4 \mapsto \gamma_4 - \mathbf{k} \cdot (\gamma_{\mu+\zeta}, \gamma_{N+\zeta}, \gamma_{N-\zeta}),$$

this means that the second cycle of the two-tori $\Lambda_{m,h}$ of the reduced system transforms as

$$\gamma_2 \mapsto \gamma_2 - \mathbf{k} \cdot (\gamma_{\mu+\zeta}, 0, 0) = \gamma_2 - k_{\mu+\zeta} \gamma_\mu,$$

and therefore k_μ in Table V and k in Sec. VI.C.1 must be equal.

3. Monodromy in R^6

Monodromy in the original physical phase space R^6 of the system with the Hamiltonian (2) can be deduced from that computed in R^8 by the same method that we used in the end of Sec. VI.C.2 to relate \mathbf{k} and k . Here we consider the KS reduction map $R^8|_{\zeta=0} \rightarrow R^6$ and analyze the map that it induces between the first homologies of the regular tori $\Lambda_{n,m,h} = T^3 \subset R^6$ and their preimages $T^4 \subset R^8|_{\zeta=0} \subset R^8$.

Note that the image of the energy-momentum maps in the two cases is the same since we only consider $\zeta=0$. The circuits Γ are also the same. The system in R^6 has two global action coordinates N and μ ; the corresponding S^1 orbits can be found explicitly after first computing them in R^8 and then bringing them down to R^6 by the KS map in Eq. (18). In particular, it can be shown that the flow of X_N and X_μ is 2π periodic in R^6 (while it has a period of 4π in R^8). We can also verify in the same way that the flow of X_ζ reduces to identity in R^6 . For the first homology identification $H_1(T^4) \rightarrow H_1(\Lambda_{n,m,h})$ this means

$$\begin{aligned} (\gamma_{\mu+\zeta}, \gamma_{N+\zeta}, \gamma_{N-\zeta}, \gamma_4) &\rightarrow (\gamma_\mu + 0, \gamma_N + 0, \gamma_N + 0, \gamma_4) \\ &\rightarrow (\gamma_\mu, \gamma_N, \gamma_N, \gamma_3) \sim (\gamma_N, \gamma_\mu, \gamma_3). \end{aligned}$$

In particular, it can be argued that the T^2 symmetry action in R^6 associated with (γ_N, γ_μ) is effective because this basis is an image $(\gamma_{\mu+\zeta}, \gamma_{N+\zeta}, \gamma_{N-\zeta})$ and the latter is associated with an effective action in R^8 . The monodromy matrix in R^6 in the basis $(\gamma_N, \gamma_\mu, \gamma_3)$ can be directly obtained from $\mathbf{k} = (k_{\mu+\zeta}, k_{N+\zeta}, k_{N-\zeta})$. Because globally defined cycles γ_N and γ_μ are fixed, this 3×3 matrix is of the same kind as in Eq. (68) with $K=3$, and it is given by two integers k_N and k_μ . For the third cycle of

$H_1(\Lambda_{n,m,h})$, the monodromy transformation is

$$\gamma_3 \mapsto \gamma_3 - \mathbf{k} \cdot (\gamma_\mu, \gamma_N, \gamma_N) = \gamma_3 - k_\mu \gamma_\mu - k_N \gamma_N$$

from where we obtain

$$k_\mu = k_{\mu+\zeta} \text{ and } k_N = k_{N+\zeta} + k_{N-\zeta}.$$

This gives the results for \mathbb{R}^6 in Table V. We observe that in \mathbb{R}^6 the Keplerian cycle γ_N does not participate in the monodromy transformation (for 1:1 systems); the matrix is $\text{diag}(1, M(k))$ with the 2×2 block $M(k)$ of the form in Eq. (71) and $k = k_\mu$ is equal to either 1 or 2. This justifies the use of the constant- n sections \mathcal{BD}_n for the classification in Table II and of the respective n -shell map \mathcal{EM}_n in Eq. (15b).

VII. QUANTUM DYNAMICAL STRATIFICATION

The classical Hamiltonian monodromy described in Sec. VI manifests itself in the corresponding quantum spectrum as explained in Sec. II.E. We quantize by replacing the classical Poisson algebra by its quantum counterpart and all classical quantities by the corresponding quantum operators marked by hats, e.g., $\hat{\mu}$. If quantum operators do not commute, such replacement becomes ambiguous. When this happens, we symmetrize the corresponding terms, e.g., $ab \rightarrow \frac{1}{2}(\hat{a}\hat{b} + \hat{b}\hat{a})$. Subsequently, we compute the joint quantum spectrum of the commuting operators $\widehat{\Delta\mathcal{E}}$, which corresponds to $\Delta\mathcal{E}$ given in Eqs. (32) and $\hat{\mu}$. Furthermore, we compute the spectrum of the first normal form $\widehat{\Delta E}$ that corresponds to ΔE given in Eq. (55) and we compare it to the joint spectrum. Since $\widehat{\Delta E}$ and $\hat{\mu}$ do not commute, there is no joint spectrum and in order to classify the eigenvalues of $\widehat{\Delta E}$ we should use the expectation value of $\hat{\mu}$ on the corresponding eigenstates.

A. Quantized second normal form

In order to find their joint spectrum, the Hamiltonian functions $\Delta\mathcal{E}$ and μ should be quantized. We work on the phase space $S^2 \times S^2$ where it is most straightforward. We now give the essentials. Dynamical variables (\mathbf{x}, \mathbf{y}) span an $\mathfrak{so}(3) \times \mathfrak{so}(3)$ Poisson algebra. Their quantum counterparts $(\hat{\mathbf{x}}, \hat{\mathbf{y}})$ span the $\mathfrak{so}(3) \times \mathfrak{so}(3)$ algebra

$$[\hat{x}_j, \hat{x}_k] = i\hbar \sum_{\ell=1}^3 \varepsilon_{jk\ell} \hat{x}_\ell, \quad [\hat{y}_j, \hat{y}_k] = i\hbar \sum_{\ell=1}^3 \varepsilon_{jk\ell} \hat{y}_\ell,$$

$$[\hat{x}_j, \hat{y}_k] = 0 \quad \text{for all } j, k.$$

Note that quantized invariants in Eqs. (47) contain only products of commuting components of $\hat{\mathbf{x}}$ and $\hat{\mathbf{y}}$, and moreover, to the principal order $k_+ + k_-$ (which is linear in π_1), terms that appear in the $k_- : k_+$ resonant normal form $\Delta\mathcal{E}$ are of this kind. In higher orders of $\Delta\mathcal{E}$, replacing (\mathbf{x}, \mathbf{y}) by $(\hat{\mathbf{x}}, \hat{\mathbf{y}})$ should eventually produce products of noncommuting operators which make the resulting $\widehat{\Delta\mathcal{E}}$

$O(\hbar)$ ambiguous. However, sufficiently close to the classical limit (large n) this well-known ambiguity⁵¹ may be disregarded.

The matrix representation of $\widehat{\Delta\mathcal{E}}$ can be given in a suitable common eigenfunction basis

$$|j_1, j_2; m_1, m_2\rangle =: |j; m_1, m_2\rangle \quad \text{with } j_1 = j_2 = j$$

of operators $\hat{x}_1, \hat{y}_1, \hat{\mathbf{x}}^2$, and $\hat{\mathbf{y}}^2$. The quantum number $j \geq 0$ can be integer or half integer, while the quantum numbers m_1 and m_2 take the values $-j, -j+1, -j+2, \dots, j-1, j$. It follows that the total number of states is $(2j+1)^2$ which corresponds to the shell with principal quantum number $n = 2j+1 \in \mathbb{Z}_{>0}$.

Operators $\hat{x}_1, \hat{y}_1, \hat{\mathbf{x}}^2, \hat{\mathbf{y}}^2$ act on $|j; m_1, m_2\rangle$ as follows:⁵²

$$\hat{x}_1 |j; m_1, m_2\rangle = m_1 \hbar |j; m_1, m_2\rangle,$$

$$\hat{y}_1 |j; m_1, m_2\rangle = m_2 \hbar |j; m_1, m_2\rangle,$$

$$\hat{\mathbf{x}}^2 |j; m_1, m_2\rangle = \hat{\mathbf{y}}^2 |j; m_1, m_2\rangle = j(j+1) \hbar^2 |j; m_1, m_2\rangle.$$

Furthermore, we note

$$\hat{\mu} |j; m_1, m_2\rangle = (m_1 + m_2) \hbar |j; m_1, m_2\rangle = m |j; m_1, m_2\rangle,$$

where $m = -2j\hbar, \dots, 2j\hbar$ is an integer multiple of \hbar which corresponds to the value of the classical action μ , and we impose

$$\hat{N} |j; m_1, m_2\rangle = (2j+1) \hbar |j; m_1, m_2\rangle.$$

Equality $j_1 = j_2 = j$ reflects Eq. (7) from where the value of the classical action N is obtained,

$$n = 2\sqrt{j(j+1)}\hbar \simeq (2j+1)\hbar \quad \text{for } j \gg 1. \quad (72)$$

First normalization defines the n -shell approximation (see Sec. IV.A). So both first and, of course, second normalized energy operators $\widehat{\Delta E}$ and $\widehat{\Delta\mathcal{E}}$ commute with \hat{N} and their matrix representations in the basis $|j; m_1, m_2\rangle$ factorize into blocks which describe noninteracting shells. In other words, for each fixed value of quantum number $n = 2j+1$, we can work on the n^2 -dimensional n -shell Hilbert space

⁵¹Advantages and accuracy of different approaches to quantization are beyond this review. In general, we can distinguish two issues here: (i) to which extent a classical canonical transformation, such as normalization, followed by quantization in new variables agrees with analogous direct quantum transformation; (ii) to which extent quantization commutes with Euler-Poisson reduction. Issue (i) goes back to the origins of quantum mechanics. It was examined particularly extensively for molecular Hamiltonians [see, e.g., Louck (1976)]. For an exposition of (ii), see Ginzburg *et al.* (2002, Chap. 8). Computing joint spectra from semiclassically quantized normal forms was discussed by Laurent and Vũ Ngọc (2008).

⁵²In atomic units, \hbar equals 1, but we may use different values to increase artificially the density of states.

$$\mathbb{H}_j = L^2(|j; m_1, m_2\rangle; m_1, m_2 = -j, \dots, j).$$

Furthermore, since $\widehat{\Delta\mathcal{E}}$ also commutes with μ , this space can be further split into subspaces

$$\mathbb{H}_{j,m} = L^2(|j; m_1, m_2\rangle; (m_1 + m_2)\hbar = m) \subset \mathbb{H}_j$$

invariant under $\widehat{\Delta\mathcal{E}}$ and $\hat{\mu}$. In order to find joint eigenvalues of $\widehat{\Delta\mathcal{E}}$ and $\hat{\mu}$ with quantum number m , we diagonalize the matrix of $\widehat{\Delta\mathcal{E}}$ in the basis of $\mathbb{H}_{j,m}$. In the energy-momentum domain, the resulting joint spectrum of $\widehat{\Delta\mathcal{E}}$ and $\hat{\mu}$ is represented by points (m, h) where for each $m = -2j\hbar, \dots, 2j\hbar$ the energies h are given by the respective eigenvalues of $\widehat{\Delta\mathcal{E}}$.

B. Quantized first normal form $\widehat{\Delta E}$

For many reasons, such as avoiding possible discrepancies introduced by the integrable approximation and its quantization (see footnote 51), quantum calculations are better performed for the second normalized system but for the Keplerian normalized system (n -shell approximation) or even for the initial system with the Hamiltonian (2). An extensive calculation of this kind may be considered as “experimental data” which can be interpreted using the results for the normalized system. In this case, the main difficulty is the absence of strictly defined joint eigenspectrum. For the original system, the quantum operators $\hat{\mu}$ and \hat{N} no longer commute with the Hamiltonian \hat{H} . However, for each eigenfunction ψ of \hat{H} we can obtain an estimate of the corresponding classical value m (and n) as the average $\langle \hat{\mu} \rangle = \langle \psi | \hat{\mu} | \psi \rangle$ (and $\langle \hat{N} \rangle$). Additionally, for each eigenstate, we can estimate the uncertainty

$$\Delta\mu = \sqrt{\langle \psi | \hat{\mu}^2 | \psi \rangle - \langle \psi | \hat{\mu} | \psi \rangle^2},$$

which we expect to be smaller than \hbar and which is smaller for the eigenstates for which μ is conserved better. Another similar characteristic is given by

$$-\langle \psi | [\widehat{\Delta E}, \hat{\mu}]^2 | \psi \rangle.$$

This uncertainty can be improved using normalized $\hat{\mu}$ (and \hat{N}) which will be denoted $\bar{\mu}$. We give more detail on the example of the first normalized system where the role of H is played by the first normalized energy ΔE in Sec. IV.B, n is an exact quantum number, and we use $\langle \hat{\mu} \rangle$ to approximate m .

Transforming $\Delta E(\mathbf{x}, \mathbf{y})$ into $\widehat{\Delta E}$ and computing the eigenspectrum of $\widehat{\Delta E}$ can also be done as outlined in Sec. VII.A. Two specific aspects should be noted. Certain terms in $\widehat{\Delta E}$ contain products of noncommuting operators which require symmetrization. Furthermore, since $[\widehat{\Delta E}, \hat{\mu}] \neq 0$, we should use the $n^2 \times n^2$ matrix representation of $\widehat{\Delta E}$ in the basis of \mathbb{H}_j .

TABLE VI. Normalizing correction $\bar{\mu}^{(2)}$ to momentum μ expressed in the coordinates (\mathbf{x}, \mathbf{y}) of the first normalized near 1:1 resonant system; $d_s = \sqrt{1-2d}$ and $d_c = \sqrt{1+2d}$.

Term	Coefficient $\times -6d_s^3 d_c^3 (d_s + d_c)/s$
$x_2 y_2 - x_3 y_3$	$-6d_s^2 d_c^2 [(d_s d_c - 1)a^2 + 2d^2]$
$x_2^2 - x_3^2$	$d_c^3 (d_c + d_s)(-a^4 + a^2 - d^2)$
$y_2^2 - y_3^2$	$d_s^3 (d_s + d_c)(-a^4 + a^2 - d^2)$
$x_2 y_1$	$d_c^2 d_s (d_s + d_c)(1 - 10d)\sqrt{-a^4 + a^2 - d^2}$
$x_1 y_2$	$-d_s^2 d_c (d_c + d_s)(1 + 10d)\sqrt{-a^4 + a^2 - d^2}$
$x_1 x_2$	$2d_c^3 (d_c + d_s)(2a^2 - 4d + 1)\sqrt{-a^4 + a^2 - d^2}$
$y_1 y_2$	$-2d_s^3 (d_s + d_c)(2a^2 + 4d + 1)\sqrt{-a^4 + a^2 - d^2}$

The momentum μ in Eq. (47) and ΔE Poisson commute only in the first order. An improved estimate of m can be obtained using the normalized

$$\bar{\mu} = \bar{\mu}^{(1)} + \bar{\mu}^{(2)} = x_1 + y_1 + \bar{\mu}^{(2)}, \quad (73)$$

which commutes with ΔE to the third order; i.e., the lowest-order contribution to $\{\Delta E, \bar{\mu}\}$ is $\{\Delta E^{(2)}, \bar{\mu}^{(2)}\} \neq 0$. Table VI gives an example of $\bar{\mu}^{(2)}$ obtained by Efsthathiou *et al.* (2009) for the 1:1 systems. To understand how it was computed, recall that the second normalization is a near unity coordinate transformation \mathcal{L} on $S^2 \times S^2$ defined so that in the transformed coordinates the second normalized energy correction $\Delta\mathcal{E}$ (or Hamiltonian) commutes with $\mu = x_1 + y_1$ up to second degree terms. The series (73) is the preimage $\mathcal{L}^{-1}(\mu)$ of μ defined in the same (original) coordinates as the first normal form ΔE .

C. Quantum joint spectra

The first interpretation of the joint spectrum of the perturbation (2) in terms of monodromy was given by Cushman and Sadovskii (1999, 2000) for A_2 -type systems. They used $\widehat{\Delta\mathcal{E}}$ and their elementary cell diagram is reproduced in Fig. 26. Schleif and Delos (2007, 2008) obtained this diagram using a quantized initial Hamiltonian (2) and expectation values $\langle \hat{\mu} \rangle$ of the momentum (cf. Sec. VII.B); they also extended the analysis to near orthogonal systems and uncovered other types, notably the $A_{1,1}$ also shown in Fig. 26. The same diagrams were obtained by Efsthathiou *et al.* (2009) using $\widehat{\Delta\mathcal{E}}$ and $\widehat{\Delta E}$.

Quantum lattices for the B -type 1:1 systems can also be found in the works cited above. Their specific feature is the presence of two sublattices corresponding to the two overlapping leaves of their respective BD . Figure 27 shows how such structures change for the 1:2 resonance. In this case, the multileaf B -type BD is replaced by a single-leaf self-overlapping BD with two internal walls due to the presence of curled tori. A double cell can be moved across these walls and can reach everywhere in order to define the third global quantum number k .

Another interesting aspect of quantum joint spectra of our systems is their simple relation to the Duistermaat-

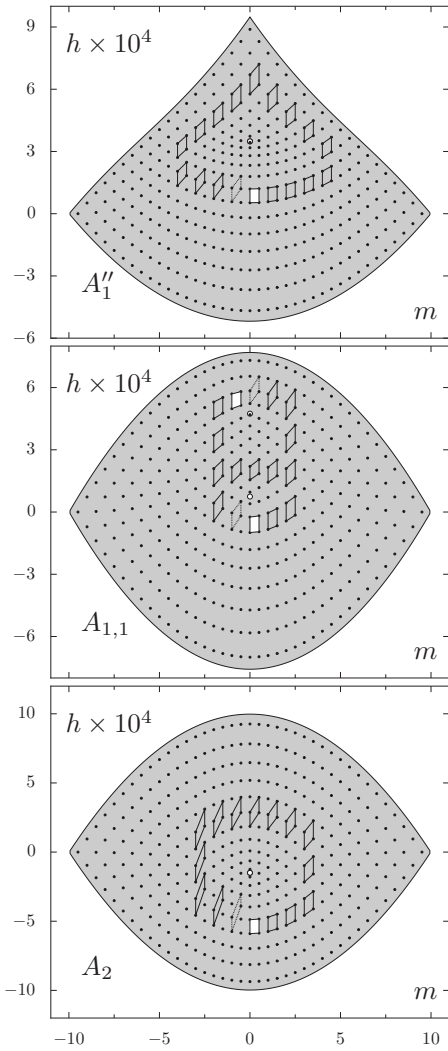


FIG. 26. Joint energy-momentum spectrum (black dots) and elementary cell diagrams of 1:1 systems with monodromy (cf. Fig. 16 and Table II). In each case, the initial elementary cell is painted white and is parallel transported in a counterclockwise direction around a critical value (opaque circle) or a set of critical values of the \mathcal{EM} map. The final cell is represented by a cell with a dashed boundary.

Heckman (DH) theorem,⁵³ the theory of lattice defects (Zhilinskiĭ, 2005) and, for the A -type systems, the theory of almost toric fibrations (Sec. II.F) for which the base space can be described as a convex polytope with cuts in the action space, i.e., in the space of global quantum numbers.

We now comment on the DH theorem. Consider the Hamiltonian S^1 action on the Keplerian reduced phase

⁵³Duistermaat and Heckman (1982) considered orbit spaces P_j obtained by reducing a proper Hamiltonian S^1 action on a compact symplectic manifold M . They showed that the Liouville volume of P_j is a piecewise-linear continuous function of the value j of the associated momentum J and that the slope change is given by the change of the Chern index of the S^1 bundle over P_j . See also Atiyah and Bott (1984), Ginzburg *et al.* (2002), Nguyễn Tiên (2002), and Guillemin (2007).

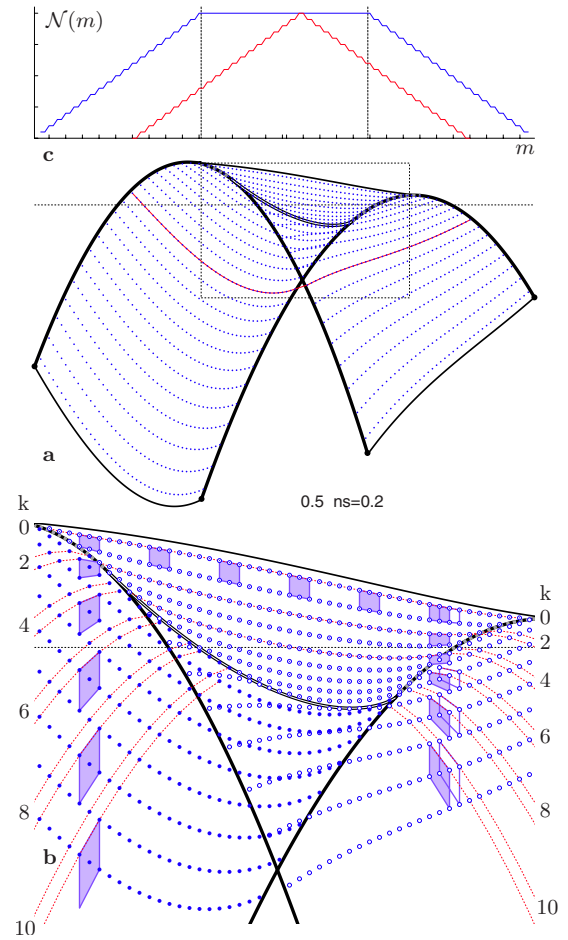


FIG. 27. (Color online) Joint spectrum and number of states of the 1:2 resonant system. (a) and (b) Joint energy-momentum spectrum (lattice dots) and classical energy-momentum bifurcation diagram (lines) of the 1:2 resonant system with $s = 1/200$, $a^2 = 0.5$, and $d = 0.3$ for $n = 40$ and $\hbar = 1$. (b) Dashed lines join states with the same value of the global quantum number k defined by the parallel transport of the elementary cell; below the $T^2_{[1/2]}$ wall these lines branch in two. (c) Corresponding number of states \mathcal{N} as a function of the value m of the 1:2 momentum μ . Adapted from Efsthathiou *et al.*, 2008.

space $S^2 \times S^2$ (which is a compact symplectic manifold) defined by momentum μ for some fixed $n > 0$. Sufficiently far in the semiclassical limit, the phase space volume of $P_{n,m}$ is well approximated by the total number of states $\mathcal{N}(m)$ with the same quantum number m . We observe that $\mathcal{N}(m)$ is a piecewise linear function of m that changes slope when $m = \pm m_{\text{crit}}$, i.e., when $P_{n,m}$ is singular. Thus in the 1:2 example in Fig. 27(c), the slopes are $\approx +\frac{1}{2}$, 0, and $\approx -\frac{1}{2}$ when $m < -m_{\text{crit}}$, $|m| < m_{\text{crit}}$, and $m > m_{\text{crit}}$, respectively, and, furthermore, $\mathcal{N}(m)$ has an oscillatory component typical for resonances of order $k_+ + k_- > 2$ [cf. Sadovskii and Zhilinskiĭ (1995)].

VIII. BIBLIOGRAPHIC REMARKS

We provide further discussion of the literature on the perturbation problem of the hydrogen atom by static

homogeneous electric and magnetic fields, one of the oldest in atomic physics. A complete survey of the vast stream of papers on this subject is beyond our scope. Within this stream it is important to identify clearly specific papers which are related in spirit and technique to the global approach described here. To this end we (i) give a summary of the guiding ideas of this approach, (ii) move aside all work that is not directly relevant, and (iii) review concisely the remaining body of work.

To assess the pertinence of such discussion, it can be noted that despite a great number of detailed studies of concrete perturbations in the 1980s and 1990s, no general, concise and meaningful classification of the family of all perturbations was provided while the interest had shifted gradually from the perturbation regime to a predominantly chaotic one. It appears that physicists focused largely on the complicated dynamical behavior for concrete fixed values of first integrals (energy, Keplerian action, angular momentum, etc.) and neglected establishing a (global) connection between systems with different values. Subsequently, as it often happens to intensely studied topics, the problem demanded a disengagement and a refreshed point of view.

While selecting the papers for this review, we used their contribution towards the above classification as a primary criterion and tried to exclude any other bias. This structuring idea helped in the vast publications on the subject. Indeed, given the large number of papers, it is hardly possible to review everything adequately.

A. The general idea of our approach

Our approach is a natural continuation of the geometric methods initiated in the theory of Hamiltonian dynamical systems during the last two decades.⁵⁴ Considered most generally, our above problem is a study of a perturbation which depends essentially on three parameters. Additionally, for sufficiently small parameter values, an integral approximation to this system always has two momenta, i.e., two Hamiltonian functions in involution which by their respective Hamiltonian flows define a \mathbb{T}^2 Lie symmetry group action on the phase space. In order to analyze this system as a perturbation, we consider a three-parameter family of three-dimensional bifurcation diagrams (or stratified images of the energy-momentum map \mathcal{EM}). This gives potentially a comprehensive classification of all possible perturbations and thus describes the problem as a whole.

In our view, as long as the features of a particular nonintegrable system under study, such as surviving Lagrange tori, tangles, and lower-dimensional (non-

Lagrangian) tori, can be related to the respective elements of the integrable approximation, namely, invariant tori, singular fibers, relative equilibria, or relative periodic orbits, this relation must be fully uncovered. Only when such a relation is shown not to exist, the features under study can be attributed as truly specific features of the individual system (or of a narrower class of systems).

B. Topics outside our scope

We leave out all numerous studies which (for sufficiently large fields with $ns > 1$) treat the system as completely chaotic; this includes the work based on the closed orbit theory, an offspring of periodic orbit quantization methods, and the related topics of recurrence spectroscopy, near-threshold field ionization, etc. Furthermore, we restrict ourselves to static homogeneous fields and to the standard Keplerian two-body setup in the limit of the infinite mass of the proton. Hence we do not discuss modifications due to nonhydrogenic core effects, time dependent (periodic) fields, quadrupole fields, finite proton mass, spin, and relativistic corrections. At the energies we study, the classical motion remains bound; this excludes all work on the continuous quantum spectrum and resonances (not to be confused with resonances of our integrable approximation). Because we rely on basic quantum-classical correspondence, we will not cover the effects of broadening due to the tunneling interaction with the continuous spectrum. Additionally, we will not discuss purely quantum studies of individual levels, typically at low quantum numbers for which the quantum-classical correspondence principle is difficult to apply. And equally, we are not interested in the studies of local “phase space structures,” typically centered on specific elliptic periodic orbits, which are studied starting at the chaotic end without relation to any possible global structure of the phase space.

The last point deserves mention. For an example of such local structures see [Gekle et al. \(2006, 2007\)](#), where a numerical technique to track some non-Lagrangian (two-dimensional) tori of the system is implemented. Persistence of such invariant manifolds under perturbation can be regarded within the framework of the refined KAM theories or more generally that of periodic orbits ([Nekhoroshev, 2002, 2005](#)). In the former case, such structures can be related to two-dimensional relative equilibria, i.e., two tori which are orbits of the dynamical symmetry \mathbb{T}^2 or relative periodic orbits of the integrable approximation (normal form), and it is possible that the ones studied by [Gekle et al. \(2006, 2007\)](#) are similar. However, with no such analysis provided we cannot comment on this work any further.

C. Review of relevant literature

[Pauli \(1926\)](#)⁵⁵ formulated the linear problem. He suggested a treatment of perturbations of the hydrogen

⁵⁴See [Cushman and Bates \(1997\)](#), [Michel and Zhilinskiĭ \(2001b\)](#), [Bolsinov and Fomenko \(2004\)](#); and [Efsthathiou \(2005\)](#) for a general survey and [Sadovskii et al. \(1996\)](#), [Sadovskii and Zhilinskiĭ \(1998, 1999\)](#), [Cushman and Sadovskii \(2000\)](#), [Michel and Zhilinskiĭ \(2001a\)](#), [Efsthathiou, Cushman, and Sadovskii \(2007\)](#), and [Efsthathiou, Sadovskii, and Zhilinskiĭ \(2007\)](#) for concrete applications to our present system.

⁵⁵See [Van der Waerden \(1968\)](#) and [Valent \(2003\)](#).

TABLE VII. Experimentally scaled field strengths attained in the perturbation regime $ns \ll 1$.

Reference	F (kV/cm)	B (T)	n	f	g	ns	a^2
Garton and Tomkins, 1969	0	2.4	30	0	0.009	0.27	1
Cacciani, Liberman, <i>et al.</i> , 1988; Cacciani <i>et al.</i> , 1986	0.025	3.11	30	3.9×10^{-4}	0.012	0.35	0.9989
	0.1	1.65	30	0.0015	0.0063	0.19	0.94
Wiebusch <i>et al.</i> , 1989	2	6	21	0.010	0.011	0.32	0.52
	4	6	21	0.021	0.011	0.51	0.21

atom within the framework of the *neue Quantenmechanik* and obtained the first-order perturbation Hamiltonian by averaging over hydrogenic states. In our context [see Valent (2003)], his most essential contribution was the proposition that after the Keplerian averaging, i.e., in the n -shell approximation, the perturbed system for any configuration of electric and magnetic fields has automatically an additional (second) approximate dynamical symmetry S^1 associated with the linear flow of the momentum μ . So this symmetry can be rightfully called Paulian. We should also attribute to Pauli the general approach based on a reduced (averaged) n -shell Hamiltonian which has the advantage over quantum perturbation corrections to individual levels in that it gives a global view at the particular system and at the parametric family of these systems and can potentially be related to classical dynamics.

Higher-order theory, notably for the pure magnetic field (Edmonds, 1970) perturbations known as quadratic Zeeman effect (QZE) or diamagnetism of hydrogen or Rydberg atoms, was encouraged by advances in high resolution atomic spectroscopy (Garton and Tomkins, 1969). Many detailed experiments followed, and some are listed in Table VII. The early attempt to obtain the second-order correction to the n -shell energy levels in the presence of both fields (Demkov *et al.*, 1969) was unsuccessful due to the difficulty of accounting for the electric field [see Manakov *et al.* (1976)]. However, these studies set the stage for the subsequent comprehensive analysis. The setup was completed by Clark and Taylor (1980, 1981) and Zimmerman *et al.* (1980), who conjectured that the typical regular level patterns observed in QZE (for $m=0$), the so-called “quasi-Landau” sequences, which resembled those of a rotator and an oscillator, reflected an “approximate dynamical symmetry.” The precise meaning of this similarity remained unresolved (see Sec. VIII.C.5).

1. Second-order perturbation theory of the 1980s

The major advancement of the early 1980s was extending Pauli’s analysis to the second-order Hamiltonian of the QZE system, which was obtained by Solov’ev (1981, 1982) and Grozdanov and Solov’ev (1984) by di-

rect classical averaging over Keplerian orbits⁵⁶ and, at about the same time, by Herrick (1982), who constructed a quantum n -shell effective operator [cf. Delande and Gay (1984)]. Recall that for QZE the Paulian symmetry is simply the axial symmetry $SO(2)$ and, therefore, the reduced Hamiltonian they obtained corresponds to the particular form of the second-order \mathcal{H}_2 of our second reduced Hamiltonian \mathcal{H} . A study for orthogonal fields followed by Grozdanov and Solov’ev (1982) and Solov’ev (1983) and later by Braun and Solov’ev (1984a, 1984b).

Two additional important ideas appeared at this stage: the use of classical mechanics and the search for a relation between global quantum level patterns and the reduced Hamiltonian. Specifically, from the quasidegeneracies of the level patterns, all states within one n shell and m multiplet, i.e., all states of the second reduced system, were separated by Herrick (1982) into vibrational and rotational. The former are doublets which lie in the dark gray shaded part of the B_0 \mathcal{BD} where the two of its three cells overlap, while the latter lie above that part in a single cell (see row B_0 in Table II). In the physical phase space \mathbb{R}^6 , vibrations correspond to the motion near one of the two equivalent stable Keplerian S^1 RE with $m=0$ (lower tip of the \mathcal{BD}), which go up and down the field axis, while rotations correspond to the localization near the T^2 RE (upper boundary of the \mathcal{BD}).

A further important technical development was the implementation of the regularization of the Kepler Hamiltonian, followed by the normalization of the resulting coupled oscillator system, and quantization of the reduced Hamiltonian. This combined approach was implemented by Robnik and Schrüfer (1985) for the QZE system, which after reduction of the axial symmetry can be regularized by the Levi-Civita method; quantization followed from the Poisson algebra of the oscillator system (Robnik, 1984). This scheme was, essentially, a direct predecessor of our techniques.

A number of studies of concrete field configurations followed [see, e.g., Cacciani *et al.* (1986), Cacciani, Luckoenig, *et al.* (1988), and Braun (1993)]. These were mostly restricted to systems with axial symmetry (QZE or parallel fields) and quite often to states with zero pro-

⁵⁶See a simplified derivation given by Reinhardt and Farrelly (1982) and Gay *et al.* (1983).

jection of the angular momentum on the field axis ($m=0$). Furthermore, it was customary to rescale the energies by the magnetic field amplitude which suited the case of relatively weak electric fields, i.e., B_0 and B_1 in Table II. Thus Cacciani *et al.* (1986) and Cacciani, Luckoenig, *et al.* (1988), who represented, arguably, the best of the perturbation results of 1980s,⁵⁷ explored what we call today the 1:1 zone⁵⁸ and, in particular, they distinguished three types of localized states in the B_1 system: (I) near the minimum energy RE of the larger cell, (II) near the minimum energy RE of the smaller cell, and (III) near the maximum energy RE. Naturally, states of types I and II are called vibrational, while those of type III are called rotational. Because their study is limited to $m=0$, Cacciani *et al.* do not notice that there is, in fact, a smooth transition between states of types I and III at $m \neq 0$ which does not exist for pure QZE. For further comparison, it may be helpful to consider more recent work on the same subject⁵⁹ and it is also instructive to recall the similarity to the spherical pendulum (type A_1) and its quadratic deformations (type B_1) discussed by Efsthathiou (2005, Sec. 4.2).

2. Geometry of the reduction map

The above-mentioned (see footnote 59) work by Salas *et al.* (1998) affords us to now comment on certain misleading conclusions, mistakes in a strict geometrical and physical sense, which are both somewhat implicit and quite characteristic to a number of similar studies. They observed correctly the two stability changes of one of the two Keplerian REs with $m=0$ (which they denoted E_2 and which corresponds to one of the singular tips of the second reduced space $P_{n,0}$). They saw these events as pitchfork bifurcations involving two unstable RE (which they denote $E_{3,4}$) for the B_1 system and two stable RE ($E_{5,6}$) at the maximum energy of the B_1 and A_1 systems. Comparing to what really goes on in $S^2 \times S^2$, the two unstable RE should correspond to only one singular circle on the $m=0$ bitorus, while the two stable RE should represent a single S^1 orbit; both lift to a T^2 RE in the physical phase space R^6 . On the other hand, Salas *et al.* saw no orbit “doubles” for $m \neq 0$ where they have

⁵⁷Such studies come essentially to the reduced dynamics on the $m=0$ space $P_{n,0}$ whose two singular tips get lost in polar coordinates (called typically angle action) that map $P_{n,0}$ to a cylinder [cf. Delos *et al.* (1983b, 1984), Waterland *et al.* (1987), and Braun (1993), and Secs. VIII.C.2 and VIII.C.5].

⁵⁸See Cacciani, Luckoenig, *et al.* (1988, Fig. 3) where the 1:1 zone corresponds to the range of \parallel field ratio parameter β whose values 0 , $(0, \frac{1}{5})$, $(\frac{1}{5}, 1)$, and $\beta > 1$ represent systems of types B_0 , B_1 , A_1 , and A_0 , respectively. Compare to quantum levels of Sadovskii *et al.* (1996, Fig. 2).

⁵⁹See Deprit *et al.* (1996), Salas and Lanchares (1998), and Salas *et al.* (1998). In Fig. 1 of Salas and Lanchares (1998), the parameter λ goes from $\lambda=1$ (QZE system B_0) to $\lambda=0$ (Stark limit), in the intervals $(1, \frac{3}{4})$ and $(\frac{3}{4}, \frac{3}{8})$ we have systems B_1 and A_1 , respectively, for $\lambda < \frac{3}{8}$ the type becomes A_0 , and we quit the 1:1 zone.

standard fold catastrophes (Deprit *et al.*, 1996; Salas and Lanchares, 1998). Since $m=0$ and $m \neq 0$ are treated in separate papers and no reconstruction of invariant sets in R^6 is undertaken, the discontinuity of the description remains well hidden.⁶⁰ As for the nature of the two bifurcations, both are in fact Hamiltonian Hopf bifurcations (van der Meer, 1985), possibly modified by a Z_2 symmetry (Efsthathiou, Cushman, and Sadovskii, 2004), and are specific phenomena in two degrees of freedom which cannot be analyzed adequately on the two-dimensional reduced phase space of Salas *et al.* (1998).

At the origin of these discrepancies is the use by Salas *et al.* (1998) of (certain combinations of) Delaunay variables.⁶¹ These variables are not global (Cordani, 2000) and care should be taken to avoid distorting the geometry of the flow of the system (Efsthathiou and Sadovskii, 2005). More specifically, in many studies⁶² reduced phase spaces for all m become smooth spheres⁶³ S^2 . We can see from Sec. IV.D.2.c that such a representation is adequate for $n > |m| > 0$, while for $m=0$ it fails because the true (in the sense one orbit–one point) reduced phase space $P_{n,0}$ of any 1:1 system is a sphere with two conical singularities (Cushman and Sadovskii, 2000, see Sec. 5.4). This singularity is masked by that of polar coordinates themselves or worse, it is assumed, as in Salas *et al.* (1998), to be “removed.” Yet it does not go away without a price. For Salas *et al.* (1998) this is working with a twofold covering of $P_{n,0}$ by a smooth S^2 sphere⁶⁴ which explains the doubling of RE.

3. Restrictions to specific systems

Classification of all possible perturbations was impeded in the 1990s by certain popular restrictions. Thus, in many papers of that and earlier period,⁶⁵ the dynamics and quantum levels in the presence of the axial symmetry (parallel fields, QZE) were often studied at different fixed values of the projection m of the angular

⁶⁰Following Cushman, we note that the main problem of Salas *et al.* (1998) is that after reducing axial symmetry and using Levi-Civita regularization, their regularized energy surface becomes not the unit tangent bundle to the two-sphere (which is real projective three-space RP^3) but a three-sphere S^3 . The latter is a double covering of RP^3 , and this caused discrepancies in the subsequent analysis.

⁶¹See Eq. (7) of Salas *et al.* (1998) and compare to Eq. (43) of Farrelly *et al.* (1992) and to Uzer (1990), Farrelly and Krantzman (1991), Farrelly and Milligan (1992), Krantzman *et al.* (1992), and Gourlay *et al.* (1993).

⁶²See Uzer (1990), Farrelly and Krantzman (1991), Farrelly and Milligan (1992), Farrelly *et al.* (1992), Krantzman *et al.* (1992), Gourlay *et al.* (1993), and Salas *et al.* (1998) and Sec. VIII.C.5.

⁶³Represented in polar coordinates as $S^1 \times [0, 1]$ cylinders.

⁶⁴Using the notation of Salas *et al.* (1998), points (u, v, w) and $(-u, v, -w)$ on the smooth S^2 represent the same S^1 orbit on $S^2 \times S^2$ and should be identified, giving thus $P_{n,0}$.

⁶⁵See, e.g., Braun and Solov'ev (1984b), Cacciani *et al.* (1986), Cacciani, Luckoenig, *et al.* (1988), Uzer (1990), and Farrelly and Krantzman (1991).

momentum almost as if they were different systems and often only the case $m=0$, the most accessible in experiments, was considered. One would display diagrams of quantum energies of the $m=0$ states as a function of field strengths (Braun and Solov'ev, 1984a; Braun, 1993) ignoring the presence of many other close energy levels of the same n shell. Similarly, Salas *et al.* (1998) can see nothing outside the 1:1 zone while they followed the single $m=0$ submanifold continuously all the way to the Stark limit. This is one of the reasons why such basic phenomena as collapse (Sadovskii *et al.*, 1996) and higher resonances (Efsthathiou, Sadovskii, and Zhilinskii, 2007) remained unnoticed for a long time (cf. Sec. IV.C).

Other frequent restrictions occur due to the choice of scaling and the resulting ordering of the perturbing terms. Thus Cacciani, Luckoenig, *et al.* (1988) (see footnote 58) focused exclusively on the 1:1 zone using a field configuration parameter β that suits the near Zeeman limit. Similarly, unlike the uniform scaling in Eq. (3), the scaling of Salas *et al.* (1998) placed the QZE term and the linear Stark term in the same order of the perturbation and is therefore preferential to the amplitude G of the magnetic field. Another similar frequent choice, implying relatively weak electric fields with $F \ll G$, is to scale the n -shell energies by G . Neither choice is adequate for the description of the whole parametric family.

4. Dynamical symmetry, equivalent operators

The SO(4) dynamical symmetry approach to the hydrogen atom (Fock, 1935; Bargmann, 1936) was formulated ten years after Pauli (1926) and Schrödinger (1926). The subject was discussed widely (Bander and Itzykson, 1966; Englefield, 1972; Prince and Eliezer, 1981; Guillemin and Sternberg, 1990) and its potential applications to perturbations were analyzed by Kalnins *et al.* (1976), Avron *et al.* (1979), and Barut *et al.* (1979). The approach provides the so-called equivalent operators and supplies convenient wave function bases and techniques to calculate matrix elements and can be used to model complicated systems without tracing everything explicitly back to the original formulation (Adams *et al.*, 1982). Concrete results begin with Herrick (1982), who is closely related to the original ideas of Fock (1935). These are followed by extensive applications to the axially symmetric case including QZE and parallel fields.⁶⁶

Note that in our systems equivalent operators are invariants of the action of the dynamical symmetry, which can be studied explicitly (on \mathbb{R}^6 or \mathbb{R}^8). Thus all SO(4) equivalent operators are Keplerian invariants and are functions of the six components in Eq. (28) for which the quantum n -shell calculus is rather straightforward (see Sec. VII). Note also that an n -shell equivalent of the Hamiltonian is its one-time Keplerian average, which may differ in the second and higher orders from the

Keplerian normal form, such as \bar{H}_{KS} in Eq. (25), because the latter may accumulate contributions from the lower orders. In principle, a normal form gives a more accurate description than an SO(4) equivalent operator. This limits the technical value of the equivalent operator approach, while the importance of the dynamical symmetry analysis persists in the use of invariants and in the geometry of corresponding Hamiltonian flows. More generally, outside the n -shell approximation, Lie algebraic methods (Adams *et al.*, 1988) explicitly related to classical invariants and their Poisson algebra seem to be the most appropriate strategy of treating dynamical symmetries. Such an approach is essentially a continuation of the thread beginning with Pauli (1926) and Bargmann (1936).

5. Reduced dynamics, rotator models

We saw in Sec. IV that after the reduction of Keplerian and Pauliean S^1 symmetries corresponding to momenta N and μ with values n and m , the original system with the Hamiltonian (2) becomes (for $|m| < n$) a one-degree-of-freedom reduced system on a compact two-dimensional phase space $P_{n,m}$, which is diffeomorphic for most m or homeomorphic for specific critical m_c to a smooth S^2 sphere.⁶⁷ Quantization of this system can be done in two ways. (i) We can return to the first reduced (n -shell) system and quantize it straightforwardly as a system of two coupled angular momenta \mathbf{x} and \mathbf{y} [Eqs. (34)] with fixed amplitudes $n/2$ [Eq. (7)] (see Sec. VII). (ii) Alternatively, we can deform the Poisson algebra in Eq. (58) into an algebra with standard so(3) structure and quantize the latter (for each m separately). The deformation preserves the Poisson structure on $P_{n,m}$ but the resulting map $P_{n,m} \rightarrow S^2$ is necessarily singular⁶⁸ for $m=m_c$. This approach was developed generally by Karasev and Novikova (2005) as a natural realization of the ideas of Poisson quantization.⁶⁹

The above discussion appears straightforward. Historically, however, it was a source of considerable confusion because the second reduced system (often considered only for $m=0$) is only topologically similar to an

⁶⁷For the 1:1 case with $m_c=0$, i.e., for orthogonal and near-orthogonal fields, this has been shown by Cushman and Sadovskii (2000), for other resonances see Theorem 5.1 of Karasev and Novikova (2005), where $P_{n,m}$ is called closure of a symplectic leaf, and Efsthathiou, Sadovskii, and Zhilinskii (2007).

⁶⁸For the 1:1 case, the explicit deformation of Cushman and Sadovskii (2000, Sec. V.D.2) is singular for $m=0$ at points $\pi_1 = \pm 1$, i.e., at the conical tips of $P_{n,0}$. It is inspired by action-angle coordinates of Uzer (1990), Farrelly and Krantzman (1991), Farrelly and Milligan (1992), Farrelly *et al.* (1992), Krantzman *et al.* (1992), and Gourlay *et al.* (1993).

⁶⁹See Karasev and Maslov (1982), Vorob'ev and Karasev (1987), and Karasev (1998) and also Sniatycki and Weinstein (1983), Weinstein (1994), and Bates *et al.* (2009).

⁶⁶See, in particular, Delande and Gay (1984, 1986, 1991) and Iu *et al.* (1991).

Euler top and is different geometrically from the latter,⁷⁰ i.e., their flows, orbits, and reduced phase spaces are geometrically different (Sec. VIII.C.2). This difference was often implied but remained implicit until Cushman and Sadovskii (2000). Thus ten years after Solov'ev (1981, 1982) obtained the second normal form \mathcal{H}_2 followed closely by Grozdanov and Solov'ev (1982) and Reinhardt and Farrelly (1982), Farrelly and Milligan (1992) wrote⁷¹ “Despite much study, an outstanding problem in the theory of QZE is the semiclassical quantization.”

After conjectures of Clark and Taylor (1980, 1981, 1982) and Zimmerman *et al.* (1980), Delos *et al.* (1983a, 1983b, 1984) reproduced correctly the quantum QZE energies by reducing axial symmetry and following numerically classical trajectories in Delaunay angle coordinates. In that way, the double well nature of the lower part of the spectrum and, separately, the higher energy states were described. The corresponding trajectories were shown to be librational and rotational, respectively.⁷² This reproduced the quantum results of Herrick (1982) and separated clearly the Keplerian component of the flow of the QZE system that Solov'ev (1981, 1982) used for averaging. However, such an essentially local approach did not uncover what if any approximate dynamical symmetry there was. Neither was the relation of the trajectory analysis to the global integrable approximation by Solov'ev (1981, 1982), Grozdanov and Solov'ev (1982), and Reinhardt and Farrelly (1982) and its quantum analog by Herrick (1982) given.⁷³

The situation was slightly helped by applying Coulomb scattering theory by Fano *et al.* (1988). A description was obtained separately for the two kinds of states. Interestingly, in this approach, the rotational states were viewed as localized near a “ridge” of an effective potential (Fano, 1980a, 1980b, 1988; Rau and Armen, 2000) and this was singled out as a specific phenomenon. Of

⁷⁰For this reason, we prefer to speak of the rotator analogy instead of dynamical symmetry $so(3)$; we reserve the latter terminology for Lie symmetries with free action on the phase space.

⁷¹More generally, we may interpret this remark of Farrelly and Milligan (1992) as referring to the problem of quantizing systems with singular phase spaces [cf. Vũ Ngọc (2000) and Colin de Verdière and Vũ Ngọc (2003)].

⁷²We see in Delos *et al.* (1983a, 1983b, 1984) the distant origins of the trajectory-based analysis, used later to study the chaotic dynamics at large field amplitudes for which any “inconvenient” (global and local) integrability was presumed to be destroyed.

⁷³To assess geometric limitations of such descriptions, consider the $m=0$ restricted \perp fields (B_0 and A_2 systems) study by Braun and Solov'ev (1984b) (see footnote 57) and Cushman and Sadovskii (2000, Sec. 5.6). We see that the doubly pinched torus $\mathbb{T}_{[2]}^2$ (Sec. II.C.3) in A_2 appears in Braun and Solov'ev (1984b) and Braun (1993) as a specific “quasibarrier” singularity of the $m=0$ effective potential, while the bitorus $\mathbb{T}_{b_1}^2$ in B_0 is a different “barrier” separating rotational and vibrational motions.

course, on a compact space, such as $S^2 \times S^2$, or $P_{n,m}$, or an S^2 of the reduced Euler top, localization near any elliptic equilibrium comes as no surprise, but this may be different within the scattering theory context, where compactification and self-interference are achieved via the boundary conditions. The ridge is most likely related to the axial (and in general to Pauliean) symmetry. So the reduced Hamiltonian \bar{H}_{KS} on $S^2 \times S^2$ has an S^1 ridge maximum (the image of the \mathbb{T}^2 RE) and two equivalent minimum equilibrium points. Since scattering methods moved, naturally, into high energy-field chaotic regimes, we will not discuss them further.

Effective potentials also appear in the so-called discrete semiclassical methods (Braun, 1993) which gave again a description without a clear analysis of global integrability, i.e., without geometry (see footnote 72). Such methods were equally successfully applied to describe quantum rotators and 1:1 resonant oscillators, but the differences were lost in technical details of the comparison (Braun, 1993; Appendix C).

The first direct attempts to relate the system of the $\hat{\mathcal{H}}_2$ eigenstates as a whole to that of a rotator can be found in Rau (1986) and Rau and Zhang (1990). The decisive step was made by Uzer (1990), who stated explicitly the $SO(3)$ dynamical symmetry⁷⁴ and the correspondence between the classical QZE system and the Euler top on the basis of the discussed results (Robnik, 1981, 1982; Robnik and Schrüfer, 1985) on the regularized and normalized QZE Hamiltonian. This rotator analogy was thoroughly analyzed and exploited by Farrelly and Krantzman (1991), Farrelly and Milligan (1992), Farrelly *et al.* (1992), and Krantzman *et al.* (1992) and extended subsequently to nonaxial, i.e., Pauliean, symmetry of Gourlay *et al.* (1993).⁷⁵ Extension to $k_-:k_+$ resonances other than 1:1 is detailed in Sec. IV.D.2.e. Unfortunately, the singularity of the mapping that leads to the explicit rotator analogy went unnoticed at the time. This incompleteness propagated into later important work on general field configurations (von Milczewski *et al.*, 1994a, 1994b, 1997a, 1997b; Uzer and Farrelly, 1995; von Milczewski and Uzer, 1997a, 1997b) where a systematic attempt was made to understand the family of the regular \mathbb{T}^3 tori of these systems. Because the singularity and the underlying singular fiber that plays a central role in the global geometry of the respective toric fibration were ignored, the description of the family could not be completed until Cushman and Sadovskii (2000).

6. KS regularization and applications

The initial quantum-mechanical description of the hydrogen atom and its perturbations (Pauli, 1926; Schrödinger, 1926; Fock, 1935; Bargmann, 1936) was based on the three-dimensional Hamiltonian (2) and so

⁷⁴See footnote 70.

⁷⁵These studies are in many ways direct predecessors of our later computations Sadovskii *et al.* (1996), Sadovskii and Zhilinskii (1998), and Cushman and Sadovskii (2000).

was the work by Solov'ev (1981, 1982, 1983) and Herrick (1982). At the same time, the virtues of regularizing the $1/r$ singularity of the Kepler-Coulomb potential in Eq. (2) began to become acknowledged.⁷⁶ In the absence of the exact axial symmetry, the Hamiltonian (2) can be regularized following the Kustaanheimo-Stiefel (KS) method.⁷⁷ Surveying mathematical aspects of this transformation, its different formulations (e.g., using quaternions, Clifford algebras, etc.) and generalizations would make a subject of specialized review. We remain focused on applications in quantum and classical analysis of our system.

Chen (1980, 1982) used the quantum KS transformation to relate quantum hydrogen atom and quantum isotropic four-dimensional oscillator. This relation was further detailed by Kibler and Negadi (1983a, 1983b, 1984a), Chen and Kibler (1985) and Chen (1987) with particular attention paid to eigenbases (Kibler *et al.*, 1985; Cahill, 1990; Campigotto and Smirnov, 1991) and applications to the analysis of perturbations (Kibler and Negadi, 1984b). However, the latter were analyzed using matrix perturbation theory and only for small n (Chen, 1983, 1984) and no connection to the second-order normalized Hamiltonian \mathcal{H}_2 was established [cf. Delande and Gay (1984) and Robnik and Schrüfer (1985)].

Remaining within the quantum context, we point out that the so-called dilated semiparabolic coordinates,⁷⁸

$$\xi_1 = \frac{1}{\beta} \sqrt{r + Q_1}, \quad \xi_2 = \frac{1}{\beta} \sqrt{r - Q_1}, \quad \phi = \tan^{-1} \frac{y}{x},$$

used extensively⁷⁹ for numerical calculations and for the realization of the SO(4,2) dynamical group are nothing but specific polar coordinates on the KS configuration space \mathbb{R}^4 . Indeed, from Eq. (18), we find

$$\xi_1 = \frac{\sqrt{2}}{\beta} \sqrt{q_1^2 + q_4^2}, \quad \xi_2 = \frac{\sqrt{2}}{\beta} \sqrt{q_2^2 + q_3^2},$$

and, furthermore, we can show that $\phi = \phi_1 + \phi_2$, where

$$\phi_1 = \tan^{-1} \frac{q_4}{q_1}, \quad \phi_2 = \tan^{-1} \frac{q_3}{q_2}.$$

In the original KS coordinates in Eq. (18) and for ζ in Eq. (20) equal to 0, the first component of the angular momentum is

$$L_1 = q_1 p_4 - q_4 p_1 + q_2 p_3 - q_3 p_2.$$

So it follows that $(\xi_1, \phi_1, \xi_2, \phi_2)$ are polar coordinates on \mathbb{R}^4 which respect the S^1 symmetries generated by the

⁷⁶See Reinhardt and Farrelly (1982), Johnson *et al.* (1983), and Robnik and Schrüfer (1985).

⁷⁷See Kustaanheimo (1964), Kustaanheimo and Stiefel (1965), Stiefel (1970), and Stiefel and Scheifele (1971) and Sec. IV.A.1.

⁷⁸Compare Eq. (1) in Delande and Gay (1984) and Eq. (2) in Main *et al.* (1998) with notation $Q = (z, x, y)^T$ and dilatation $\beta = (-2E)^{-1/4}$.

⁷⁹See Delande and Gay (1984, 1986, 1991), Wiebusch *et al.* (1989), Iu *et al.* (1991), Main and Wunner (1992, 1994), and Main *et al.* (1998).

Hamiltonian flows of the vector fields X_ζ and X_{L_1} [which are rotations of two planes (q_1, q_4) and (q_2, q_3)] and, furthermore, ϕ is the angle conjugate to L_1 , while $\phi_\zeta = \phi_1 - \phi_2$ is the vanishing angle (since the symmetry associated with ζ is the strict symmetry of the KS map). Therefore, quantum computations using dilated semiparabolic coordinates (see footnote 79) give examples of generalized spectral calculus within the KS framework.

Note also that the semiparabolic coordinates ξ are used in the Levi-Civita transformation of systems with axial symmetry [for example, of Robnik and Schrüfer (1985)]. The above expressions of ξ in terms of KS coordinates q give a starting point for an explicit comparison [see also Cordani (2000, 2003), Cordani and Merlini (2001), and Celletti (2006)]. One finds that in both cases time is rescaled by r (times a constant). In other words, the actual regularization step precedes either transformation as done in Sec. IV.A.1.

The Hamiltonian \mathcal{H}_2 was obtained by Kuwata *et al.* (1990) using the classical KS transformation. The approach was used extensively later by Farrelly *et al.* (1992) for parallel fields and by Gourlay *et al.* (1993) for orthogonal fields, where the KS transformation is essential. This thread of work leads directly to Sadovskii *et al.* (1996), Sadovskii and Zhilinskii (1998), Cushman and Sadovskii (2000), Efsthathiou, Cushman, and Sadovskii (2004), and Efsthathiou, Sadovskii, and Zhilinskii (2007) and the techniques discussed in Sec. IV.A. Note also that the classical four-oscillator analogy and its perturbations were studied by Kummer (1996).

7. Other regularization and normal form techniques

The KS method is not the only one to regularize and normalize a perturbed Kepler system with the Hamiltonian (2), although, arguably, it is the most straightforward one. A discussion of various regularization techniques, their variants, and their relation can be found in Cushman (1992), Cordani (2003), and Celletti (2006). Of these, the most important alternative is Moser's approach (Moser, 1970a, 1970b; Kummer, 1982; Guillemin and Sternberg, 1990) and the related constrained normalization techniques of van der Meer (1986), van der Meer and Cushman (1986), and Cushman and Sanders (1989).⁸⁰

The Lie series algorithm for normalizing near elliptic equilibria was detailed by Deprit (1969) and Henrard (1970) independently from the earlier work of Gröbner (1960, 1967). Deprit himself turned later to normalization in terms of Delaunay angles (Coffey *et al.*, 1987) that are traditionally used for Keplerian systems in astronomy. We discussed implementations of this approach (Deprit *et al.*, 1996; Salas *et al.*, 1998) in Sec. VIII.C.2.

Some mostly local geometric analysis and normalization can equally be accomplished in the angle-action co-

⁸⁰See an early application by Cushman and van der Meer (1987) which treated an astronomical equivalent of the orthogonal fields system of Cushman and Sadovskii (2000).

ordinates in Eqs. (53) and (54). Note that in the 1:1 case, which is the only one studied in this context in the literature, definitions in Sec. IV.D.2.e become

$$\varphi = \phi_1 - \phi_3 - \phi_2 + \phi_4 \quad \text{and} \quad \nu = (n - |m|)\cos \theta,$$

where φ and θ can be related to Delaunay angles. All such coordinates have special definition domains similar to that of polar coordinates or one-oscillator action-angle variables. They can be used for an algorithmic normalization similar to that in Deprit (1969),⁸¹ but, as shown in Sec. VIII.C.2, they are masking proper singularities of the system and its monodromy through their own distorted geometry.

Recent work of Schleif and Delos (2007, 2008) demonstrated the difficulties of working in polarlike coordinates without regularization. This study continued earlier work⁸² and may be considered essentially as the approach of Pauli (1926) and Solov'ev (1981, 1982) applied to arbitrary field orientations. Knowing beforehand where and what to look for, Schleif and Delos (2008) uncovered monodromy where their predecessors, who used similar techniques, have not seen it. So the particular value of their study is in its explicit relation to the preceding body of work.

8. Studies of parametric families, classification, and bifurcations

Parametric families of quantum states or of dynamically invariant sets of the classical system arise naturally in our problem. Already in the early work,⁸³ plots of $m=0$ quantum levels and extrema of the effective potential (see footnote 72) as a function of field configuration became standard without relating the extrema to the actual invariant sets. For perpendicular fields, Flöthmann *et al.* (1994) considered the most basic one-parameter family, that of four Keplerian S^1 RE (or *Kepler ellipses*), the “bones” of the n shell (Sec. V.A.2). Sadovskii and Zhilinskiĭ (1998) completed the analysis by showing explicitly the relation between these RE and the four equilibria of the first normal form on $S^2 \times S^2$.

In early attempts⁸⁴ to classify individual regular tori, physicists did not characterize fully all critical fibers, i.e., no complete \mathcal{BD} was given. So the unstable Keplerian RE, the corresponding singular fiber, and their \mathcal{EM} image were not considered; neither were the tori con-

nected. Furthermore, the $k_-:k_+$ resonances were not properly acknowledged until Karasev and Novikova (2005).

Michel and Zhilinskiĭ (2001a) introduced the parameter space in Fig. 2 and gave the general topological classification of perturbations of the hydrogen atom by considering reduced Hamiltonian \mathcal{H} as a function on the orbit space \mathcal{O} (cf. Sec. III.A). They reconstructed families of regular and singular fibers which differ qualitatively for qualitatively different perturbations.⁸⁵ No connections between regular fibers were established and, therefore, no monodromy was considered.

Cushman and Sadovskii (2000) uncovered monodromy and classified all orthogonal field systems (strata A_2 and B_0 in Table II). Their classification was extended⁸⁶ later to all nearly orthogonal systems. Finally the zone concept of Efstathiou, Sadovskii, and Zhilinskiĭ (2007) provided the basis to complete the classification of all perturbations, the original program of Pauli (1926).

A one-parameter family of all quantum states within one n shell was studied for parallel fields by Sadovskii *et al.* (1996), a predecessor of Michel and Zhilinskiĭ (2001a). At the first (linear) order of the second reduced energy correction (36) such a family is shown in Fig. 28 where low-order resonances show up as characteristic “gaps” in the spectral density. At $d=1/2$, when one of the frequencies ω_{\pm} vanishes, we observe the structure characteristic of the dynamical symmetry $\mathfrak{su}(2) \times \mathfrak{su}(2)$ which Sadovskii *et al.* (1996) called *collapsed*. This gave a first clear indication of the existence of $k_-:k_+$ resonances and close near-resonant systems which Efstathiou, Sadovskii, and Zhilinskiĭ (2007) called zones. About the same time, Lutwak *et al.* (1997) considered the adiabatic evolution of subfamilies of an n -shell and used it to populate the so-called circular states⁸⁷ which are not ac-

⁸⁵This is equivalent to our \mathcal{BD} -based classification and is an application of the general program of Bolsinov and Fomenko (2004).

⁸⁶See Efstathiou, Sadovskii, and Zhilinskiĭ (2007), Schleif and Delos (2007, 2008), and Efstathiou *et al.* (2009). The initiation of the study of the 1:1 zone should be attributed to Schleif, who did quantum computations for nearly orthogonal systems with Delos and discovered the $A_{1,1}$ systems. Schleif and Delos (2007) shared their observations with Sadovskii in 2006.

⁸⁷Elliptic or circular states are states close to the respective stable Keplerian RE of the 1:1 system with maximal absolute value of momentum $\mu = \pm n$ [see Delande and Gay (1988), Gay *et al.* (1989), Brecha *et al.* (1993), Germann *et al.* (1995), Lutwak *et al.* (1997), Kristensen *et al.* (1998), and Suno *et al.* (1999)]. Typically, to produce a circular state, a $\mu=0$ state is populated spectroscopically and an adiabatic change of field parameters equivalent to our a^2 and/or d is used to bring the energies of Keplerian RE with $\mu=0$ and $\pm n$ together. One obtains correlation diagrams similar to Fig. 1 of Sadovskii *et al.* (1996) and Figs. 1 and 3 of Lutwak *et al.* (1997); note in Fig. 5 of the latter study a tentative energy-momentum diagram for \parallel fields near the S limit. At close energies, additional small perturbations cause population shifting. For other resonances, analogous states with $\mu = \pm(k_- + k_+)n/2$ have never been considered.

⁸¹See, e.g., Meyer and Hall (1992).

⁸²See Delos *et al.* (1983a, 1983b, 1984), Noid *et al.* (1983), and Waterland *et al.* (1987) and discussion in Sec. VIII.C.5.

⁸³Notably Braun and Solov'ev (1984b) (see footnote 72) and Cacciani, Luckoenig, *et al.* (1988) (see footnote 58).

⁸⁴For orthogonal systems see von Milczewski and Uzer (1997a, 1997b), von Milczewski *et al.* (1997c), and Cushman and Sadovskii (2000, Sec. 5). General configurations were considered by Main *et al.* (1998) and later by Berglund and Uzer (2001). Usual problems of traditional polarlike coordinates made analyzing critical fibers and uncovering $k_-:k_+$ resonances difficult.

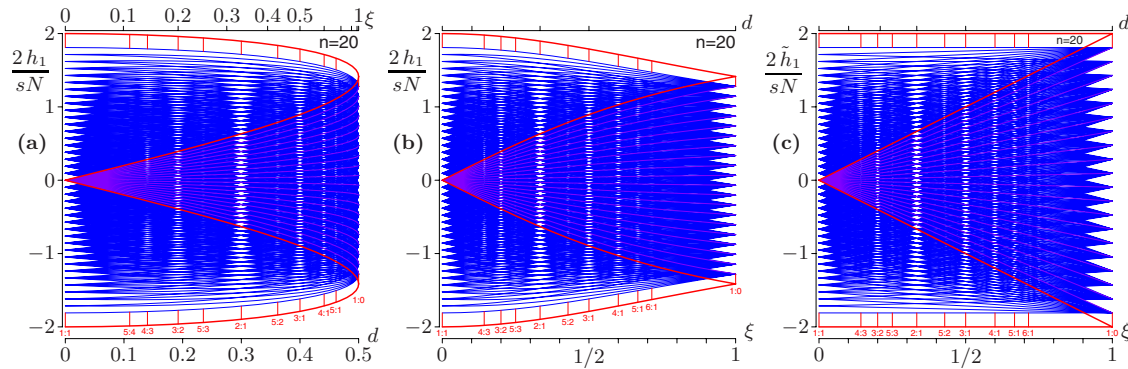


FIG. 28. (Color online) Quantum spectrum (fine solid lines) for $n=20$ and classical equilibrium energies (bold lines) for $N=n+1$ of the linear second reduced Hamiltonian $\Delta\mathcal{E}^{(1)}$ (a) and (b) in Eq. (36) and the scaled Hamiltonian $\tilde{\mathcal{H}}_1 = \Delta\mathcal{E}^{(1)}\sqrt{1+\xi^2}$ (c) on $S^2 \times S^2$ as a function of configuration parameters for \parallel fields (a) $d \in [0, 1/2]$ and (b) and (c) $\xi \in [0, 1]$ with $d = \xi/(1+\xi^2)$. Energies are scaled by $Ns/2$; vertical bars mark several low-order resonances. Fine differences between (c) and the results of Sadovskii *et al.* (1996, Fig. 1), are due to the higher-order term $\Delta\mathcal{E}^{(2)}$.

cessible directly to dipole absorption transitions from low-lying states with small μ due to prohibitive selection rules. The renewed interest in such studies for systems with monodromy, such as systems of type A_1 or A_2 , may be due to the suggestion of Delos *et al.* (2008) to manifest monodromy in a physical process.

Back on the more local scale, transitions between different dynamical strata involve various bifurcations of individual S^1 and T^2 RE (Sec. III.B and Fig. 16). These have been studied extensively⁸⁸ as bifurcations of the features of the second reduced effective potentials (see footnote 72). However, because they occur at the singularity, bifurcations of the $m=0$ Keplerian S^1 RE⁸⁹ cannot be analyzed adequately that way, and this remained widely unknown. As conjectured by Cushman and Sadovskii (2000) (Sec. III.E) and later demonstrated by Efsthathiou, Cushman, and Sadovskii (2004) and Efsthathiou (2005), these bifurcations are irreducibly four-dimensional phenomena known as Hamiltonian Hopf bifurcations⁹⁰ that involve a CH equilibrium and should be analyzed on $S^2 \times S^2$. Furthermore, to remove degeneracies remaining in the local second-order approximation for perpendicular fields, Efsthathiou, Cushman, and Sadovskii (2004) had to go to the fourth order.

D. Monodromy

Any reasonably complete review of Hamiltonian monodromy is a matter of a specialized paper. The key references are given in Sec. II. We mention additionally

⁸⁸See Deprit *et al.* (1996), Salas *et al.* (1998), and Salas and Lanchares (1998) (see footnote 59) and Farrelly *et al.* (1992), Gourlay *et al.* (1993), and von Milczewski and Uzer (1997a) (see footnote 41) discussed in Secs. VIII.C.2 and VIII.C.5, respectively.

⁸⁹For example, at $\beta = \frac{1}{5}$ and 1 in Cacciani, Luckoenig, *et al.* (1988) (see footnote 58).

⁹⁰See van der Meer (1985) and Duistermaat (1998) for a general introduction.

the place of Hamiltonian monodromy within the larger domain of mathematics, notably that of complex algebraic geometry and singularity theory. Monodromy is used to classify elliptic fibrations which in the real case⁹¹ correspond to singular fibrations of compact four-dimensional symplectic manifolds whose regular fibers are two-tori. With regard to the local framework of the singularity theory,⁹² Hamiltonian monodromy in the basic case of a nondegenerated FF equilibrium becomes equivalent to the Picard-Lefschetz⁹³ monodromy of the Morse singularity A_1 after proper identification of the far ends of the regular fibers that turns them into tori.⁹⁴ From this perspective, the work of Nekhoroshev (1969, 1972) and later of Duistermaat (1980) was coherent with contemporary developments in other domains. A number of other leading mathematicians, including Bolsinov and Fomenko, Lerman and Umanskiĭ, worked in the 1980s on the general topological theory of integrable systems. Beginning with the description of typical constant energy level sets, they focused naturally on Bott

⁹¹Classification of elliptic fibrations and their singular fibers was given in the early 1960s by Kodaira (Barth *et al.*, 1984, p. 150). Though all of them have formal Hamiltonian counterparts, concrete physical realizations are known only for a few simplest types. Understanding these systems from a physicist's perspective is a fascinating project.

⁹²See introductory chapters of Arnol'd *et al.* (1984, 1993), Arnol'd, Gusein-Zade, and Varchenko (1988), and Zoladek (2006).

⁹³Solomon Lefschetz (1884–1972), an American mathematician, introduced monodromy in geometry and topology in the 1930s following the ideas and results of Charles Emile Picard (1856–1941), professor at the École Centrale in Paris and a known French mathematician.

⁹⁴The relation between the Hamiltonian and Picard-Lefschetz monodromy was discussed in a number of papers [see, e.g., Audin (2002), Bates and Cushman (2005), and Bates and Cushman (2007)].

singularities⁹⁵ and came to recognize the importance of connections and of the FF singularity which results in monodromy⁹⁶ by the mid-1990s. Presently, Duistermaat's monodromy is regarded as their principal concept.⁹⁷

There was a number of examples of simple mechanical systems with monodromy, notably (a) the spherical pendulum (Cushman, 1983) used by Duistermaat (1980) and its quadratic deformations (Bates and Zou, 1993; Cushman and Bates, 1995; Efsthathiou, 2005); (b) the “Mexican hat” or the “champagne bottle” potential (Bates, 1991), its simplified billiard analog (Delos *et al.*, 2008), and a more abstract 1:(−1) resonance system (Nekhoroshev *et al.*, 2002, 2006); (c) the Lagrange top (Cushman and Bates, 1997) to which Sadovskii and Zhilinskiĭ (1999) added (d) systems of coupled “spins.” We also mention the 1:(−2) (Nekhoroshev *et al.*, 2006) and higher-order (Nekhoroshev, 2007, 2008; Giacobbe, 2008; Sugny *et al.*, 2008), resonance oscillator systems that exhibit fractional monodromy, as well as situations without global S^1 symmetry (Efsthathiou *et al.*, 2003; Efsthathiou and Sadovskii, 2004).

By 2000, due to Cushman, monodromy has made its way in real physical systems.⁹⁸ For most of the examples above, a concrete physical analog system was found: (a) floppy triatomic molecules (Joyeux *et al.*, 2003; Efsthathiou, Joyeux, and Sadovskii, 2004); (b) rotating quasilinear molecules such as H_2O (Child *et al.*, 1999; Zobov *et al.*, 2005) and others (Winnewisser *et al.*, 2006) and trapped Bose-Einstein condensate (Waalkens, 2002); (c) rotating molecules in external electric field (Kozin and Roberts, 2003; Arango *et al.*, 2004, 2005) and Ezra; and of course (d) systems considered in this review. This list is by no means exhaustive. Important systems with more complex three-dimensional \mathcal{BD} , such as the H_2^+ molecular ion (Waalkens *et al.*, 2003, 2004) and the 2:1:1 Fermi resonance in the CO_2 molecule (Cushman *et al.*, 2004)⁹⁹ must be added to it.

E. Similar systems

There is a number of model integrable Hamiltonian systems with properties similar to those of the normalized perturbations of the hydrogen atom discussed here.

⁹⁵In this context singular fibers that continue in parameter such as energy h ; an ubiquitous example are bitori T_{bi}^2 .

⁹⁶See Lerman and Umanskiĭ (1994a, 1994b, 1994c, 1995), Matveev (1996), and Nguyễn Tiên (1997, 2002).

⁹⁷Thus Bolsinov and Fomenko (2004) introduced a special elaborate construction of “marked loop molecule” that is essentially our regular torus bundle over Γ (the “loop molecule”) with a connection (the “mark”).

⁹⁸Applications of monodromy in atomic and molecular physics were first discussed at the workshop *Nonlinear Dynamics and Spectra*, organized by Mark Roberts at the Mathematics Institute of Warwick University, U.K., March 18–21, 1997. Discussions were initiated by Child and Zhilinskiĭ (see Zhilinskiĭ 2005).

⁹⁹See also Dullin *et al.* (2004), Giacobbe *et al.* (2004), Sanrey *et al.* (2006), and Sadovskii and Zhilinskiĭ (2007).

However, our system is the first real physical example where we observe such nontrivial topologically different fibrations of the phase space for the integrable approximation.

Thus exactly the same qualitative kinds A_1 , $A_{1,1}$, A_2 , and B_1 of systems with monodromy and the B_0 system can be modeled in a family of spherical pendula with quadratic potentials (Efsthathiou, 2005), which can be considered as deformations of the usual spherical pendulum with linear gravitational potential (Cushman and Bates, 1997; Efsthathiou and Sadovskii, 2005). Recently it was shown by Sugny *et al.* (2009) that description of the polarization exchange of counterpropagating intense laser beams in a nonlinear media reduces to a Hamiltonian system on $S^2 \times S^2$, where points of the two-spheres represent polarization vectors of the beams. In this system, it is possible to reproduce experimentally all the above qualitative types.

Other systems on the same (reduced) phase space $S^2 \times S^2$ (see Sec. IV) have been analyzed before. Sadovskii and Zhilinskiĭ (1999) and recently Hansen *et al.* (2007) studied monodromy of a system of coupled angular momenta. Davison and Dullin (2007) and Davison *et al.* (2007) obtained similar results for the geodesic flow on four-dimensional ellipsoids. Comparison to this latter system is particularly interesting. It is an integrable system on $S^2 \times S^2$, which is otherwise known as *Manakov top* (Sinitsyn and Zhilinskiĭ, 2007) and which has generally no momentum (and, obviously, no global action-angle variables). Similar to that of the Euler top, its Hamiltonian H is a homogeneous quadratic polynomial in the components of angular momenta \mathbf{x} and \mathbf{y} . In the particular case when H has S^1 symmetry and $|\mathbf{x}|=|\mathbf{y}|$ [cf. Sec. IV of Davison and Dullin (2007)], we come to our 1:1 systems.

A general Manakov top is a more complicated system on $S^2 \times S^2$ which possesses a HH singularity. Unfolding its \mathcal{EM} image (Sinitsyn and Zhilinskiĭ, 2007) may require further development of the concepts in Sec. II.C.4. To those looking for realistic physical examples of the HH singularities (Dullin and Vũ Ngọc, 2007), it may come as a disappointment that our system is unsuitable. In order to produce such fibers, the perturbing fields should be nonhomogeneous, axial symmetry must be broken, and the linear $\Delta E^{(1)}$ part should be made insignificant. An atomic realization of such system does not seem straightforward.

IX. CONCLUSION AND PERSPECTIVES

Completing this survey, the most general observation is that of the gradually developing hierarchical complexity of our system. Several times it seemed that nothing could have been further learned about it, and each time the truth was that nothing new could indeed be found without new techniques. As a result Klein's¹⁰⁰ skepticism

¹⁰⁰Felix Christian Klein (1849–1925), a leading German mathematician.

about the limited practical value of the abstract theory of Hamiltonian dynamical systems, made infamous by Arnol'd (1989), can be repeated here with regard to the modern global theories of integrable systems.¹⁰¹

The idea of describing an individual state within a family of all possible states of the system and the latter as a member in the parametric family of systems is intrinsic to physics. This idea is the reason why physicists value global actions and respective quantum numbers and why action-angle variables, an intrinsically local concept, have become overexploited. Modern mathematical theories come to our rescue when global actions are either complicated functions or simply do not exist. As we have seen this happens quite regularly in our system.

We went through the main stages of the analysis of systems with the Hamiltonian (2): linear study initiated by Pauli (1926), second normalized Hamiltonian ($\Delta\mathcal{E}$ in our notation) of Solov'ev (1981, 1982, 1983), Grozdanov and Solov'ev (1982), and Herrick (1982), complete joint spectra of parametric families of n -shell systems [e.g., Sadovskii *et al.* (1996), Michel and Zhilinskiĭ (2001a), and others], global analysis of the integrable approximation started by Cushman and Sadovskii (1999, 2000), and the respective dynamical stratification of the parameter space by Efsthathiou, Sadovskii, and Zhilinskiĭ (2007). Each time facts, which were (or could have been) known previously, (re)appeared in a new light. This happened with the second-order integrable approximation, which was given a "new life" by Cushman and Sadovskii (1999, 2000), resonances (Efsthathiou, Sadovskii, and Zhilinskiĭ, 2007), and deformation of the known structures (see footnote 86).

Each time the new results came belated. Thus one had to wait 55 years after Pauli (1926) to compute a "simple" second average and another 20 years to come up with correct complete images of the \mathcal{EM} map. The only essentially new mathematical idea used by Cushman and Sadovskii (1999, 2000), who constructed these images, was that of the global connection between different states (different tori) of the system which resulted in the discovery of monodromy. Similarly, the importance of resonances in the linear (Pauliean) approximation went unacknowledged for too long. They could have been noticed right after Pauli (1926), but instead, despite early indications by Sadovskii *et al.* (1996) and later by Karasev and Novikova (2005), it took time (Efsthathiou, Sadovskii, and Zhilinskiĭ, 2007) to understand their true significance. Finally, general reduction of the Pauliean symmetry and the analysis of the whole 1:1 zone was accessible already to Cushman and Sadovskii (1999, 2000) but only came seven years later (see footnote 86).

One can argue as to the reasons of such slow advance. These are, essentially, of three kinds: motivation, techniques, and ideas. Possibilities of experimental investigation of the quadratic Zeeman splittings stimulated the

second-order theories of the 1980s. Later the interest in integrable approximations diminished due to the obvious interest in the chaotic regime. Certainly, modern regularization and normalization techniques, reduction of symmetries, and invariant theory, all combined with computer algebra, become indispensable. New mathematics plays the central role in the present stage of the analysis.

It may be tempting to think that now, some 80 years after Pauli (1926), we have a complete understanding of the family of classical systems with the Hamiltonian (2) and its quantum analogs. Our progress is substantial: we do have a general framework for a meaningful classification of all these systems, and we do have a global detailed understanding of an important three-parameter subfamily of them, the 1:1 zone. However, higher-order resonance zones remain essentially unknown. We do not have meaningful estimates of their widths, neither do we know much about their dynamical stratification which promises to be quite complex. Even within the 1:1 zone, we have left out certain small regions of complex structures that require higher-order approximations and we did not analyze fully the related bifurcation phenomena. The effects of nonintegrability and the limits of our analysis should be investigated further.

Finally, it seems that our current advanced state of theoretical understanding of these systems may give motivation to other fields. What significance do all these complex collective structures of tori and of corresponding eigenstates have to physics? How can we "observe" monodromy? The answer is unclear, but the collective behavior of several states seems to be the key element (Delos *et al.*, 2008). The ultimate reward for this review will be the involvement of the broader physics community in solving these questions.

LIST OF SYMBOLS

\mathcal{BD}	bifurcation diagram for \mathcal{EM}
\mathcal{BD}_n	constant n section of the \mathcal{BD} , i.e., the bifurcation diagram for \mathcal{EM}_n
$E(\mathbf{X}, \mathbf{Y})$	first normalized energy [see Eqs. (32)]
\mathcal{EM}	energy-momentum map (N, μ, \mathcal{H})
\mathcal{EM}_n	energy-momentum map (μ, \mathcal{H}) for fixed value $N=n$
$\mathbf{F}=(F_b, F_e, 0)$	electric field
$\mathbf{G}=(G, 0, 0)$	magnetic field
H_{3D}, E	Hamiltonian in physical space and its value
H_{KS}	Kustaanheimo-Stiefel transformed Hamiltonian [see Eq. (21)]
\tilde{H}_{KS}	first normalized Kustaanheimo-Stiefel Hamiltonian [see Eqs. (30)]
\mathcal{H}, h	the Hamiltonian function on $P_{n,m}$ and its value. \mathcal{H} is defined

¹⁰¹See Nguyễn Tiên (1996, 2003), Cushman and Bates (1997), Symington (2003), and Bolsinov and Fomenko (2004).

	as the nontrivial part of $\Delta\mathcal{E}$, i.e., it does not contain the terms of $\Delta\mathcal{E}$ that depend only on n, m and are thus constant on $P_{n,m}$ [see Eq. (56)].
N, n	Keplerian integral and its value [see Eq. (22)]
$P_{n,m}$	second reduced phase space (see Sec. IV.D.2.c); N, μ are constant on $P_{n,m}$ with values n, m , respectively
$S^2 \times S^2$	phase space for the first normalized and reduced system defined by E (see Sec. IV.A)
$T_{[1]}^2, T_{[2]}^2, T_{[1/2]}^2, T_{\text{bi}}^2$	singly pinched torus, doubly pinched torus, curled torus, and bitorus, respectively (see Figs. 7 and 8)
(\mathbf{X}, \mathbf{Y})	
$= (X_1, X_2, X_3, Y_1, Y_2, Y_3)$	coordinates in space $\mathbb{R}^6 \supset S^2 \times S^2$ [see Eq. (28)]
X_F	the Hamiltonian vector field of function F
a^2, d	constant s fields parametrization [see Eq. (4b)]
g, f_e, f_b	n -scaled field amplitudes [see Eq. (3)]
$\tilde{g}, \tilde{f}_e, \tilde{f}_b$	Ω scaled field amplitudes [see Eq. (5)]
ns	the product of n and s plays the role of “small” perturbation parameter in the 1:1 resonance zone
$s = (g^2 + f_e^2 + f_b^2)^{1/2}$	combined field strength
(\mathbf{x}, \mathbf{y})	
$= (x_1, x_2, x_3, y_1, y_2, y_3)$	symmetry adapted coordinates in $\mathbb{R}^6 \supset S^2 \times S^2$ obtained from (\mathbf{X}, \mathbf{Y}) through linear transformation (34) (see Sec. IV.C)
ΔE	first normalized and reduced energy correction function [see Eqs. (32)]
$\Delta E^{(1)}, \Delta E^{(2)}$	first- and second-order terms in the first normalized energy correction function ΔE [see Eqs. (33) and (9) and Table III]
$\Delta\mathcal{E}$	second normalized and reduced energy correction function [see Eqs. (36), (37), and (55) and Table IV]
$\Delta\mathcal{E}^{(1)}, \Delta\mathcal{E}^{(2)}$	first- and second-order terms in the second normalized energy correction function $\Delta\mathcal{E}$ [see Eq. (36) and Table IV]
Ω	$(-8E)^{1/2}$
ζ	Kustaanheimo-Stiefel integral, its value is 0 [see Eq. (20)]
μ, m	second integral (momentum)

$\nu, \pi_1, \pi_2, \pi_3, \pi_4$	and its value [see Eq. (13)] invariants (together with μ) of the $k_-:k_+$ resonant S^1 action on $S^2 \times S^2$ [see Eq. (46)]. The invariants ν, π_1 , and π_2 serve as coordinates on $\mathbb{R}^3 \supset P_{n,m}$ (see Sec. IV.D.2.a).
ω_+, ω_-	frequencies on $S^2 \times S^2$ [see Eq. (10)]

ACKNOWLEDGMENTS

The authors thank Professor H. W. Broer, Professor R. H. Cushman, and Professor B. I. Zhilinskii for useful discussions and encouragement and Dr. O. V. Lukina for help with the initial version of the paper. K.E. acknowledges support from the NWO mathematics cluster NDNS+. D.A.S. thanks the University of Groningen, where part of this research was done, for its hospitality and the NDNS+ cluster for supporting his visit to Groningen.

REFERENCES

- Adams, B. G., J. Cízek, and J. Paldus, 1982, “Representation theory of $SO(4,2)$ for the perturbation treatment of hydrogenic type Hamiltonians by algebraic methods,” *Int. J. Quantum Chem.* **21**, 153–171.
- Adams, B. G., J. Cízek, and J. Paldus, 1988, “Lie algebraic methods and their applications to simple quantum systems,” *Adv. Quantum Chem.* **19**, 1–85.
- Arango, C. A., W. W. Kennerly, and G. S. Ezra, 2004, “Quantum monodromy for diatomic molecules in combined electrostatic and pulsed nonresonant laser fields,” *Chem. Phys. Lett.* **392**, 486–492.
- Arango, C. A., W. W. Kennerly, and G. S. Ezra, 2005, “Quantum and classical mechanics of diatomic molecules in tilted fields,” *J. Chem. Phys.* **122**, 184303.
- Arms, J. M., 1986, “Symmetry and solution set singularities in Hamiltonian field-theories,” *Acta Phys. Pol. B* **17**, 499–523.
- Arms, J. M., 1988, “Reduction of Hamiltonian systems for singular values of momentum,” *Contemp. Math.* **81**, 99–110.
- Arms, J. M., R. H. Cushman, and M. J. Gotay, 1991, in *Geometry of Hamiltonian Systems*, edited by T. Ratiu (Springer, New York), pp. 33–51.
- Arms, J. M., M. J. Gotay, and G. Jennings, 1990, “Geometric and algebraic reduction for singular momentum maps,” *Adv. Math.* **79**, 43–103.
- Arnol’d, V. I., 1989, *Mathematical Methods of Classical Mechanics*, 2nd ed., *Graduated Texts in Mathematics* Vol. 60 (Springer-Verlag, New York), translated by K. Vogtmann and A. Weinstein.
- Arnol’d, V. I., S. M. Gusein-Zade, and A. N. Varchenko, 1988, *Singularities of Differentiable Maps*, *Monographs in Mathematics* Vol. 83 (Birkhäuser, Boston), p. 492, translated from Russian by Hugh Porteous. Translation revised by the authors and James Montaldi.
- Arnol’d, V. I., V. V. Kozlov, and A. I. Neishtadt, 1988, *Mathematical Aspects of Classical and Celestial Mechanics: Dynamical Systems III*, *Encyclopedia of Mathematical Sciences* Vol. 3 (Springer-Verlag, Berlin).

- Arnol'd, V. I., A. N. Varchenko, and S. M. Gusein-Zade, 1984, *Singularities of Differentiable Maps: Monodromy and Asymptotics of Integrals* (Nauka, Moscow) [in Russian, see English translation (Arnol'd, Gusein-Zade, and Varchenko, 1988)].
- Arnol'd, V. I., V. A. Vassil'ev, V. V. Goryunov, and O. V. Lyashko, 1993, *Singularities—Local and Global Theory: Dynamical Systems VI*, Encyclopedia of Mathematical Sciences Vol. 6 (Springer-Verlag, Berlin) (Russian original published in 1988).
- Atiyah, M. F., 1982, “Convexity and commuting Hamiltonians,” *Bull. London Math. Soc.* **14**, 1–15.
- Atiyah, M. F., 1983, “Angular momentum, convex polyhedra and algebraic geometry,” *Proc. Edinb. Math. Soc.* **26**, 121–133.
- Atiyah, M. F., and R. Bott, 1984, “The moment map and equivariant cohomology,” *Topology* **23**, 1–28.
- Audin, M., 2002, “Hamiltonian monodromy via Picard-Lefschetz theory,” *Commun. Math. Phys.* **229**, 459–489.
- Avron, J. E., B. G. Adams, J. Cizek, M. Clay, M. L. Glasser, P. Otto, J. Paldus, and E. Vrscaj, 1979, “Bender-Wu formula, the SO(4,2) dynamical group, and the Zeeman effect in hydrogen,” *Phys. Rev. Lett.* **43**, 691–693.
- Bander, M., and C. Itzykson, 1966, “Group theory and hydrogen atom 1,” *Rev. Mod. Phys.* **38**, 330–345.
- Bargmann, V., 1936, “Theory of the hydrogen atom,” *Z. Phys.* **99**, 578–582.
- Barth, W., C. Peters, and A. Van de Ven, 1984, *Compact Complex Surfaces* (Springer-Verlag, Berlin).
- Bartsch, T., S. Gekle, J. Main, and T. Uzer, 2007, “Gluing torus families across a singularity: The lens space for the hydrogen atom in crossed fields,” *Prog. Theor. Phys. Suppl.* **166**, 45–55.
- Barut, A. O., C. K. E. Schneider, and R. Wilson, 1979, “Quantum theory of infinite component fields,” *J. Math. Phys.* **20**, 2244–2256.
- Bates, L., R. Cushman, M. Hamilton, and J. Śniatycki, 2009, “Quantization of singular reduction,” *Rev. Math. Phys.* **21**, 315–371.
- Bates, L., and R. H. Cushman, 2005, “Complete integrability beyond Liouville-Arnol'd,” *Rep. Math. Phys.* **56**, 77–91.
- Bates, L., and R. H. Cushman, 2007, “Scattering monodromy and the A_1 singularity,” *Cent. Eur. J. Math.* **5**, 429–451.
- Bates, L. M., 1991, “Monodromy in the champagne bottle,” *ZAMP* **42**, 837–847.
- Bates, L. M., and M. R. Zou, 1993, “Degeneration of Hamiltonian monodromy cycles,” *Nonlinearity* **6**, 313–335.
- Berglund, N., and T. Uzer, 2001, “The averaged dynamics of the hydrogen atom in crossed electric and magnetic fields as a perturbed Kepler problem,” *Found. Phys.* **31**, 283–326.
- Bolsinov, A. V., and A. T. Fomenko, 2004, *Integrable Hamiltonian Systems: Geometry, Topology, Classification* (Chapman and Hall, London/CRC, Boca Raton, FL).
- Braun, P. A., 1993, “Discrete semiclassical methods in the theory of Rydberg atoms in external fields,” *Rev. Mod. Phys.* **65**, 115–161.
- Braun, P. A., and E. A. Solov'ev, 1984a, “The Stark effect for the hydrogen atom in a magnetic field,” *Zh. Eksp. Teor. Fiz.* **86**, 68–83 [*Sov. Phys. JETP* **59**, 38–46 (1984)].
- Braun, P. A., and E. A. Solov'ev, 1984b, “Transformation of the spectrum of atomic hydrogen in crossed electric and magnetic fields,” *J. Phys. B* **17**, L211–L216.
- Brecha, R. J., G. Raithel, C. Wagner, and H. Walther, 1993, “Circular Rydberg states with very large n ,” *Opt. Commun.* **102**, 257–264.
- Broer, H., R. Cushman, F. Fassò, and F. Takens, 2007, “Geometry of KAM tori for nearly integrable Hamiltonian systems,” *Ergod. Theory Dyn. Syst.* **27**, 725–741.
- Cacciani, P., S. Liberman, E. Luckoenig, J. Pinard, and C. Thomas, 1988, “Rydberg atoms in parallel magnetic and electric fields. 1. Experimental studies of the odd diamagnetic multiplet of lithium- n mixing and core effects,” *J. Phys. B* **21**, 3473–3498.
- Cacciani, P., E. Luckoenig, J. Pinard, C. Thomas, and S. Liberman, 1986, “Experimental study and analysis of the lithium atom in the presence of parallel electric and magnetic fields,” *Phys. Rev. Lett.* **56**, 1467–1470.
- Cacciani, P., E. Luckoenig, J. Pinard, C. Thomas, and S. Liberman, 1988, “Rydberg atoms in parallel magnetic and electric fields. 2. Theoretical analysis of the Stark structure of the diamagnetic manifold of hydrogen,” *J. Phys. B* **21**, 3499–3522.
- Cahill, E., 1990, “The Kustaanheimo-Stiefel transformation applied to the hydrogen atom: Using the constraint equation and resolving a wavefunction discrepancy,” *J. Phys. A* **23**, 1519–1522.
- Campigotto, C., and Y. F. Smirnov, 1991, “On connections between the four-dimensional harmonic oscillator and the Coulomb-problem in the representation with the discrete basis,” *Helv. Phys. Acta* **64**, 48–60.
- Celletti, A., 2006, in *Chaotic Worlds: From Order to Disorder in Gravitational n -Body Dynamical Systems*, edited by B. A. Steves, A. J. Maciejewski, and M. Hendry, Proceedings of the 11th Conference of the NATO Advanced Study Institute on Chaotic Worlds (Springer, Dordrecht), Vol. 227, pp. 203–230.
- Chen, A. C., 1980, “Hydrogen atom as a four-dimensional oscillator,” *Phys. Rev. A* **22**, 333–335; **22**, 2901(E) (1980).
- Chen, A. C., 1982, “Addition to hydrogen atom as a four-dimensional oscillator,” *Phys. Rev. A* **25**, 2409–2410.
- Chen, A. C., 1983, “Degenerate perturbative treatment of the hydrogenic Zeeman effect,” *Phys. Rev. A* **28**, 280–286.
- Chen, A. C., 1984, “Second-order perturbative calculation of hydrogenic Zeeman levels,” *Phys. Rev. A* **29**, 2225–2227.
- Chen, A. C., 1987, “Coulomb Kepler problem and the harmonic oscillator,” *Am. J. Phys.* **55**, 250–252.
- Chen, A. C., and M. Kibler, 1985, “Connection between the hydrogen atom and the four-dimensional oscillator,” *Phys. Rev. A* **31**, 3960–3963.
- Child, M. S., 1998, “Quantum states in a champagne bottle,” *J. Phys. A* **31**, 657–670.
- Child, M. S., 2001, “Quantum level structures and nonlinear classical dynamics,” *J. Mol. Spectrosc.* **210**, 157–165.
- Child, M. S., 2007, “Quantum monodromy and molecular spectroscopy,” *Adv. Chem. Phys.* **136**, 39–94.
- Child, M. S., T. Weston, and J. Tennyson, 1999, “Quantum monodromy in the spectrum of H_2O and other systems: New insight into the level structure of quasi-linear molecules,” *Mol. Phys.* **96**, 371–379.
- Clark, C. W., and K. T. Taylor, 1980, “The quadratic Zeeman effect in hydrogen Rydberg series,” *J. Phys. B* **13**, L737–L743.
- Clark, C. W., and K. T. Taylor, 1981, “Dynamical symmetry in the quadratic Zeeman effect,” *Nature (London)* **292**, 437–439.
- Clark, C. W., and K. T. Taylor, 1982, “Diamagnetism in excited states of hydrogen,” *J. Phys. (Paris), Colloq.* **43**, 127–135.
- Coffey, S. L., A. Deprit, B. Miller, and C. A. Williams, 1987, “The quadratic Zeeman effect in moderately strong magnetic fields,” *Ann. N.Y. Acad. Sci.* **497**, 22–36.
- Colin de Verdière, Y., and S. Vũ Ngọc, 2003, “Singular Bohr-Sommerfeld rules for 2D integrable systems,” *Ann. Sci. Ec.*

- Normale Super. **36**, 1–55.
- Cordani, B., 2000, “Perturbations of the Kepler problem in global coordinates,” *Celest. Mech. Dyn. Astron.* **77**, 185–200.
- Cordani, B., 2003, *The Kepler Problem: Group Theoretical Aspects, Regularization and Quantization with Applications to the Study of Perturbations* (Birkhäuser, Basel).
- Cordani, B., and G. Merlini, 2001, “Perturbations of the Kepler problem in global coordinates: A program,” *Celest. Mech. Dyn. Astron.* **81**, 313–319.
- Cushman, R. H., 1983, “Geometry of the energy-momentum mapping of the spherical pendulum,” *C.W.I. Newsl.* **1**, 4–18.
- Cushman, R. H., 1992, in *Dynamics Reported—Expositions in Dynamical Systems*, edited by C. K. R. T. Jones, U. Kirchgraber, and H. O. Walther (Springer-Verlag, Berlin), pp. 54–112.
- Cushman, R. H., and L. Bates, 1997, *Global Aspects of Classical Integrable Systems* (Birkhäuser, Basel).
- Cushman, R. H., and L. M. Bates, 1995, “The magnetic spherical pendulum,” *Meccanica* **30**, 271–289.
- Cushman, R. H., and J. J. Duistermaat, 1988, “The quantum-mechanical spherical pendulum,” *Bull., New Ser., Am. Math. Soc.* **19**, 475–479.
- Cushman, R. H., and J. J. Duistermaat, 2001, “Non-Hamiltonian monodromy,” *J. Differ. Equations* **172**, 42–58.
- Cushman, R. H., H. R. Dullin, A. Giacobbe, D. D. Holm, M. Joyeux, P. Lynch, D. A. Sadovskii, and B. I. Zhilinskiĭ, 2004, “CO₂ molecule as a quantum realization of the 1:1:2 resonant swing-spring with monodromy,” *Phys. Rev. Lett.* **93**, 024302.
- Cushman, R. H., and D. A. Sadovskii, 1999, “Monodromy in perturbed Kepler systems: Hydrogen atom in crossed fields,” *Europhys. Lett.* **47**, 1–7.
- Cushman, R. H., and D. A. Sadovskii, 2000, “Monodromy in the hydrogen atom in crossed fields,” *Physica D* **142**, 166–196, Eq. (3), which defines the KS map, is missing $\frac{1}{2}$.
- Cushman, R. H., and J. A. Sanders, 1989, “The constrained normal form algorithm,” *Celest. Mech.* **45**, 181–187.
- Cushman, R. H., and R. Sjamaar, 1991, in *Symplectic Geometry in Mathematical Physics*, edited by P. Donato (Birkhäuser, Boston), pp. 114–128.
- Cushman, R. H., and J. C. van der Meer, 1987, in *Proceedings of the XV International Conference on Differential Geometric Methods in Theoretical Physics*, edited by H. Doebner and J. Henning (World Scientific, Singapore), p. 403.
- Cushman, R. H., and S. Vũ Ngọc, 2002, “Sign of the monodromy for Liouville integrable systems,” *Ann. Henri Poincaré* **3**, 883–894.
- Cushman, R. H., and B. I. Zhilinskiĭ, 2002, “Monodromy of a two degrees of freedom Liouville integrable system with many focus-focus singular points,” *J. Phys. A* **35**, L415–L419.
- Davison, C. M., and H. R. Dullin, 2007, “Geodesic flow on three-dimensional ellipsoids with equal semi-axes,” *Regular Chaotic Dyn.* **12**, 172–197.
- Davison, C. M., H. R. Dullin, and A. V. Bolsinov, 2007, “Geodesics on the ellipsoid and monodromy,” *J. Geom. Phys.* **57**, 2437–2454.
- Delande, D., and J. C. Gay, 1984, “Group theory applied to the hydrogen atom in a strong magnetic field—Derivation of the effective diamagnetic Hamiltonian,” *J. Phys. B* **17**, L335–L340.
- Delande, D., and J. C. Gay, 1986, “The hydrogen atom in a magnetic field—Spectrum from the Coulomb dynamic group approach,” *J. Phys. B* **19**, L173–L178.
- Delande, D., and J. C. Gay, 1988, “A new method for producing circular Rydberg states,” *Europhys. Lett.* **5**, 303–308.
- Delande, D., and J. C. Gay, 1991, “Supersymmetric factorization for Rydberg atoms in parallel electric and magnetic fields,” *Phys. Rev. Lett.* **66**, 3237–3240.
- Delos, J. B., G. Dhont, D. A. Sadovskii, and B. I. Zhilinskiĭ, 2008, “Dynamical manifestation of Hamiltonian monodromy,” *Europhys. Lett.* **83**, 24003.
- Delos, J. B., G. Dhont, D. A. Sadovskii, and B. I. Zhilinskiĭ, 2009, “Dynamical manifestations of Hamiltonian monodromy,” *Ann. Phys.* **324**, 1953–1982.
- Delos, J. B., S. K. Knudson, and D. W. Noid, 1983a, “High Rydberg states of an atom in a strong magnetic field,” *Phys. Rev. Lett.* **50**, 579–583.
- Delos, J. B., S. K. Knudson, and D. W. Noid, 1983b, “Highly excited states of a hydrogen atom in a strong magnetic field,” *Phys. Rev. A* **28**, 7–21.
- Delos, J. B., S. K. Knudson, and D. W. Noid, 1984, “Trajectories of an atomic electron in a magnetic field,” *Phys. Rev. A* **30**, 1208–1218.
- Delzant, T., 1988, “Periodic Hamiltonians and convex images of momentum mapping,” *Bull. Soc. Math. France* **116**, 315–339.
- Demkov, Y. N., B. S. Monozon, and V. N. Ostrovskii, 1969, “Energy levels of the hydrogen atom in crossed electric and magnetic fields,” *Zh. Eksp. Teor. Fiz.* **57**, 1431–1434 [Sov. Phys. JETP **30**, 775–776 (1970)].
- Deprit, A., 1969, “Canonical transformations depending on a small parameter,” *Celest. Mech.* **1**, 12–30.
- Deprit, A., J. Henrard, J. F. Price, and A. Rom, 1969, “Birkhoff’s normalization,” *Celest. Mech.* **1**, 222–251.
- Deprit, A., V. Lanchares, M. Inarrea, J. P. Salas, and J. D. Sierra, 1996, “Teardrop bifurcation for Rydberg atoms in parallel electric and magnetic fields,” *Phys. Rev. A* **54**, 3885–3893.
- Duistermaat, J. J., 1980, “On global action-angle coordinates,” *Commun. Pure Appl. Math.* **33**, 687–706.
- Duistermaat, J. J., 1998, “The monodromy in the Hamiltonian Hopf bifurcation,” *ZAMP* **49**, 156–161.
- Duistermaat, J. J., and G. J. Heckman, 1982, “On the variation in the cohomology of the symplectic form of the reduced phase space,” *Invent. Math.* **69**, 259–268.
- Dullin, H., A. Giacobbe, and R. Cushman, 2004, “Monodromy in the resonant swing spring,” *Physica D* **190**, 15–37.
- Dullin, H., and S. Vũ Ngọc, 2007, “Symplectic invariants for hyperbolic-hyperbolic singularities,” *Regular Chaotic Dyn.* **12**, 687–716.
- Edmonds, A. R., 1970, “The theory of the quadratic Zeeman effect,” *J. Phys. Colloq.* **31**, C4-71–C4-74.
- Efsthathiou, K., 2005, *Metamorphoses of Hamiltonian Systems with Symmetries*, Lecture Notes in Mathematics Vol. 1864 (Springer-Verlag, New York).
- Efsthathiou, K., R. Cushman, and D. A. Sadovskii, 2007, “Fractional monodromy in the 1:–2 resonance,” *Adv. Math.* **209**, 241–273.
- Efsthathiou, K., R. H. Cushman, and D. A. Sadovskii, 2004, “Hamiltonian Hopf bifurcation of the hydrogen atom in crossed fields,” *Physica D* **194**, 250–274.
- Efsthathiou, K., M. Joyeux, and D. A. Sadovskii, 2004, “Global bending quantum number and the absence of monodromy in the HCN ↔ CNH molecule,” *Phys. Rev. A* **69**, 032504.
- Efsthathiou, K., O. Lukina, and D. A. Sadovskii, 2008, “Most typical 1:2 resonant perturbation of the hydrogen atom by weak electric and magnetic fields,” *Phys. Rev. Lett.* **101**,

253003.

- Efsthathiou, K., O. Lukina, and D. A. Sadovskii, 2009, "Complete classification of qualitatively different perturbations of the hydrogen atom in weak near orthogonal electric and magnetic fields," *J. Phys. A: Math. Theor.* **42**, 055209.
- Efsthathiou, K., and D. A. Sadovskii, 2004, "Perturbations of the 1:1:1 resonance with tetrahedral symmetry: A three degree of freedom analogue of the two degree of freedom Hénon-Heiles Hamiltonian," *Nonlinearity* **17**, 415–446.
- Efsthathiou, K., and D. A. Sadovskii, 2005, in *Geometric Mechanics and Symmetry: The Peyresq Lectures*, edited by J. Montaldi and T. Ratiu, London Mathematical Society Lecture Note Series No. 306 (Cambridge University Press, Cambridge, England), pp. 211–302.
- Efsthathiou, K., D. A. Sadovskii, and R. H. Cushman, 2003, "Linear Hamiltonian Hopf bifurcation for point-group-invariant perturbations of the 1:1:1 resonance," *Proc. R. Soc. London, Ser. A* **459**, 2997–3019.
- Efsthathiou, K., D. A. Sadovskii, and B. I. Zhilinskiĭ, 2007, "Classification of perturbations of the hydrogen atom by small static electric and magnetic fields," *Proc. R. Soc. London, Ser. A* **463**, 1771–1790.
- Englefield, M. J., 1972, *Group Theory and the Coulomb Problem* (Wiley-Interscience, New York).
- Fano, U., 1980a, "Formation of Landau standing waves in Rydberg spectra," *J. Phys. B* **13**, L519–L523.
- Fano, U., 1980b, "Wave propagation and diffraction on a potential ridge," *Phys. Rev. A* **22**, 2660–2671.
- Fano, U., 1988, "Half-scattering and the diamagnetism of Rydberg states," *Comments At. Mol. Phys.* **22**, 97–113.
- Fano, U., F. Robicheaux, and A. R. P. Rau, 1988, "Semianalytic study of diamagnetism in a degenerate hydrogenic manifold," *Phys. Rev. A* **37**, 3655–3665.
- Farrelly, D., and K. Krantzman, 1991, "Dynamic symmetry of the quadratic Zeeman effect in hydrogen—Semiclassical quantization," *Phys. Rev. A* **43**, 1666–1668.
- Farrelly, D., and J. A. Milligan, 1992, "Action-angle variables for the diamagnetic Kepler problem," *Phys. Rev. A* **45**, 8277–8279.
- Farrelly, D., T. Uzer, P. E. Raines, J. P. Skelton, and J. A. Milligan, 1992, "Electronic structure of Rydberg atoms in parallel electric and magnetic fields," *Phys. Rev. A* **45**, 4738–4751.
- Fassò, F., 1996, "The Euler-Poincaré top: A non-commutatively integrable system without global action-angle coordinates," *ZAMP* **47**, 953–976.
- Fassò, F., 2008, private communication.
- Flöthmann, E., J. Main, and K. H. Welge, 1994, "The Kepler ellipses of the hydrogen atom in crossed electric and magnetic fields," *J. Phys. B* **27**, 2821–2833.
- Fock, V., 1935, "Theory of the hydrogen atom," *Z. Phys.* **98**, 145–154.
- Gaeta, G., 1997, "Reduction of Poincaré normal forms," *Lett. Math. Phys.* **42**, 103–114.
- Gaeta, G., 1999, "Poincaré renormalized forms," *Ann. Inst. Henri Poincaré, Sect. A* **70**, 461–514.
- Gaeta, G., 2001, "Algorithmic reduction of Poincaré-Dulac normal forms and Lie algebraic structure," *Lett. Math. Phys.* **57**, 41–60.
- Garton, W. R. S., and F. S. Tomkins, 1969, "Diamagnetic Zeeman effect and magnetic configuration mixing in long spectral series of BaI," *Astrophys. J.* **158**, 839–845.
- Gay, J. C., D. Delande, F. Biraben, and F. Penent, 1983, "Diamagnetism of the hydrogen atom—An elementary derivation of the adiabatic invariant," *J. Phys. B* **16**, L693–697.
- Gay, J. C., D. Delande, and A. Bommier, 1989, "Atomic quantum states with maximum localization on classical elliptical orbits," *Phys. Rev. A* **39**, 6587–6590.
- Gekle, S., J. Main, T. Bartsch, and T. Uzer, 2006, "Extracting multidimensional phase space topology from periodic orbits," *Phys. Rev. Lett.* **97**, 104101.
- Gekle, S., J. Main, T. Bartsch, and T. Uzer, 2007, "Hydrogen atom in crossed electric and magnetic fields: Phase space topology and torus quantization via periodic orbits," *Phys. Rev. A* **75**, 023406.
- Germann, T. C., D. R. Herschnach, M. Dunn, and D. K. Watson, 1995, "Circular Rydberg states of the H atom in magnetic field," *Phys. Rev. Lett.* **74**, 658–661.
- Giacobbe, A., 2008, "Fractional monodromy: Parallel transport of homology cycles," *Diff. Geom. Applic.* **26**, 140–150.
- Giacobbe, A., R. H. Cushman, D. A. Sadovskii, and B. I. Zhilinskiĭ, 2004, "Monodromy of the quantum 1:1:2 resonant swing spring," *J. Math. Phys.* **45**, 5076–5100.
- Ginzburg, V. L., V. Guillemin, and Y. Karshon, 2002, *Moment Maps, Cobordisms, and Hamiltonian Group Actions*, Mathematical Surveys and Monographs Vol. 98 (AMS, Providence, RI).
- Goldstein, H., 1975, "Prehistory of the Runge-Lenz vector," *Am. J. Phys.* **43**, 737–738.
- Goldstein, H., 1976, "More on the prehistory of the Runge-Lenz vector," *Am. J. Phys.* **44**, 1123–1124.
- Gourlay, M. J., T. Uzer, and D. Farrelly, 1993, "Asymmetric-top description of Rydberg electron dynamics in crossed external fields," *Phys. Rev. A* **47**, 3113–3117; **48**, 2508(E) (1993).
- Gröbner, W., 1960, *Die Lie-Reihen und ihre Anwendungen*, Mathematische Monographien Vol. 3 (Deutscher Verlag der Wissenschaften, Berlin).
- Gröbner, W., 1967, *Contributions to the Method of Lie Series*, B. I. Hochschulschriften Vol. 802/802a (Bibliographisches Institut, Mannheim).
- Gross, M., 2001, "Topological mirror symmetry," *Invent. Math.* **144**, 75–137.
- Grozdanov, T. P., and E. A. Solov'ev, 1982, "Semi-classical quantization of the hydrogen atom in crossed electric and magnetic fields," *J. Phys. B* **15**, 1195–1204.
- Grozdanov, T. P., and E. A. Solov'ev, 1984, "The quadratic Zeeman effect for highly excited hydrogen atoms in weak magnetic fields," *J. Phys. B* **17**, 555–570.
- Guillemin, V., and S. Sternberg, 1982, "Convexity properties of the moment mapping," *Invent. Math.* **67**, 491–513.
- Guillemin, V., and S. Sternberg, 1984, "Convexity properties of the moment mapping—II," *Invent. Math.* **77**, 533–546.
- Guillemin, V., and S. Sternberg, 1990, *Variations on a Theme by Kepler*, AMS Colloquium Publications Vol. 42 (AMS, Providence, RI).
- Guillemin, V. W., 2007, *Geometric Aspects of Analysis and Mechanics: A Conference in Honor of the 65th Birthday of Hans Duistermaat* (Utrecht University, Utrecht).
- Hansen, M. S., F. Faure, and B. I. Zhilinskiĭ, 2007, "Fractional monodromy in systems with coupled angular momenta," *J. Phys. A: Math. Theor.* **40**, 13075–13089.
- Henrard, J., 1970, "On a perturbation theory using Lie transforms," *Celest. Mech.* **3**, 107–120.
- Herrick, D. R., 1982, "Symmetry of the quadratic Zeeman effect for hydrogen," *Phys. Rev. A* **26**, 323–329.
- Iu, C.-H., G. R. Welch, M. M. Kash, D. Kleppner, D. Delande,

- and J. C. Gay, 1991, “Diamagnetic Rydberg atom: Confrontation of calculated and observed spectra,” *Phys. Rev. Lett.* **66**, 145–148.
- Johnson, B. R., K. F. Scheibner, and D. Farrelly, 1983, “Large-order perturbation theory in the Stark-Zeeman effect for parallel fields,” *Phys. Rev. Lett.* **51**, 2280–2283.
- Joyeux, M., D. A. Sadovskii, and J. Tennyson, 2003, “Monodromy of the LiNC/NCLi molecule,” *Chem. Phys. Lett.* **382**, 439–442.
- Kalnins, E. G., W. Miller, and P. Winternitz, 1976, “Group $O(4)$, separation of variables and hydrogen atom,” *SIAM J. Appl. Math.* **30**, 630–664.
- Karasev, M. V., 1998, Ed., *Coherent Transform, Quantization, and Poisson Geometry* (AMS, Providence, RI), Vol. 187.
- Karasev, M. V., and V. P. Maslov, 1982, “Quantization of symplectic manifolds with conical points,” *Theor. Math. Phys.* **53**, 1186–1195.
- Karasev, M. V., and E. M. Novikova, 2005, “Algebra with polynomial commutation relations for the Zeeman-Stark effect in the hydrogen atom,” *Teor. Mat. Fiz.* **142**, 530 [*Theor. Math. Phys.* **142**, 447–469 (2005)], see Theorem 5.1 on p. 459 where resonances, Poisson algebras, and reduced spaces are all defined.
- Kibler, M., and T. Negadi, 1983a, “On the connection between the hydrogen atom and the harmonic oscillator,” *Lett. Nuovo Cimento Soc. Ital. Fis.* **37**, 225–228.
- Kibler, M., and T. Negadi, 1983b, “On the connection between the hydrogen atom and the harmonic oscillator: The continuum case,” *J. Phys. A* **16**, 4265–4268.
- Kibler, M., and T. Negadi, 1984a, “Connection between the hydrogen atom and the harmonic oscillator: The zero-energy case,” *Phys. Rev. A* **29**, 2891–2894.
- Kibler, M., and T. Negadi, 1984b, “Hydrogen atom in a uniform electromagnetic field as an anharmonic oscillator,” *Lett. Nuovo Cimento Soc. Ital. Fis.* **39**, 319–323.
- Kibler, M., T. Negadi, and A. Ronveaux, 1985, “The Kustaanheimo-Stiefel transformation and certain special functions,” *Lect. Notes Math.* **1171**, 497–505.
- Kontsevich, M., and Y. Soibelman, 2006, in *Unity of Mathematics—In Honor of the 90th Birthday of I. M. Gelfand*, edited by P. Etingof, V. Retakh, and I. M. Singer, Progress in Mathematics Vol. 244 (Birkhäuser, Basel), pp. 321–385.
- Kozin, I. N., and R. M. Roberts, 2003, “Monodromy in the spectrum of a rigid symmetric top molecule in an electric field,” *J. Chem. Phys.* **118**, 10523–10533.
- Kozlov, V. V., 1974, “Geometry of “action-angle” variables in the Euler-Poinsot system,” *Vestn. Mosk. Univ., Ser. 1: Mat., Mekh.* **29**, 74–79.
- Krantzman, K. D., J. A. Milligan, and D. Farrelly, 1992, “Semi-classical mechanics of the quadratic Zeeman effect,” *Phys. Rev. A* **45**, 3093–3103.
- Kristensen, L., E. Horsdal-Pedersen, and P. Sorensen, 1998, “Coherent elliptic states of atoms in non-orthogonal E and B fields,” *J. Phys. B* **31**, 1049–1057.
- Kummer, M., 1982, “On the regularization of the Kepler problem,” *Commun. Math. Phys.* **84**, 133–152.
- Kummer, M., 1996, “Anharmonic oscillators in classical and quantum mechanics with applications to the perturbed Kepler problem,” *Fields Inst. Commun.* **8**, 35–63.
- Kustaanheimo, P. E., 1964, “Spinor regularization of the Kepler motion” (Turun yliopisto, Turku, Finland, 1964).
- Kustaanheimo, P. E., and E. Stiefel, 1965, “Perturbation theory of Kepler motion based on spinor regularization,” *J. Reine Angew. Math.* **218**, 204–219.
- Kuwata, M., A. Harada, and H. Hasegawa, 1990, “Derivation and quantization of Solov’ev constant for the diamagnetic Kepler motion,” *J. Phys. A* **23**, 3227–3244.
- Lagrange, S., A. Picozzi, H. R. Jauslin, and D. Sugny, 2010, “Singular tori as attractors of four-wave-interaction systems,” *Phys. Rev. E* **81**, 016202.
- Laurent, C., and S. Vũ Ngọc, 2008, “Spectral asymptotics via the semiclassical Birkhoff normal form,” *Duke Math. J.* **143**, 463–511.
- Lerman, L. M., and I. L. Umanskiĭ, 1994a, “Classification of 4-dimensional integrable Hamiltonian systems and Poisson actions of $R(2)$ in extended neighborhoods of simple singular points. 1,” *Russ. Acad. Sci. Sb. Math.* **77**, 511–542.
- Lerman, L. M., and I. L. Umanskiĭ, 1994b, “Classification of 4-dimensional integrable Hamiltonian systems and Poisson actions of $R(2)$ in extended neighborhoods of simple singular points. 2,” *Russ. Acad. Sci. Sb. Math.* **78**, 479–506.
- Lerman, L. M., and I. L. Umanskiĭ, 1994c, “Isoenergetic classification of integrable Hamiltonian systems in a neighborhood of a simple elliptic point,” *Math. Notes* **55**, 496–501.
- Lerman, L. M., and I. L. Umanskiĭ, 1995, “Classification of 4-dimensional integrable Hamiltonian systems and Poisson actions of $R(2)$ in extended neighborhoods of simple singular points. 3. Realization,” *Sb. Math.* **186**, 1477–1491.
- Louck, J. D., 1976, “Derivation of the molecular vibration-rotation Hamiltonian from the Schrödinger equation for the molecular model,” *J. Mol. Spectrosc.* **61**, 107–137.
- Lutwak, R., J. Holley, P. P. Chang, S. Paine, D. Kleppner, and T. Ducas, 1997, “Circular states of atomic hydrogen,” *Phys. Rev. A* **56**, 1443–1452.
- Main, J., M. Schwacke, and G. Wunner, 1998, “Hydrogen atom in combined electric and magnetic fields with arbitrary mutual orientations,” *Phys. Rev. A* **57**, 1149–1157.
- Main, J., and G. Wunner, 1992, “Ericson fluctuations in the chaotic ionization of the hydrogen atom in crossed magnetic and electric fields,” *Phys. Rev. Lett.* **69**, 586–589.
- Main, J., and G. Wunner, 1994, “Rydberg atoms in external fields as an example of open quantum systems with classical chaos,” *J. Phys. B* **27**, 2835–2848.
- Manakov, N. L., V. D. Ovsyannikov, and L. P. Rapoport, 1976, “Perturbation theory for quasi energy spectrum of atoms in an intense monochromatic field,” *Zh. Eksp. Teor. Fiz.* **70**, 1697–1712.
- Marsden, J., R. Montgomery, and T. Ratiu, 1990, *Memoirs AMS* (AMS, Providence, RI), Vol. 88.
- Matveev, V. S., 1996, “Integrable Hamiltonian systems with two degrees of freedom: The topological structure of saturated neighbourhoods of points of focus-focus and saddle-saddle type,” *Sb. Math.* **187**, 495–524.
- Meyer, K. R., and G. R. Hall, 1992, *Introduction to Hamiltonian Dynamical Systems and the N -Body Problem* (Springer-Verlag, Berlin).
- Michel, L., and B. I. Zhilinskiĭ, 2001a, “Rydberg states of atoms and molecules. Basic group-theoretical and topological analysis,” *Phys. Rep.* **341**, 173–264.
- Michel, L., and B. I. Zhilinskiĭ, 2001b, “Symmetry, invariants, topology: Basic tools,” *Phys. Rep.* **341**, 11–84.
- Mineur, H., 1937, “Etude des systèmes admettant n intégrales premières uniformes en involution. Extension à ces systèmes des conditions de quantification de Bohr-Sommerfeld,” *J. Ec. Polytech., Sér. III* **143**, 237–270.
- Moser, J., 1970a, “Regularization of Kepler’s problem and av-

- eraging method on a manifold," *Commun. Pure Appl. Math.* **23**, 609–636.
- Moser, J., 1970b, "The regularization of the Kepler problem and the averaging method," *Bull. Am. Astron. Soc.* **2**, 249–250.
- Nekhoroshev, N. N., 1969, "Two theorems on the action-angle variables," *Usp. Mat. Nauk* **24**, 237–238.
- Nekhoroshev, N. N., 1972, "Angle-action variables and their generalizations," *Trans. Mosc. Math. Soc.* **26**, 180–198.
- Nekhoroshev, N. N., 1994, "The Poincaré-Lyapunov-Liouville-Arnol'd theorem," *Funct. Anal. Appl.* **28**, 128–129.
- Nekhoroshev, N. N., 2002, "Generalizations of Gordon theorem," *Regular Chaotic Dyn.* **7**, 239–247.
- Nekhoroshev, N. N., 2005, "Types of integrability on a submanifold and generalizations of Gordon's theorem," *Trans. Mosc. Math. Soc.* **66**, 169–241.
- Nekhoroshev, N. N., 2007, "Fractional monodromy in the case of arbitrary resonances," *Sb. Math.* **198**, 383–424.
- Nekhoroshev, N. N., 2008, "Fuzzy fractional monodromy and the section-hyperboloid," *Milan J. Math.* **76**, 1–14, presented at the Seminario Matematico e Fisico di Milano, 2004.
- Nekhoroshev, N. N., D. A. Sadovskii, and B. I. Zhilinskiĭ, 2002, "Fractional monodromy of resonant classical and quantum oscillators," *C. R. Math.* **335**, 985–988.
- Nekhoroshev, N. N., D. A. Sadovskii, and B. I. Zhilinskiĭ, 2006, "Fractional Hamiltonian monodromy," *Ann. Henri Poincaré* **7**, 1099–1211.
- Nguyễn Tiên, Z., 1995, "Decomposition of nondegenerate singularities of integrable Hamiltonian systems," *Lett. Math. Phys.* **33**, 187–193.
- Nguyễn Tiên, Z., 1996, "Symplectic topology of integrable Hamiltonian systems. I: Arnol'd-Liouville with singularities," *Compos. Math.* **101**, 179–215.
- Nguyễn Tiên, Z., 1997, "A note on focus-focus singularities," *Diff. Geom. Applic.* **7**, 123–130.
- Nguyễn Tiên, Z., 2002, "Another note on focus-focus singularities," *Lett. Math. Phys.* **60**, 87–99.
- Nguyễn Tiên, Z., 2003, "Symplectic topology of integrable Hamiltonian systems. II: Topological classification," *Compos. Math.* **138**, 125–156.
- Noid, D. W., S. K. Knudson, and J. B. Delos, 1983, "Resonant states of the hydrogen atom in strong magnetic fields," *Chem. Phys. Lett.* **100**, 367–370.
- Ortega, J. P., and T. S. Ratiu, 1998, "Singular reduction of Poisson manifolds," *Lett. Math. Phys.* **46**, 359–372.
- Pauli, W., 1926, "Über das Wasserstoffspektrum vom Standpunkt der neuen Quantenmechanik (The hydrogen spectrum from the viewpoint of the new quantum mechanics)," *Z. Phys. A* **36**, 336–363.
- Postell, V., and T. Uzer, 1990, "Quantization of the asymmetric top using quantum action-angle variables," *Phys. Rev. A* **41**, 4035–4037.
- Prince, G. E., and C. J. Eliezer, 1981, "On the Lie symmetries of the classical Kepler problem," *J. Phys. A* **14**, 587–596.
- Rau, A. R. P., 1986, "Rydberg states in crossed fields—The gyropendulum," *Phys. Rev. A* **34**, 4501–4503.
- Rau, A. R. P., and G. B. Armen, 2000, "Effective potentials for high Rydberg states in a magnetic field," *Phys. Essays* **13**, 400–407.
- Rau, A. R. P., and L. J. Zhang, 1990, "Mapping degenerate perturbations in atoms onto an asymmetric rotor," *Phys. Rev. A* **42**, 6342–6353.
- Reinhardt, W. P., and D. Farrelly, 1982, "The quadratic Zeeman effect in hydrogen: An example of semi-classical quantization of a strongly non-separable but almost integrable system," *J. Phys. Colloq.* **43**, 29–43.
- Rink, B. W., 2004, "A Cantor set of tori with monodromy near a focus-focus singularity," *Nonlinearity* **17**, 347–356.
- Robnik, M., 1981, "Hydrogen atom in a strong magnetic field—On the existence of the 3rd integral of motion," *J. Phys. A* **14**, 3195–3216.
- Robnik, M., 1982, "Hydrogen atom in strong magnetic fields—Regular and irregular motions," *J. Phys. Colloq.* **43**, 45–61.
- Robnik, M., 1984, "The algebraic quantization of the Birkhoff-Gustavson normal form," *J. Phys. A* **17**, 109–130.
- Robnik, M., and E. Schrüfer, 1985, "Hydrogen atom in a strong magnetic field—Calculation of the energy levels by quantizing the normal form of the regularized Kepler Hamiltonian," *J. Phys. A* **18**, L853–L859.
- Sadovskii, D. A., and B. I. Zhilinskiĭ, 1995, "Counting levels within vibrational polyads: Generating function approach," *J. Chem. Phys.* **103**, 10520–10536.
- Sadovskii, D. A., and B. I. Zhilinskiĭ, 1998, "Tuning the hydrogen atom in crossed fields between the Zeeman and Stark limits," *Phys. Rev. A* **57**, 2867–2884.
- Sadovskii, D. A., and B. I. Zhilinskiĭ, 1999, "Monodromy, diabolic points, and angular momentum coupling," *Phys. Lett. A* **256**, 235–244.
- Sadovskii, D. A., and B. I. Zhilinskiĭ, 2007, "Hamiltonian systems with detuned 1:1:2 resonance: Manifestation of bidromy," *Ann. Phys.* **322**, 164–200.
- Sadovskii, D. A., B. I. Zhilinskiĭ, and L. Michel, 1996, "Collapse of the Zeeman structure of the hydrogen atom in the external electric field," *Phys. Rev. A* **53**, 4064–4067.
- Salas, J. P., A. Deprit, S. Ferrer, V. Lanchares, and J. Palacian, 1998, "Two pitchfork bifurcations in the polar quadratic Zeeman-Stark effect," *Phys. Lett. A* **242**, 83–93.
- Salas, J. P., and V. Lanchares, 1998, "Saddle-node bifurcation for Rydberg atoms in parallel electric and magnetic fields," *Phys. Rev. A* **58**, 434–439.
- Sanrey, M., M. Joyeux, and D. A. Sadovskii, 2006, "Classical and quantum-mechanical plane switching in CO₂," *J. Chem. Phys.* **124**, 74318.
- Schleif, C. R., and J. B. Delos, 2007, "Monodromy and the structure of the energy spectrum of hydrogen in near perpendicular electric and magnetic fields," *Phys. Rev. A* **76**, 013404.
- Schleif, C. R., and J. B. Delos, 2008, "Semiclassical theory of the structure of the hydrogen spectrum in near-perpendicular electric and magnetic fields: Derivations and formulas for Einstein-Brillouin-Keller-Maslov quantization and description of monodromy," *Phys. Rev. A* **77**, 043422.
- Schrödinger, E., 1926, "The non-relativistic equation of the De Broglie waves," *Ann. Phys.* **79**, 361–376.
- Sinitsyn, E., and B. I. Zhilinskiĭ, 2007, "Qualitative analysis of the classical and quantum Manakov top," *Symmetry, Integr. Geom.: Methods Appl.* **3**, 046.
- Śniatycki, J., and A. Weinstein, 1983, "Reduction and quantization for singular momentum mappings," *Lett. Math. Phys.* **7**, 155–161.
- Solov'ev, E. A., 1981, "Approximate integral of motion of H atoms in a magnetic field," *Pis'ma Zh. Eksp. Teor. Fiz.* **34**, 278–281.
- Solov'ev, E. A., 1982, "Hydrogen atom in a weak magnetic field," *Zh. Eksp. Teor. Fiz.* **82**, 1762–1771.
- Solov'ev, E. A., 1983, "Second-order perturbation theory for a hydrogen atom in crossed electric and magnetic fields," *Zh.*

- Eksp. Teor. Fiz. **85**, 109–114 [Sov. Phys. JETP **58**, 63–66 (1983)].
- Stiefel, E. L., 1970, “Remarks on numerical integration of Keplerian orbits,” *Celest. Mech.* **2**, 274–281.
- Stiefel, E. L., and G. Scheifele, 1971, *Linear and Regular Celestial Mechanics* (Springer-Verlag, Berlin).
- Sugny, D., P. Mardešić, M. Pelletier, A. Jebrane, and H. R. Jauslin, 2008, “Fractional Hamiltonian monodromy from a Gauss-Manin monodromy,” *J. Math. Phys.* **49**, 042701.
- Sugny, D., A. Picozzi, S. Lagrange, and H. R. Jauslin, 2009, “On the role of singular tori in the spatiotemporal dynamics of nonlinear wave systems,” *Phys. Rev. Lett.* **103**, 034102.
- Suno, H., L. Andric, T. P. Grozdanov, and R. McCarroll, 1999, “Circular Rydberg states in parallel electric and magnetic fields,” *Phys. Rev. A* **59**, 524–530.
- Symington, M., 2003, “Four dimensions from two in symplectic topology,” in *Topology and Geometry of Manifolds*, Proceedings of Symposia in Pure Mathematics, edited by G. Matic and C. McCrory (AMS, Providence, RI), Vol. 71, pp. 153–208.
- Uzer, T., 1990, “Zeeman effect as an asymmetric top,” *Phys. Rev. A* **42**, 5787–5790.
- Uzer, T., and D. Farrelly, 1995, “Threshold ionization dynamics of the hydrogen atom in crossed electric and magnetic fields,” *Phys. Rev. A* **52**, R2501–R2504.
- Valent, G., 2003, “The hydrogen atom in electric and magnetic fields: Pauli’s 1926 article,” *Am. J. Phys.* **71**, 171–175.
- van der Meer, J. C., 1985, *The Hamiltonian Hopf Bifurcation*, Lecture Notes in Mathematics Vol. 1160 (Springer-Verlag, New York).
- van der Meer, J. C., 1986, “Corrections to: Constrained normalization of Hamiltonian system and perturbed Keplerian motion,” *ZAMP* **37**, 931.
- van der Meer, J. C., and R. H. Cushman, 1986, “Constrained normalization of Hamiltonian systems and perturbed Keplerian motion,” *ZAMP* **37**, 402–424.
- Van der Waerden, B. L., 1968, Ed., *Sources of Quantum Mechanics* (Dover, London).
- von Milczewski, J., G. H. F. Diercksen, and T. Uzer, 1994a, “Classical dynamics of Rydberg electrons in crossed fields—The structure of phase space and chaos order alternations,” *Int. J. Bifurcation Chaos Appl. Sci. Eng.* **4**, 905–920.
- von Milczewski, J., G. H. F. Diercksen, and T. Uzer, 1994b, “Intramanifold chaos in Rydberg atoms in external fields,” *Phys. Rev. Lett.* **73**, 2428–2431.
- von Milczewski, J., D. Farrelly, and T. Uzer, 1997a, “ $1/r$ dynamics in external fields: 2D or 3D?” *Phys. Rev. Lett.* **78**, 2349–2352.
- von Milczewski, J., D. Farrelly, and T. Uzer, 1997b, “Frequency analysis of 3D electronic $1/r$ dynamics: Tuning between order and chaos,” *Phys. Rev. Lett.* **78**, 1436–1439.
- von Milczewski, J., D. Farrelly, and T. Uzer, 1997c, “Role of the atomic Coulomb center in ionization and periodic orbit selection,” *Phys. Rev. A* **56**, 657–670.
- von Milczewski, J., and T. Uzer, 1997a, “Canonical perturbation treatment of a Rydberg electron in combined electric and magnetic fields,” *Phys. Rev. A* **56**, 220–231.
- von Milczewski, J., and T. Uzer, 1997b, “Chaos and order in crossed fields,” *Phys. Rev. E* **55**, 6540–6551.
- Vorob’ev, Y. M., and M. V. Karasev, 1987, “Corrections to the classical dynamics and quantization conditions arising at Poisson bracket deformation,” *Dokl. Akad. Nauk SSSR* **297**, 1294–1298.
- Vũ Ngọc, S., 1999, “Quantum monodromy in integrable systems,” *Commun. Math. Phys.* **203**, 465–479.
- Vũ Ngọc, S., 2000, “Bohr-Sommerfeld conditions for integrable systems with critical manifolds of focus-focus type,” *Commun. Pure Appl. Math.* **53**, 143–217.
- Vũ Ngọc, S., 2007, “Moment polytopes for symplectic manifolds with monodromy,” *Adv. Math.* **208**, 909–934.
- Waalkens, H., 2002, “Quantum monodromy in trapped Bose condensates,” *Europhys. Lett.* **58**, 162–168.
- Waalkens, H., H. R. Dullin, and P. H. Richter, 2004, “The problem of two fixed centers: Bifurcations, actions, monodromy,” *Physica D* **196**, 265–310.
- Waalkens, H., A. Junge, and H. R. Dullin, 2003, “Quantum monodromy in the two-centre problem,” *J. Phys. A* **36**, L307–L314.
- Waterland, R. L., J. B. Delos, and M. L. Du, 1987, “High Rydberg states of an atom in parallel electric and magnetic fields,” *Phys. Rev. A* **35**, 5064–5080.
- Watson, J. K. G., 1967, “Determination of centrifugal distortion coefficients of asymmetric-top molecules,” *J. Chem. Phys.* **46**, 1935–1949.
- Watson, J. K. G., 1968, “Simplification of the molecular rotation-vibration Hamiltonian,” *Mol. Phys.* **15**, 479–490.
- Weinstein, A., 1994, “Deformation quantization,” *Sémin. Bourbaki* **36**, 389–409.
- Wiebusch, G., J. Main, K. Krüger, H. Rottke, A. Holle, and K. H. Welge, 1989, “Hydrogen atom in crossed magnetic and electric fields,” *Phys. Rev. Lett.* **62**, 2821–2824.
- Williamson, J., 1936, “On an algebraic problem concerning the normal forms of linear dynamical systems,” *Am. J. Math.* **58**, 141–163.
- Winnewisser, M., B. P. Winnewisser, I. R. Medvedev, F. C. De Lucia, S. C. Ross, and L. M. Bates, 2006, “The hidden kernel of molecular quasi-linearity: Quantum monodromy,” *J. Mol. Struct.* **798**, 1–26.
- Zhilinskiĭ, B. I., 2005, “Interpretation of quantum Hamiltonian monodromy in terms of lattice defects,” *Acta Appl. Math.* **87**, 281–307.
- Zimmerman, M. L., M. M. Kash, and D. Kleppner, 1980, “Evidence of an approximate symmetry for hydrogen in a uniform magnetic field,” *Phys. Rev. Lett.* **45**, 1092–1094.
- Zobov, N. F., S. V. Shirin, O. L. Polyansky, J. Tennyson, P.-F. Coheur, P. F. Bernath, M. Carleer, and R. Colin, 2005, “Monodromy in the water molecule,” *Chem. Phys. Lett.* **414**, 193–197.
- Żołądek, H., 2006, *The Monodromy Group*, Monografie Matematyczne, Instytut Matematyczny PAN Vol. 67 (Birkhäuser, Basel).